Single Transponder Range Only Navigation Geometry (STRONG) Applied to REMUS Autonomous Under Water Vehicles

by

Lieutenant Commander J. Carl Hartsfield, Jr.

B.S. Engineering Physics, Murray State University, 1992

Submitted in partial fulfillment of the

Requirements for the degree of

MASTER OF SCIENCE
at the
MASSACHUSETTS INSTITUTE OF TECHNOLOGY
and the
WOODS HOLE OCEANOGRAPHIC INSTITUTION
August 2005

Signature of Author ……...
Lieutenant Commander J. Carl Hartsfield Jr.
U.S. Navy Submarine Force
Joint Program in Applied Ocean Science and Engineering
Massachusetts Institute of Technology/
Woods Hole Oceanographic Institution

Certified by …….....
Professor Arthur B. Baggeroer
Ford Professor of Engineering, Professor of Mechanical Engineering, Electrical Engineering, and Computer Science
Massachusetts Institute of Technology
Thesis Supervisor

Certified by …….....
Mr. Christopher J. von Alt
Principal Engineer, Ocean Systems Laboratory
Woods Hole Oceanographic Institution

Accepted by ……..
Professor Mark A. Grosenbaugh
Chairman, Joint Committee for Applied Ocean Science and Engineering
Massachusetts Institute of Technology and Woods Hole Oceanographic Institution

Report Documentation Page

Form Approved
OMB No. 0704-0188

1. REPORT DATE	2. REPORT TYPE	3. DATES COVERED
01 AUG 2005	**N/A**	**-**

4. TITLE AND SUBTITLE	5a. CONTRACT NUMBER
Single Transponder Range Only Navigation Geometry (STRONG) Applied to REMUS Autonomous Under Water Vehicles	5b. GRANT NUMBER
	5c. PROGRAM ELEMENT NUMBER
6. AUTHOR(S)	5d. PROJECT NUMBER
	5e. TASK NUMBER
	5f. WORK UNIT NUMBER
7. PERFORMING ORGANIZATION NAME(S) AND ADDRESS(ES) **Massachusetts Institute of Technology**	8. PERFORMING ORGANIZATION REPORT NUMBER
9. SPONSORING/MONITORING AGENCY NAME(S) AND ADDRESS(ES)	10. SPONSOR/MONITOR'S ACRONYM(S)
	11. SPONSOR/MONITOR'S REPORT NUMBER(S)

12. DISTRIBUTION/AVAILABILITY STATEMENT
Approved for public release, distribution unlimited

13. SUPPLEMENTARY NOTES
The original document contains color images.

14. ABSTRACT

15. SUBJECT TERMS

16. SECURITY CLASSIFICATION OF:			17. LIMITATION OF ABSTRACT	18. NUMBER OF PAGES	19a. NAME OF RESPONSIBLE PERSON
a. REPORT	b. ABSTRACT	c. THIS PAGE			
unclassified	**unclassified**	**unclassified**	**UU**	**125**	

Standard Form 298 (Rev. 8-98)
Prescribed by ANSI Std Z39-18

Single Transponder Range Only Navigation Geometry (STRONG) Applied to REMUS Autonomous Under Water Vehicles

by
Lieutenant Commander J. Carl Hartsfield, Jr.
Submitted to Massachusetts Institute of Technology/
Woods Hole Oceanographic Institution
Joint Program in Oceanographic Engineering
on August 5, 2005 in partial fulfillment of the
requirements for the Degree of Master of Science in Ocean Engineering

ABSTRACT

A detailed study was conducted to prove the concept of an iterative approach to single transponder navigation for REMUS Autonomous Underwater Vehicles (AUVs). Although the concept of navigation with one acoustic beacon is not new, the objective was to develop a computer algorithm that could eventually be integrated into the REMUS architecture. This approach uses a least squares fit routine coupled with restrictive geometry and simulated annealing vice Kalman filtering and state vectors. In addition, to provide maximum flexibility, the single transponder was located on a GPS equipped surface ship that was free to move instead of the more common single bottom mounted beacon. Using only a series of spread spectrum ranges logged with time stamp, REMUS standard vehicle data, and reasonable initial conditions, the position at a later time was derived with a figure of merit fit score.

Initial investigation was conducted using a noise model developed to simulate the errors suspected with the REMUS sensor suite. Results of this effort were applied to a small at sea test in 3,300 meters with the REMUS 6000 deep water AUV. A more detailed test was executed in Buzzard's Bay, Massachusetts, in 20 meters of water with a REMUS 100 AUV focusing on navigation in a typical search box.

While deep water data was too sparse to reveal conclusive results, the Buzzard's Bay work strongly supports the premise that an iterative algorithm can reliably integrate REMUS logged data and an accurate time sequence of ranges to provide position fixes through simple least squares fitting. Ten navigational legs up to1500 meters in length showed that over 90% of radial position error can be removed from an AUV's position estimate using the STRONG algorithm vice dead reckon navigation with a magnetic compass and Doppler Velocity Log alone (DVL).

Thesis Supervisors: Professor Arthur B. Baggeroer
Ford Professor of Engineering, Professor of Mechanical Engineering, Electrical Engineering, and Computer Science
Massachusetts Institute of Technology
Mr. Christopher J. von Alt
Principal Engineer, Woods Hole Oceanographic Institution
Mr. Thomas C. Austin
Senior Engineer, Woods Hole Oceanographic Institution

Acknowledgments

Selection to the MIT/WHOI Joint Program has been a professional goal for over ten years. When your high school graduating class numbered 24 and the highest math offered was Algebra II, it is hard to hope for such lofty academic accolades. This unique educational experience has surpassed my expectations, and the lessons learned in this course of study will provide great personal benefit and, hopefully, advantage to the submarine service.

Admiral Cohen and Admiral West deserve many thanks not only for the wise support and administration of this program, but also for their efforts to defer my acceptance when unforeseeable conditions required me to stay where I was needed most on the USS Parche (SSN 683). Captain Nees and Commander Kennedy of my parent squadron wrote letters and made phone calls to ensure I did not miss this opportunity, and I became the only Navy Joint Program deferral in history. Sometimes the best path is not the most obvious one.

I would also like to recognize Captain Dave Leary for his continued and unilateral support on my behalf. He has been a friend, a professional sounding board, and someone I could always count in my corner.

I extend thanks to my advisors Professor Arthur Baggeroer and Chris von Alt who treated me more as a colleague than a student and provided every opportunity to succeed. I worked closest with Tom Austin who taught me with wisdom beyond the textbook. His guidance and friendship were immeasurable. I also appreciate the engineering and scientific guidance of Mike Purcell, Roger Stokey, Ben Allen, Ned Forrester, Professor Jim Irish, and Professor Eugene Terray; the technical assistance of Greg Packard and Amy Kukulya; and the general support of Marga McElroy and Gretchen McManamin. You are all great friends.

Finally, I give my deepest and most heartfelt thank you to my wife, Leigh Ann, who was diagnosed with breast cancer during the completion of this thesis. Her unwavering bravery and positive attitude while she beat cancer were, and continue to be, a profound inspirational source for all who know her. She is the strongest, smartest, and most beautiful person I will ever know.

CONTENTS

LIST OF FIGURES

LIST OF TABLES

CHAPTER 1
GENERAL BACKGROUND

1.1 Conceptual Beginnings

Although single transponder navigation is not a new concept, the combination of an iterative approach to navigate an Autonomous Underwater Vehicle with a moving, ship-mounted transponder is largely unexplored. There are many ways to solve this problem, but this research has focused on proving that a properly structured computer algorithm can apply basic principles of target tracking within empirically determined restrictive geometries to estimate vehicle position.

1.1.1 Submarine Force Inspiration

Since before World War II the U. S. submarine force has tracked targets surmising through experience the proper data inputs to yield the necessary output: target solution in course, speed, and range. From the earliest days, periscope observations with telemeter range estimations on targets at given times were laid down on paper plots that tied information together to deduce the target track and an intercept firing solution. These plots are still used today and can allow the brain at a glance to accurately integrate passive sonar, bearing only, information into a target solution. To estimate the target's position, the submarine crew must employ basic target motion analysis. Simply stated, an estimate of the solution must be made based on the targets best guess parameters and continually refined to increase confidence. The estimation is iteratively improved as the submarine maneuvers to make the data set observable and unique yielding one solution.

Development of the Single Transponder Range Only Navigation Geometry (STRONG) parallels this approach wherein an initially unobservable data set, using range only vice bearing only observations, can be estimated upon and iteratively refined to yield a solution. Mechanically applying the intuition gained from numerous tracking scenarios over several years of personal experience, a noise model algorithm was

developed and tested through various geometries. This algorithm was then revised and applied to REMUS (Remote Environment Monitoring UnitS) autonomous vehicle data sets.

1.1.2 Strengths Of An Iterative Tracking Algorithm

The eventual end application of the STRONG algorithm in a REMUS vehicle would require much of the computer processing to be done on board the vehicle since acoustic modem data rates are limited. While the computing capacity of these vehicles is substantial, the available space for executable code is by no means endless. Navigation should be a background task that doesn't over burden the processor. Current long base line navigation routines run iteratively as information is received and are integrated with streams of on board sensor data. With these restrictions in mind, a simplified computer algorithm is preferred vice a large matrix driven Kalman filter or complex estimation routine. The STRONG approach is to sequentially process measured range data against intended trajectory in a simple least squares sense until a vehicle position is produced. This geographic position, or "fix", will then be processed in the traditional REMUS architecture like current long baseline (LBL) fixes. On REMUS vehicles equipped with commercially available Kearfott Inertial Navigation Units (INUs), these fixes will become inputs to Kalman filtering and weighting routines inherent to the instrument. Modular integration would allow upgrades to vehicles in the field without major changes to the tried and true REMUS core firmware.

1.1.3 Relative Motion

A key concept in the development of STRONG involved platform relative motion. Many approaches focus data collection on a single bottom mounted transponder. From the beginning, STRONG assumed both platforms would be in motion. As will be

demonstrated in subsequent chapters, intelligent management of relative motion is the key to expedient and unique solution convergence.

1.2 Benefits and Applications of Single Transponder Navigation

Navigation with a single ship mounted transponder affords many benefits over traditional LBL navigation. The expense and time involved in AUV operations are significant metrics motivating researchers to reduce both while accomplishing the same goals. With the day rate on moderately sized research ship measured in the tens of thousands preparation time for a mission work area is costly. Transponder surveys absorb valuable ship time with the vehicle dry on deck. An acoustic field is usually a must since even moderately deep water precludes transiting a vehicle to the surface for GPS positions. However, even the most accurately surveyed bottom transponders only have so much work area "foot print" before a new field is needed. While gaining local autonomy, AUV's sacrifice the capability of older towed systems to operate in long survey transects without transponders knowing that the vehicle position was at least within a cantenary calculation from ship's GPS position. The solution to all these problems is reliable, ship mounted transducer navigation that coordinate transforms surface GPS to an AUV positional solution.

1.2.1 Transponder Seeding

A REMUS shallow water transponder costs $2,000. A deep water model with acoustic release is $20,000. With a minimum of two required, the investment is obvious. Loss of unit or failure to release is a real threat and a costly event.

While deployed on the USNS Pathfinder north of the Bahamas REMUS 6000 ran eleven missions in deep water. Two transponders were deployed approximately 2000 meters apart on a north/south axis in a subterranean trench. Two methods were attempted to "survey in" the transponders with only marginally conclusive results. The approach is summarized as follows (Stokey, 2002):

1. Determine the best average sound speed by launching a bathymetric thermograph. Review best bathymetry and estimate transponder depths, determine transponder height by subtracting mooring length from best estimate of depth.
2. Determine ranges at four stopping points around the field such that three of the four positions cluster around each transponder at optimum 120° horizontal angles. The positions should also optimally one water depth away from the transponder to get a 45° slant angle (Figure 1.1).
3. Collect range and ship position at the various stopping points. Process the results by computer algorithm or manually.

Figure 1.1
Transponder Survey Geometry

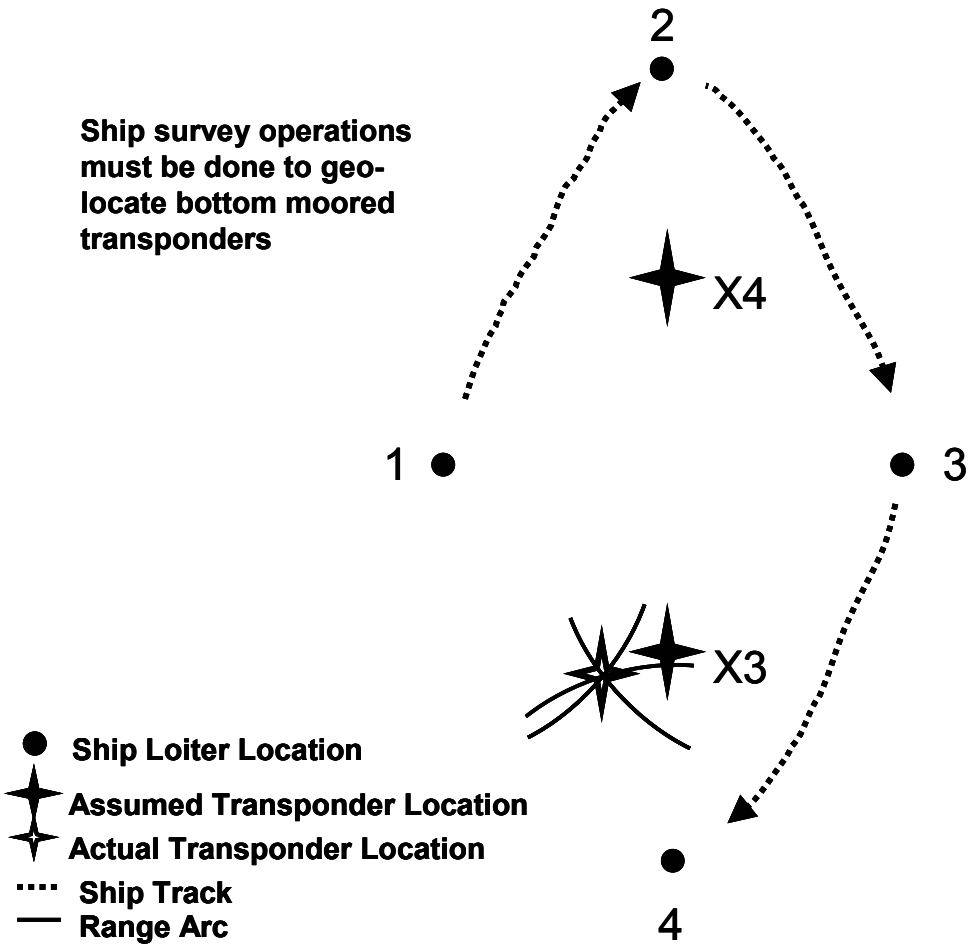

Collecting the range data to survey in the transponders precludes most other operations. Steaming between the stopping points involves over 10 nautical miles (NM) of travel while hovering between ten to twenty minutes to get consistent ranging. With ranger equipment in the water, speed is limited to only a few knots. Often, the hovering takes much longer as systems have to be shut down or shifted on the ship to lower background noise enough for range reception in deep water. The first data set took about six hours to collect. Computer processing failed to converge and produce transponder positions. The data was again collected over the next eight hours and manually processed by plotting the ranges on a scaled chart printed from Pathfinder's tracking systems. The

corrections and the drift rates (horizontal position error developed as the transponder sinks) from the surface were calculated (Table 1.1).

Table 1.1

Bahamas Transponder Offsets

	WATER DEPTH	OFFSET	DIRECTION	DRIFT RATE %
Transponder X4 (northern)	3265 m	220 m	251°	6.7 %
Transponder X3 (southern)	3312 m	130 m	240°	3.9 %

The results of the geo-location were never used in vehicle navigation and REMUS 6000 found and returned to all targets in a relative sense. If latitude and longitude of the objects surveyed were essential to mission success, the corrections would have become much more important. Irregardless, nearly 10 % of the time in this work area (one of three for the short deployment) was devoted to corrections attempted but not used. Although this deep water example was extreme, even shallow water depths in Buzzard's Bay experience positional drift rate transponder errors when GPS fluctuations and relatively strong currents are combined.

1.2.2 Long Transects

Another exciting application of single transponder navigation is the ability to conduct long linear transects without surfacing for GPS. With the ship in acoustic range and properly maneuvered, the vehicle can generally follow the ship's path to maximum endurance. With ever improving battery technology, AUV's often have sea legs longer than their navigational foot print. However, the long transect concept could allow pipeline or communication cable surveys for hundreds of miles. The REMUS 600's maximum range of 300+ kilometers could be fully utilized. For instance, cable surveys

often rely on towed systems to inspect cables over the long haul, or resort to piecewise ROV surveys. A survey system optimized for towing is often not very maneuverable so a coordinated and delicate ballet must take place between the ship drivers and the sensor operators to stay on the target. Likewise, cable tension limits often severely restrict ship's speed. Transition to a STRONG navigated vehicle would allow some relaxation in ship movement while the vehicle runs previously determined GPS waypoints of the cable or pipeline lay. The ship would most likely sprint and drift off side the survey path to force enough relative motion change to fix vehicle position.

1.2.3 Bottom Mounted Transponders Revisited

Another basic application of STRONG technology would involve the more traditional approach of operating with a reduced number of bottom transponders. Traditional long baseline navigation is briefly reviewed for comparison in subsequent chapters, but it is suffice to say that more area could be covered with fewer bottom transponders. REMUS 100 shallow water operations can be used in a simple thumbnail exercise. Current operations in Buzzard's Bay show maximum reliable linear ranges to navigational beacons to be on the order of 1500 meters. Traditional REMUS procedure would set the diagonal length of the search box at 1500 meters and the baseline to about 1000 meters. The maximum quoted reliable range is about 2 kilometers. As per standard procedure, REMUS operations are limited to one side of the baseline yielding an effective search area per transponder ratio of approximately 5×10^5 m^2 /transponder. Using only one transponder and folding coverage to all four quadrants around a single transponder results in 4×10^6 m^2/transponder effectiveness, or an eight fold increase in area for a single transponder (Figure 1.2). Although simplified, this example illustrates how much search areas can easily expand to match battery capabilities without solely relying on dead reckon navigation, diverging inertial systems, or frequent surfaces for satellite fix information.

Figure 1.2
Single Transponder Area Increase

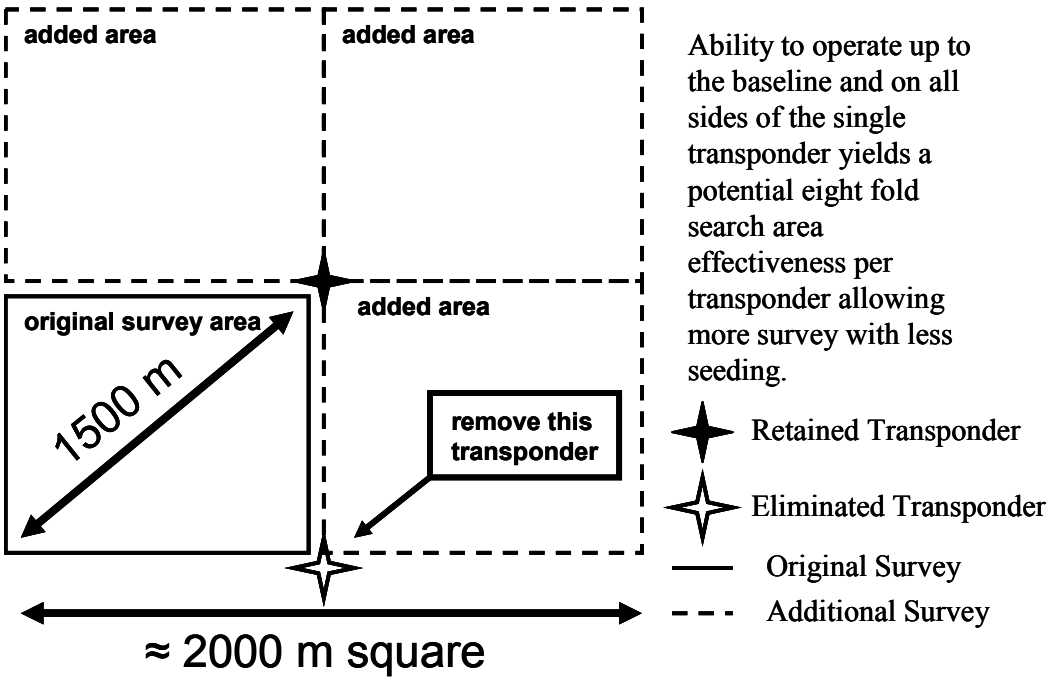

A combination of long transect navigation and single bottom mounted transponder navigation also bears mentioning. A long linear target such as a pipeline could be routinely surveyed with fewer transponders if single transponders are integrated into the physical structure periodically down its length. The surveying vehicle could stand off to the side and image the entire structure in side scan sonar. In these scenarios, it may be more useful to scale the example for REMUS 6000 operations in which the maximum transponder range would be on the order of 10,000 meters vice 1500 meters.

1.2.4 Buoy Navigation

A final application of STRONG technology involves using a single REMUS Portable Acoustic/RADIo Geo-referenced Monitoring (PARADIGM) buoy to control the navigation scheme. The buoy already has the capability to act as a bottom transponder

when anchored on the surface. Adding an acoustic modem would allow the buoy to "stand in" for the ship as the ranging platform. In deeper waters, the buoy can be allowed to drift or, in high windage or current, may be modified to rudimentarily station keep. Some buoy motion is not an issue if environmental conditions do not force the surface transponder into an unfavorable geometry before the survey is completed. With proper planning the ship can standoff within radio range and monitor, track, communicate, and acoustically command the vehicle while performing other tasks. Multiple vehicles could be managed in such a manner.

CHAPTER 2
SHORT LITERATURE REVIEW

2.1 Traditional Long Baseline Navigation (LBL)

Long baseline navigation has dominated the underwater navigation of vehicles since the late 1970s. Wide utilization of a bottom mounted, recoverable transponder gave an earth fixed reference for range measurement (Marquet, Webb, and Fairhurst, 1969). Before the days of the Global Positioning System, Pulse-Doppler long baseline concepts were employed to accurately position ships and platforms on the surface accurately as well (Spindel, Porter, Marquet, and Durham, 1976). The basic concept involves calculating range from adjusted travel time (τ) and an average sound speed (c_{avg}). Travel time must be adjusted to account for any instrument turn around (t_{delay}) and can be improved using spread spectrum techniques to reduce the inherent measuring error (ε).

$$Range = \frac{1}{2} c_{avg} \left(t_{measured} - t_{delay} \varepsilon \right) = \frac{1}{2} c_{avg} \tau$$

A minimum of two transponders result in two intersecting spheres. This union creates a circle of possible position. Measurement and application of vehicle depth further constrains the problem to two possible positions on that circle of intersection. Lacking the consideration of a third transponder, wise application of initial position results in a known relative position. Translation to the Earth frame of reference results in a vehicle "fix" that can be quoted usefully in latitude and longitude. Including the time delay error already mentioned, the considered list of LBL errors is as follows:

1. Ambiguities in the initial condition or near baseline ill effects to include slant range measurements very near actual water depth
2. Transponder position error relative to the Earth frame of reference
3. Deviation of actual sound speed from the assumed average

4. Sound bending at moderate horizontal distances
5. Vehicle advance during travel time
6. Depth errors for vehicle and transponders
7. Exact time measuring ambiguity (ε)
8. Flat earth approximation

A rigorous mathematical review of each of these errors plus their second order combinational errors (to include multiplicative and square-law errors) can be found in *Latest Highlights in Acoustic Underwater Navigation* (Ceston, Cyr, Roesler, and St. George Jr., 1976). However, this research focuses on identifying the main contributors for the specific geometry in question and operating to mitigate ones that can be controlled. The first five errors will be addressed in detail in subsequent chapters. Depth error will be discussed in detail and is driven by latitude correction and deviations from the assumed standard ocean. Depth accuracy needed to employ STRONG in deep water is within current instrument capability if advantage is made of the maximum instrument sensitivity. Time ambiguity (ε) has been greatly reduced since the Cestone paper using spread spectrum approaches developed and currently employed in the Remote Environmental Monitoring UnitS (REMUS) architecture (Austin, 1994). Finally, the earth was assumed flat for all calculations since the deviation is only about a third of a meter over a square mile and deemed insignificant.

Even though developed before the widespread revolution of affordable, dense computing capability, LBL was always intended to be an iterative computer algorithm. The hand written flow chart for the Woods Hole Oceanographic Institution's (WHOI) first LBL navigator was a simple logic tree written with computer language in mind. A simple iterative approach could be easily understood, programmed, and executed. Over the past thirty years inertial navigators have revolutionized "x marks the spot" navigation but have necessitated complex Kalman filtering routines to prioritize and promote end results. The goal of this research was to go back to the iterative approach with a single transponder and develop a simple navigator that could one day be reasonably executed in

the brain of a REMUS vehicle without stealing computing power needed to do science vice just navigate.

2.2 Synthetic Long Baseline Navigation

Synthetic Long Baseline Navigation (SLBL) is a single beacon navigational method studied for at least five years (Larsen, 2000). However, as mentioned, most approaches focus on a single sea floor mounted transponder. Likewise, the processing of inputs into an output solution is generally done by defining a state vector and creating linear functions of the individual state variables. The most prevalent estimator used is a Kalman filter. Although the overall problem is non-linear, inclusion of factors large and small creates a detailed estimation model that is exact but often overwhelming for a small AUV.

2.2.1 SLBL Concept

A traditional approach to the SLBL estimation problem can readily be found (Baccou, 2002). A vast array of parameters can be included in the state vector. Baccou applies his model to a vehicle without an Acoustic Current Doppler Profiler (ADCP), so in addition to positional coordinates (*x, y,* and *z*), he includes north and east components of current (v_{cx} and v_{cy}), vehicle velocity (u), and velocity error (du). Making the usual simplification that the z component of the transponder can be eliminated by converting the 3 dimensional "slant ranges" into two dimensional "bottom ranges", the problem is restricted to the x-y plane passing through the vehicle's depth z. Displacement over time (Δt) with a vehicle pitch (ψ) and heading (θ) is as follows:

$$\Delta y = \cos\theta \sin\Psi (u - du)\Delta t + v_{cx}\Delta t$$
$$\Delta x = \cos\theta \cos\Psi (u - du)\Delta t + v_{cy}\Delta t$$

An extended Kalman filter can be applied to the equations to estimate the *n+1* iteration knowing the *nth* parameters:

$$\begin{bmatrix} x \\ y \\ z \\ \\ v_{cx} \\ v_{cy} \\ du \end{bmatrix}_{n+1} = \begin{bmatrix} x \\ y \\ z \\ \\ v_{cx} \\ v_{cy} \\ du \end{bmatrix}_{n} + \begin{bmatrix} \cos\theta\cos\psi(u-du)+v_{cx} \\ \cos\theta\sin\psi(u-du)+v_{cy} \\ -\sin\theta(u-du) \\ 0 \\ 0 \\ 0 \end{bmatrix}_{n} \Delta t + N$$

Where N represents the state noise vector. Baccou models the currents and the speed bias as a constant. The next step is to construct an observation equation that accurately turns the measured parameter of travel time into a range. The range obtained from travel time must be corrected for significant vehicle advance as sound transverses from transponder to vehicle and back. This observation equation can also include noise and turn around time inherent to the ranging equipment in use.

2.2.2 SLBL Advantages

Traditional SLBL's Kalman filter has many attractive attributes. Having served as the Navigation Officer of a nuclear submarine, I have great confidence in an inertial Kalman filtering combination that could navigate months with sporadic fix input. As mentioned, any parameter can be included into the state vector. The component currents of the previous example are not considered in the STRONG approach since all velocities are derived from ADCP bottom lock motion. However, a Kalman filter allows defining variations large and small. STRONG seeks to simplify the estimation problem by minimizing minor effect contributors through geometry constraints and knowledge of instrument characteristics.

Second, a Kalman filter is a real time estimator in that a prediction is available in the present. Although not as iteratively simple as STRONG, Kalman filters are superior to other estimation techniques that produce significantly time late position estimates. Although a time late position may be successfully dead reckoned for a short period to

give a current fix, results must be fresh enough to give fixes in the here and now. Of course, this feature is why Kalman is so prevalent in inertial navigation routines.

Finally, the Kalman filtering SLBL routine accepts accuracy weighted input and outputs error estimates. Simply put, the information going into the filter can be assigned error bars, and the filtered output will have error bars. The richness in error estimation comes from the detailed covariance matrix that place holds and correlates both on axis and off axis matrix terms to track a complicated dimensional error. STRONG is not without its indications. A FIT VALUE is monitored to determine how well the measured ranges correspond to the predicted ranges derived from the planned geometry. However, this one dimensional value is not directly relatable to a real time radial position error. To mitigate this drawback, STRONG relies on Monte Carlo numeric simulation and real world REMUS data to show in a rudimentary sense that a simplified approach is justified in scenarios where large errors can be addressed and small ones ignored. Again, the goal of STRONG is to work towards implementation of a piecewise navigator that can yield an acceptable result without overwhelming onboard computing capability.

An example of the different error approaches of a Kalman approach and STRONG involves Geometric Dilution of Precision (GDOP). GDOP expresses the loss in accuracy due to the increasing collinear line of sight that a vehicle experiences when it is far from a transponder. Essentially, corrections for heading are not possible because outside a certain range the vehicle effectively “points” the transponder and does not show enough spatial variance in course to allow correction, i.e. it is “unobservable”. Any broader course at that range would yield a trajectory far from the transponder. Think about this effect with the small angle approximation if you like, but a vehicle advancing directly toward or away from a transponder can only correct for speed and not course. This idea is further developed later, but Larsen’s work shows that for his equipment suite, the ranges of dilution occur at around 2 kilometers for sub meter accuracy (Larsen, 2000). Since REMUS 100 operations rarely exceed 2 kilometers in shallow water, GDOP for range is ignored. As depicted in Figure 1.2, ranges for REMUS 100 are approximately 1.5 kilometers (2 kilometers maximum). Even in deep REMUS 6000 work, the ship

mounted transponder, although moveable, is usually in decent proximity to the operating vehicle. If long range operations were necessary, a transmitting buoy could stand in for the ship. An extended Kalman filter could track the degradation in GDOP dependent on range and output a position likewise degraded. STRONG drops this dependence since it is not operationally relevant.

2.2.3 SLBL Limitations

Kalman SLBL simply requires a lot of calculations. The equations are matrix equations involving large, sometimes sparse, components that must be modified and combined at every iteration. This requires processing power plus memory space. STRONG simulations used the MATLAB environment steeped in matrix capability, but the REMUS architecture relies on a processor running DOS instructions with the familiar cap on conventional memory. This space must be used for everything, not just navigation. Some of the latest Synthetic Aperture Sonar (SAS) advances in the REMUS 600 require complicated vehicle control routines to improve vehicle stability. These routines are mission necessary and should not be "robbed" by a navigational routine. Even though Pentium level upgrades with advanced languages are in the works, the amount of room for navigation will never be unlimited. STRONG aims to simplify the process by numerically determining vehicle geometry where the major components of error will describe the problem. These numerical predictions were then tested with experimentation.

A Kalman filter can divergence. Its complexity is desirable but leaves few adjustments to prevent a potential derailment. The Kalman filter on a nuclear submarine could only be altered by "weighting out" past positional inputs with numerous better estimates of position. Whether these positions were absolute GPS fixes or the near continuous inertial update of position based on accelerometer sensed movement, the solution to filter divergence was the same: sustained better input. The inner workings of the filter were unapproachable, and a contaminated Kalman inertial system could take days or weeks to heal. Even local variations in the acceleration due to gravity could produce noticeably affected output. REMUS operations with the Kearfott inertial

navigator are analogous. Likewise, error estimations do not necessarily foretell a divergence. Error estimations of fleet submarine Kalman filters are not used as a navigation quality measure. Instead, a set error was assigned to these predictions based on operational experience and a flag was thrown when any outside position source or the redundant inertial navigator violated this circle of uncertainty.

2.3 Transponder Locating on the Fly

It bears mentioning that single transponder navigation is often an approach to more accurately locate bottom mounted transponders. Submerged, on the fly calibration of transponders would allow a vehicle to navigate in a traditional LBL approach while working to improve accuracy in the process (Newman and Leonard, 2003). The transponders could be ship seeded or laid down by the AUV. The later is an attractive option for a vehicle that must travel a large standoff distance and seed a LBL field. Although the operational constraints are different, the mathematical formulation is nearly identical to covered material and usually follows the Kalman filtering estimation approach already mentioned. In the most basic sense, the information can be simply processed as the ship laid transponders were in Section 1.2.1.

CHAPTER 3
PREPARATION AND NOISE MODELING

3.1 General Application

The REMUS team's first consideration of single transponder ranging involved some simple ship/AUV geometries to allow long transect runs. The original concept proposed that REMUS 6000 would travel in a relative straight line while a USNS research vessel traveled abeam the AUV to correct heading and astern to correct speed. A small noise model was developed to prove that a simple random walk error could be removed with successive ship maneuvers to make heading and speed errors observable. STRONG's modeling extended this two position model to a continuous geometry around the ranging platform. A random walk vehicle trajectory was used to simulate the varying vehicle position of a REMUS 6000 with variance in inertial heading and ADCP speed over ground. However, the majority of actual STRONG experimental data were taken with a magnetic compass driven REMUS 100 vehicle. Although noisier in heading, the lessons learned in the original model laid a successful architecture for REMUS 100 operations that were verified by experimental measurement. The commonality of REMUS internal workings makes a generic application to all classes both desirable and realistic. Chapter 3 will explain the vehicles, underlying error assumptions, and the noise modeling used to create the STRONG algorithm.

3.1.1 General Geometry

The basic geometric approach is to convert measured slant ranges into two dimensional bottom ranges and define axial zones around the vehicle. The zones are defined for optimal course corrections (across track errors) and speed corrections (along track errors). They are defined by the vehicle's "line of sight" diagram with the ranging ship transponder (Figure 3.1). Narrow vehicle "angles to course made good (CMG)" result in speed corrections while broad angles result in course corrections. The transition

angle between these zones was determined by Monte Carlo computer simulation using the previously discussed ranges typically seen in REMUS operations. The result is an axially binned integration of range corrections based on a 0° – 180° angle-to-CMG. Since the two sides of the vehicle are symmetric and indiscernible through range measurement only, 360° coverage is possible by assuming a reasonable initial position.

Figure 3.1
Vehicle to Ship Geometry

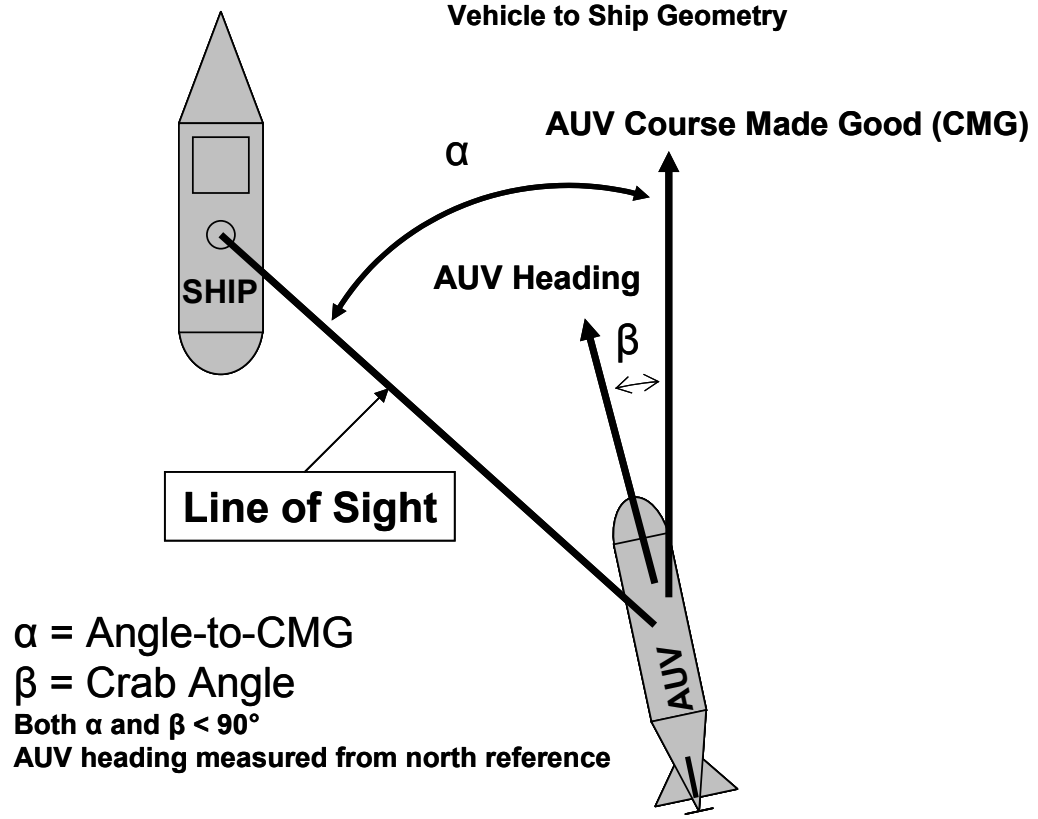

Two dimensional "line of sight" angles between the ship and AUV are angularly referenced from both north and AUV Course Made Good (CMG)

3.1.2 Ambiguous Solution

In assuming a starting position, one must rule out ambiguous solutions. Just like operations with two transponders yields two identical solutions, one on each side of the

baseline, single transponder ranging yields four potential solutions that fit a given set of range data with a fixed transponder given a known speed (Figure 3.2).

Figure 3.2
Four AUV Trajectories for Range Sequence

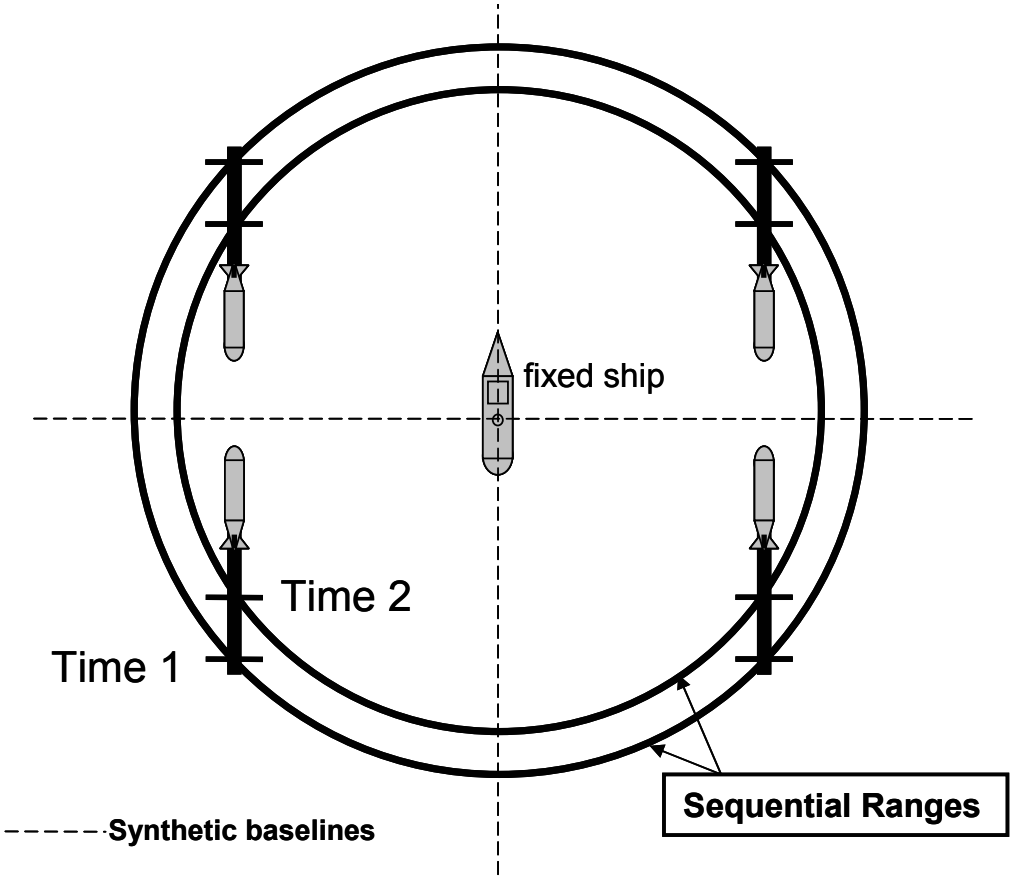

Two sequential ranges with no AUV or ship course maneuvers yield four possible ambiguous solutions that fit the data across synthetic baselines

Without a relatively large beam-forming array, bearing cannot, of course, be used to pick the correct trajectory. These potential solutions can be paired as mirror images across "synthetic" baselines. Usually, one pair can easily be ruled out with an approximate dead reckon starting position. The two cases that are not so easily ruled out are a vehicle broad at closest point of approach (CPA) or a vehicle with a very narrow angle-to-CMG. Since a tracking problem is rarely initialized with the AUV broad at CPA, the first case is rarely

an issue. Likewise, the mirrored solution in this case would only lag ahead or behind the real solution and would likely be weighed out as the AUV drives into the distance. The second case is much more probable. As the vehicle points the ranging transponder, the two close CPA solutions stay nearly identical both closing and opening with only a few range variations to discern between the two possibilities (Figure 3.3). The initial dead reckon error remains unresolved because the range sequences for a fixed ship position are indistinguishable.

Figure 3.3
Two Irresolvable Trajectories in Four Decreasing Ranges

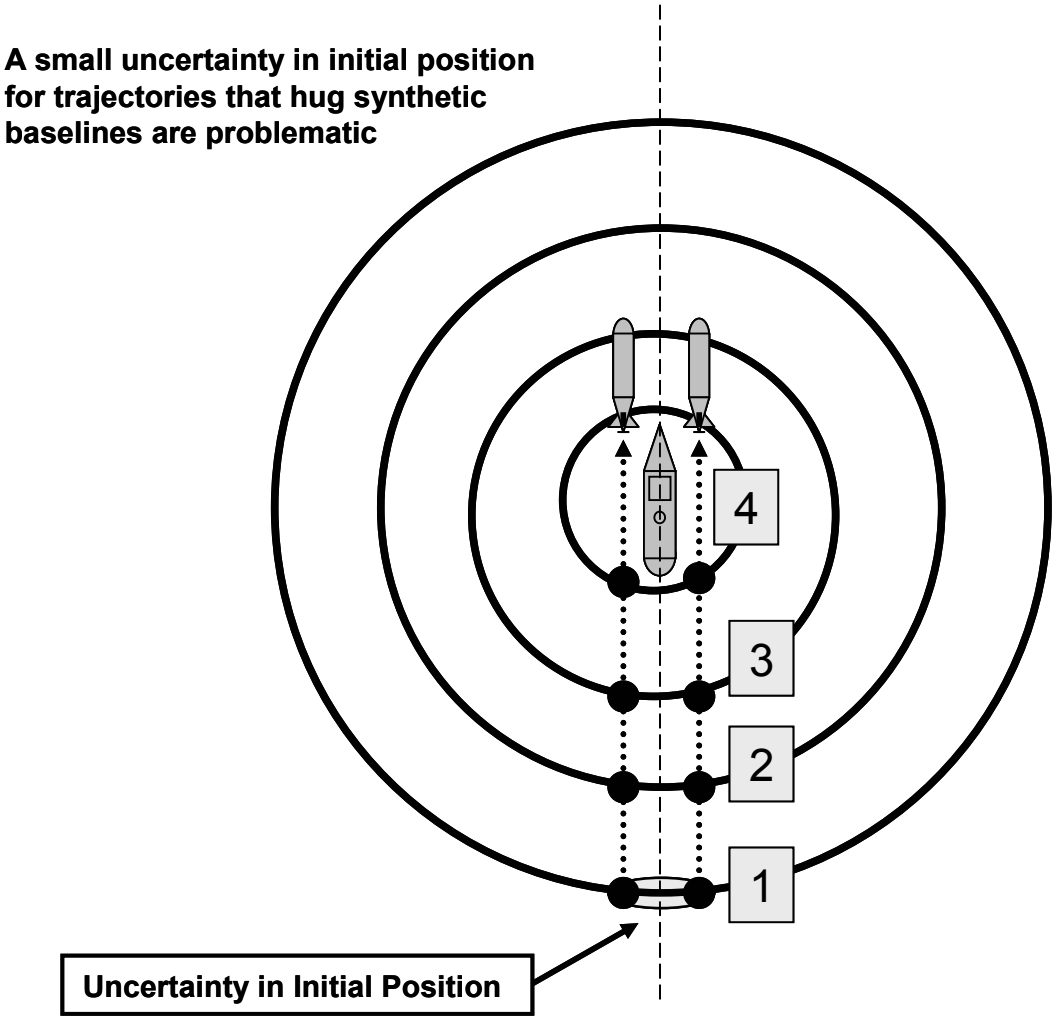

These small range variations at CPA are not enough to weigh one solution out as the winner. Therefore, the STRONG algorithm uses the results of a numerical simulation to find these zones of ambiguity for course correction (cross track) and replace them with something that can be observed – speed (along track). So, when the vehicle has a "down the throat" trajectory closing, or a similar opening aspect, the algorithm shifts to find any ADCP speed bias. Conversely, when the transponder is in the "waist" zone of the vehicle, the dead reckon initial position is used to rule out ambiguities and course is corrected (Figure 3.4). The corrections toggle between these two modes as the AUV changes heading and leaves the ranging platform at a different Angle-to-CMG (roughly analogous to a pseudo relative bearing ranging only from 0° - 180°, port or starboard side of the AUV). In Figure 3.4, the ship mounted transponder has an Angle-to-CMG of 20° relating the relative geometry between the closing AUV and its ranging transponder.

Figure 3.4
Zoned Corrections Based on AUV to Transponder Aspect

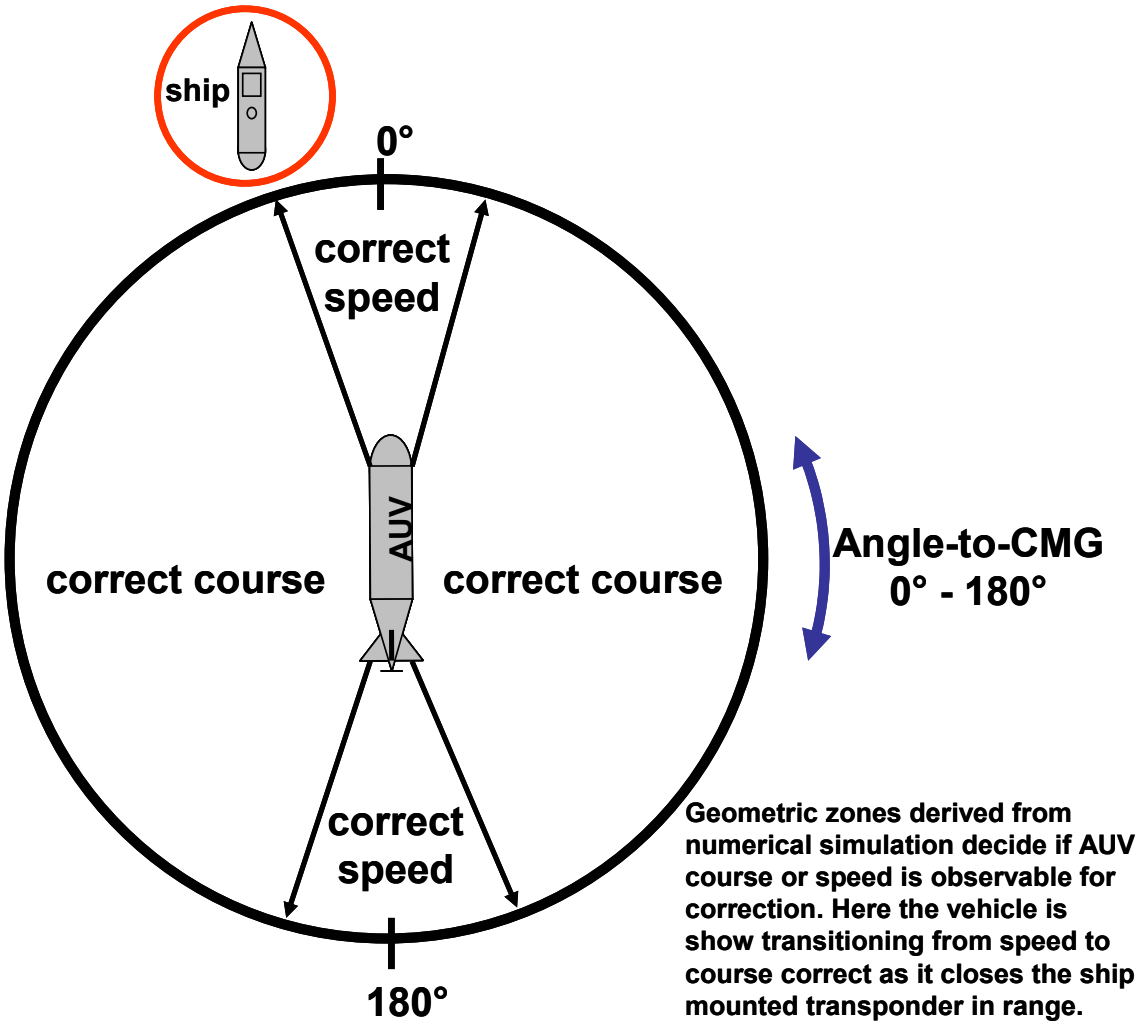

Geometric zones derived from numerical simulation decide if AUV course or speed is observable for correction. Here the vehicle is show transitioning from speed to course correct as it closes the ship mounted transponder in range.

Since REMUS only accepts positional input, these corrections would be used to update position with a fix. With a stationary ranging transponder, these zones can be thought of as based around the transponder vice the vehicle due to equal approximated reciprocal bearings (which is how they were originally conceived) (Figure 3.5). The small sub plot illustrates the range measurements that are least squared fitted by STRONG to the expected range vs. time trajectory to yield, in this case, the best speed estimate.

Figure 3.5
Zoned Corrections Transformed to a "Mowing the Lawn" Pattern

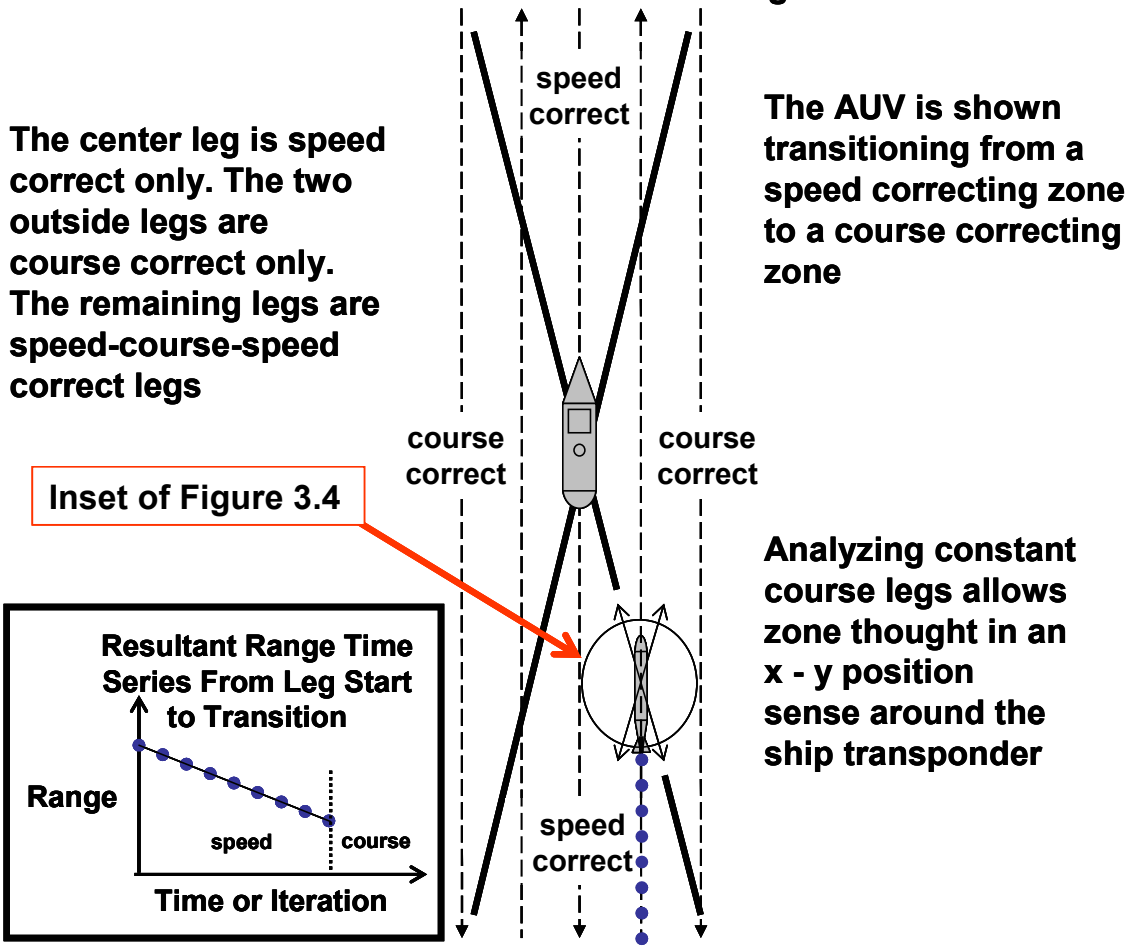

This visualization is easier to mentally picture when the AUV is mowing the lawn around a central transponder position. However, it is important to realize that the vehicle could, in concept, switch from course to speed correct geometry by simply turning to point the ranging transponder (here a ship). The Angle-to-CMG is approximated by calculating the angular offset between known transponder location (ship mounted with GPS) and vehicle dead reckon position.

The preceding discussion assumed that the ranging platform has no motion. However, STRONG corrects for a moving range transponder. In actuality a change in the motion of either the ranging platform or the AUV eliminates ambiguities. Submarine

target motion analysis (TMA) is based on this very principle. Assessing the change in target motion after a subsequent maneuver of the measuring platform specifies the solution like a key in a lock (Figure 3.6). A Fisher information matrix can be defined to rigorously mathematically prove what experience dictates (Song, 1999). This approach easily shows, for instance, that a constant bearing trajectory will not result in a cross track correction; however, STRONG would capitalize on this condition and sub plant an observable along track correction.

Figure 3.6
Relative Motion Maneuver Eliminating Ambiguities

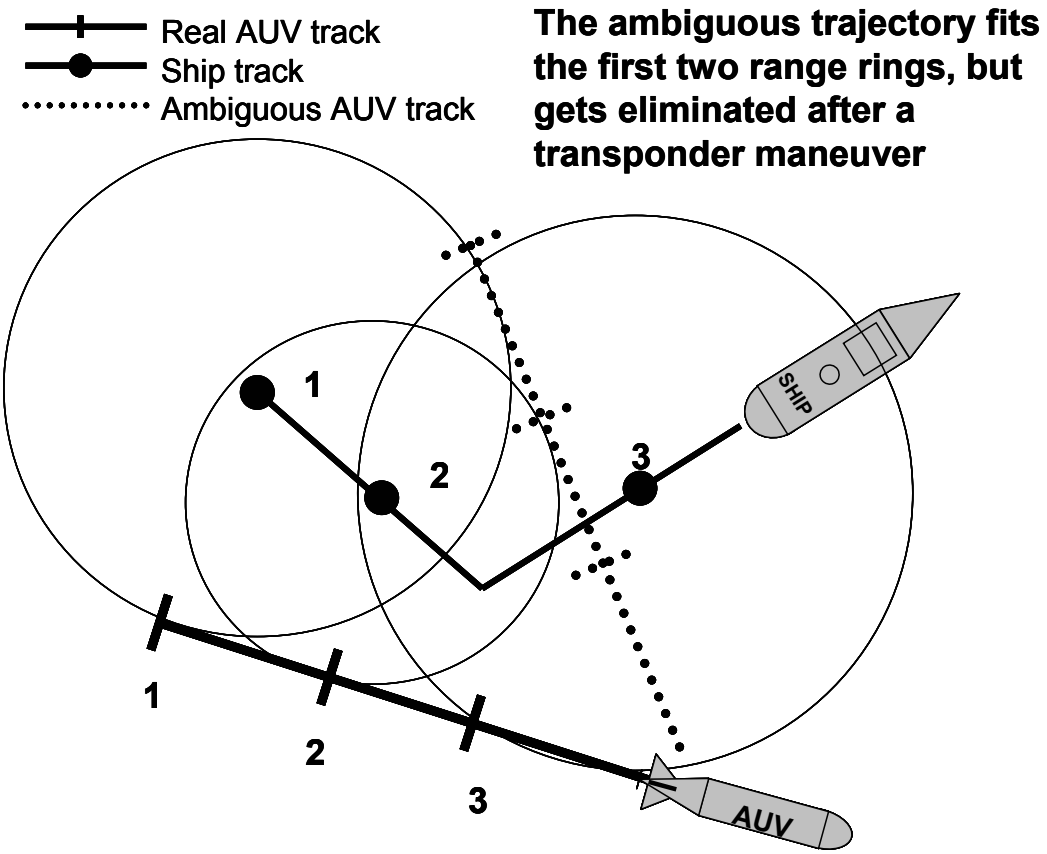

One of the great advantages of allowing the transponder to move is this relative motion convergence. Irregardless, with a zoned approach, dead reckon position is sufficient to determine the "macro" level starting point. Eliminating the "micro" variances of the starting position will be discussed later.

3.2 Vehicles

Single transponder navigation has been suggested for a number of different vehicles. As long as the vehicle can produce a reasonable dead reckon position and measure its orientation to the assumed frame of reference, Kalman filtering can weight the strength and weaknesses of the vehicle to give the best result. However, when the filter is dropped to reduce complexity, a vehicle must have enough sensor resolution to warrant simplifying assumptions.

The REMUS vehicles are good STRONG experimental work horses for many reasons. The STRONG algorithm was applied to data from two of the three REMUS open water vehicles (100 and 6000). The similarity of the vehicle architectures makes shifts from one to another seamless. Developed since the 1980's by the Ocean Sciences Laboratory, REMUS vehicles circle the globe, but they all share the same basic software to get things done. Whether REMUS 100, 600, or 6000, the user interfaces, data streams, and sensor integrations are nearly identical. Departure from the "one-of-a-kind" vehicle mentality benefits STRONG research allowing seamless migration between two different vehicle data sets and execution of experiments from Buzzards Bay to the Bahamas spanning water depths from 20 meters to 3300 meters.

The basic sensor requirements necessary to implement a STRONG single transponder routine at a minimum are:

1. Doppler velocity sonar (DVL)
2. Heading sensor (magnetic or inertial)
3. Accurate DVL integrated dead reckoning subroutine
4. Transponder interrogation for ship to vehicle ranging
5. Depth sensor
6. Ship board GPS
7. Acoustic modem (ship to vehicle communications)

The basic geometry requires an accurate DVL to provide a reliable short to moderate term velocity estimate. Vector DVL resolution of actual vehicle motion can be compared to compass heading to determine the "crab angle" offset between course over ground and steered course. With this assumed correct course and speed, the vehicle can be dead reckoned to advance a comparison position in the vehicle's brain. The only external data available to correct position errors is range to a known reference point. Slant range is determined with a ship board interrogation system that pulses the vehicle and gets a turn around reply. The spread spectrum range (Austin, 1994) accuracy of REMUS is essential since range inaccuracy translates to position uncertainty. Range is currently determined on board the ship with a REMUS Ranger circuitry and anchored to current GPS position. For position processing to eventually occur on board the vehicle, information must be sent in packets back to the vehicle via an acoustic modem. At a minimum, ship position must be sent via acoustic modem. Range determination could easily be shifted to the vehicle processor to unload the modem. For this proof of concept research, all vehicle and ship data was post processed iteratively to re-navigate vehicle fixes. Eventual real time integration will update vehicle position in a target tracking sense when the range data is spatially observable enough to produce a fix.

3.2.1 REMUS 100

The REMUS 100 is often generically referred to as "REMUS". It is the original, two man portable vehicle that was developed at the Woods Hole Oceanographic Institution and is commercially available through Hydroid, Inc. Specifications are listed in Table 3.1. The standard vehicle can sense pressure (depth), temperature, conductivity, ADCP current and bottom lock, optic light scatter, and carry side scan sonar. Over the years numerous special instruments have been fitted to the vehicle for special applications.

Table 3.1 REMUS 100 SPECIFICATIONS	
Vehicle Diameter	19 cm
Vehicle Length	160 cm
Weight in Air	37 kg
Maximum Operating Depth	100 meters
Endurance	22 hours at optimum speed of 1.5 m/s (3 knots) 8 hours at 2.5 m/s (5 knots)
Propulsion	Direct dive DC brushless motor to open three bladed propeller
Navigation	Long base line; Ultra short base line; Doppler assisted dead reckon; GPS
Transponders	20-30 kHz operating frequency range
Sensors Doppler Velocity Log	RDI 1.2 MHz up/down looking

The REMUS 100 has a 1:7 width to length ratio and a standard four fin posterior (Figure 3.7). The REMUS 100 is extremely modular. A sensor such as a camera can be inserted by removing the nose section and inserting a loaded cylinder that fairs with the body. The LBL transducer is chin mounted for optimum positioning with bottom mounted transponders. Hull shading doesn't appear to be a problem when ranging from the surface. A ranging device aptly called the REMUS Ranger is standard equipment that is used topside to range the vehicle, send acoustic commands, and receive modem messages from the vehicle. These signals are sent and received throw a streamline acoustic tow fish. Acoustic communications are done through a WHOI Micromodem developed by the Acoustic Communications Group. FSK data rates are on the order of 80 baud sending 32 kilobytes per transmission. The transmissions are a few seconds long and occur about every minute to pass vehicle data back to the operator. PSK developments could push the data rate as high as 5800 baud, but the current equipment can easily handle the requirements of this research.

Figure 3.7
REMUS FAMILY OF VEHICLES

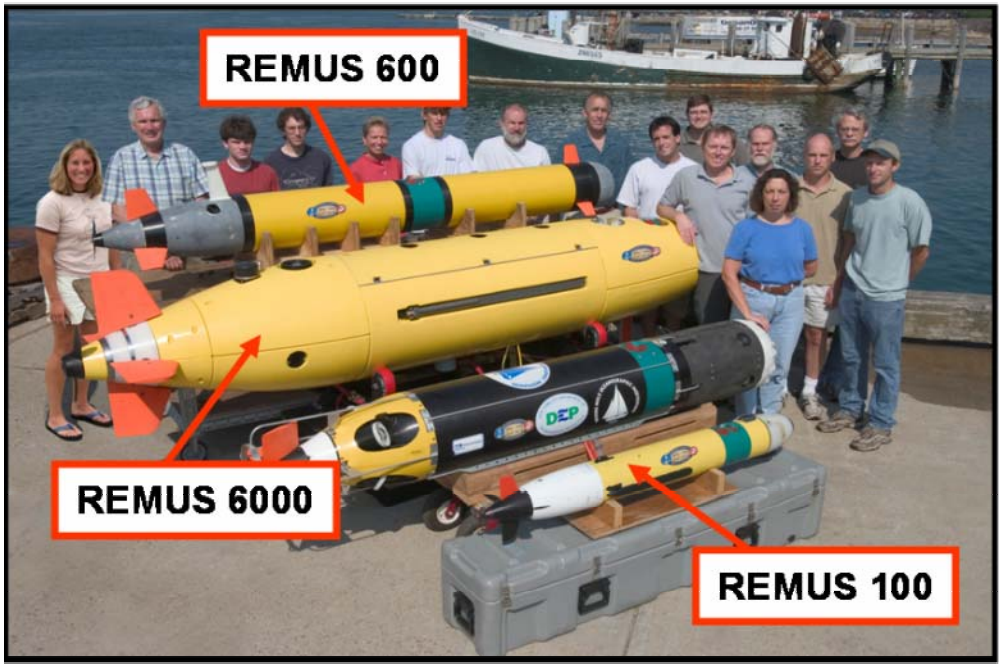

The time measurements for all ranges are done using spread spectrum processing. By coding the signals a wider bandwidth pulse in frequency can be sent at lower power levels. The signal can be accurately picked out of background noise and the narrow peak in the time domain allows travel times to be distinguished to a third of a millisecond or better (Austin, 1994). Increased accuracy and density of ranging data are highly desirable for a single ranging algorithm. The frequency of range data can be set close to the physical limits of sound speed, but environmental conditions can cause gaps or sparseness in the data set. The range data will be explored in greater detail in Chapter 4.

Navigation is done with long baseline, ultra-short baseline, and dead reckon navigation. Acoustic fixes are filtered to remove erroneous results. The dead reckon routine tracks two different vehicle positions. One dead reckon routine is initiated at time of launch and receives no resets in position. I refer to this position as the "Straight DR" in that it operates as if dead reckon was the only position routine despite available position fixing data. Another routine is influenced by fix information and will reset to a different

location if a given number of position updates suggest the vehicle is not where currently thought. I call this position “Influenced DR”. Straight DR is important because it represents the vehicle’s best guess of position if no acoustic fixes were available. Straight DR simulates on board vehicle position in the range only environment in which no LBL field would be laid. These DR positions are explored more thoroughly in the experimental set up of Chapter 4.

The REMUS user interface and data management software is user friendly and nearly identical for different vehicle variations. Mission planning is done in a very simple pseudo language format that is intuitive and concise. This plan is in the form of an initialization file that the vehicle executes while on the bottom. While the vehicle conducts the mission, it records oceanographic data for analysis. It also records all the parameters pertaining to its own condition from moment to moment. State parameters include dead reckon position, depth, heading, and crab angle. Data streams from the ADCP are recorded as well including velocity in three directions and heading. The moment to moment measurements are averaged and saved in approximate 1 to 3 second intervals. These data streams can be exported in a MATLAB or text format.

3.2.2 REMUS 600

REMUS commonality makes an introduction to a new vehicle easy since the heart of the machine is the same. The REMUS 600 (Figure 3.7) departs from the two man portable entering argument and uses its larger size for deeper depths and extended ranges (Table 3.2). The sensor payload is robust with room for more capable side scan sonars and cameras. The fin configuration is quite different from the rear traditional four fin configuration. The REMUS 600 prototype has six fins, three forward - three aft, in an attempt to provide more vehicle control in synthetic aperture sonar experiments. However, the vehicle can be configured with the more traditional fin configuration. The vehicle is highly modular and can be broken apart in sections quickly to roll in different sensors. REMUS 600 data was not processed for this research only because the vehicle

was busy with a myriad of developmental tests. Long transect testing will be done with the REMUS 600 and STRONG as vehicle time becomes available.

Table 3.2
REMUS 600 SPECIFICATIONS

Vehicle Diameter	32.4 cm
Vehicle Length	297 cm
Weight in Air	250 kg
Maximum Operating Depth	600 meters
Endurance	300+ km at 4 knots
Propulsion	Direct dive DC brushless motor to open two bladed propeller
Navigation	Long base line; Doppler assisted dead reckon; Kearfott INU; GPS
Transponders	20-30 kHz operating frequency range
Sensors Doppler Velocity Log	RDI 1.2 MHz up/down looking

3.2.3 REMUS 6000

The REMUS 6000 design has two fielded vehicles with extensive bottom time. The vehicle is larger to accommodate its impressive diving depth of 6000 meters (Figure 3.7). Endurance figures fall between the two shallower models (Table 3.3). Again most of the internal electronics are identical to the smaller cousins. The electronics housings are titanium and mounted within a titanium frame. The navigation transponders obviously have to be deep water capable, so commercial units are employed. The commercial units do not benefit from the spread spectrum accuracy of shallower models, but custom transponders are in the works. The surface ranger technology does use spread spectrum, so the STRONG range data set benefits from the extra accuracy discussed earlier. The vehicle surface antenna arrangement is advanced containing GPS, Iridium, and wireless connectivity. The Iridium allows satellite tracking with positions provided by satellite

phone on over the horizon recoveries. When within line of site, the vehicle comes up on the wireless network aboard ship. Mission data download can occur reliably before vehicle recovery.

Table 3.3
REMUS 6000 SPECIFICATIONS

Vehicle Diameter	66 cm
Vehicle Length	394 cm
Weight in Air	718 kg
Maximum Operating Depth	6000 meters
Endurance	12 hours at optimum speed of 2 m/s (4 knots)
Propulsion	Direct dive DC brushless motor to open two bladed propeller
Navigation	Long base line; Doppler assisted dead reckon; Kearfott INU; GPS
Transponders	7.5-16 kHz operating frequency range
Sensors Doppler Velocity Log	RDI 0.6 MHz down looking

3.3 Instrument Errors

As mentioned, REMUS vehicles have state of the art instrumentation. As with any measurement, there is error with every recorded value. The STRONG algorithm corrects errors in position generated by the cumulative errors of instruments. The instruments modeled and accounted for are the heading sensor and the speed sensor. These errors are considered first order and remaining errors such as in the measurement of depth and range are assumed second order and negligible. These assumptions are not made lightly and due consideration is given to the mitigation and quantification of the errors in question. Moreover, application of STRONG requires accuracy not normally needed in typical data logging to qualify as negligible. Measuring ranges through the water column required a little more research to prove how much inaccuracy would be incurred due to the ray trace bending of sound. Also, in deep water geometries very close to beneath the

ship, small errors in the range or the depth instrument can yield negatives under the square root in simple Pythagorean calculations. These errors are typical near "baseline" in traditional LBL and have this analog in the synthetic approach. The only way to minimize the error exclusion zones is to push the accuracy limits of the instrumentation. Although more work has to be done in this area, reasonable attempts were made to quantify these errors. Future calibration procedures are in development to squeeze all of the available accuracy out of the instrumentation.

3.3.1 Compass

The base REMUS 100 is equipped with a magnetic compass. The optional heading source for the REMUS 100 (and used exclusively on the 600 and 6000) is the Kearfott Inertial Measuring Unit (IMU). The magnetic compass is a TCM2-20 electronic compass manufactured by Precision Navigation Incorporated. The sensor is an electronically gimbaled, tri-axial magnetometer with an integral two-axis tilt sensor. The compass has an accuracy of +/- 1° when tilted and a resolution of 0.1°. When level and still, the instrument has an accuracy of +/- 0.5°. These specifications rely on the integrated tilt sensor which is an electrolytic device that measure the slope of an alcohol based salt solution contained in a small dome. The slope of the solution is measured by detecting the range of resistance in three wires caused by the electrolytic solution moving up and down on them as the sensor is tilted. The tilt limits of +/- 20° would rarely be reached. The tilt sensor is also affected by any acceleration forces experienced by the vehicle. The coupling of theses forces by the compass yields small random errors in heading. As a result, the compass has an undesirable "hunting" behavior. To mitigate this affect, a yaw rate sensor is integrated into the vehicle.

The yaw rate sensor is a QRS14-00100-103 solid-state inertial sensor manufactured by BEI Systron Donner Inertial Division. The sensor measures the vehicle's angular rate in yaw and is used to stabilize the dynamic errors of the heading sensor. This yaw rate sensor uses a vibrating quartz tuning fork to conduct its

measurement and has a component footprint smaller than a quarter. The combination of the two instruments has never been assessed by REMUS engineers for an overall accuracy. Since the magnetic compass requires the vehicle to complete a calibration circle on the surface, a poor calibration could exceed this level of accuracy. In operational experience the vehicle often exhibits a larger compass error in a certain direction due to magnetic heading deviation. A software routine compares reciprocal headings and compensates for this effect when LBL fixes are available to ground truth the heading source. In any event, a 0.5° error over a typical 1500 meter leg yields over 13 meters of cross error so even the best of magnetic course errors are first order and need correction.

The Kearfott heading source can be much more accurate and stable. The original noise modeling of STRONG was done by approximating the error of this inertial sensor. The Kearfott IMU has been used extensively in aviation and has now found a successful market in AUV navigation. Although a Kearfott has been integrated with REMUS for several years, no dedicated study has been performed to assess its performance in heading or position. Since STRONG provides a position by integrating out errors in heading and speed, only the heading output of the inertial sensor is questioned in this research. An in depth comparison of the synergy between a STRONG algorithm feeding an inertial unit's Kalman filtering routines would be interesting. Meaningful comparisons of parameters were not available since REMUS Kearfott integration is still largely in a developmental stage. Since the machine is essentially a "black box" that takes input and returns position, the sensor has often been blindly used to provide heading or position.

The Kearfott IMU is a three-axis ring laser gyro with accelerometers that sense vehicle motion in angle and direction updating position based on that movement. The system has a filtering routine that weighs fix input by both time and accuracy combining the twice integrated acceleration with the external position information to return a best position. The inertial unit is about the size of a coffee can with modest electronics. REMUS 6000 has a more advanced build in which the Kearfott IMU has been integrated inside an ADCP housing. Done for space considerations, this arrangement efficiently provides two compact navigation devices in the space of one. REMUS 100 and 600 use

the T-16 IMU while the REMUS 6000 combination unit utilizes a T-24 IMU. The ring laser gyro is a one dither instrument with three orthogonal axes. Each gyro uses two lasers traveling in opposite directions around a square mirror box to meet in a diffraction fringe pattern. Angular motion about the axis normal to laser motion causes one beam to arrive faster and the other slower changing the diffraction pattern based on the beam frequency differences. Since the laser beams are spawned from the same device, there is a "lock on" region at low rotations in which a false frequency is predicted. A "dither" mechanism is used to angularly vibrate the mechanism in a tight Gaussian manner to disrupt the false convergence. The model number of 16 and 24 depict the laser path lengths around the square in centimeters. As a navigator, the T-16 and T-24 show an approximate 0.15 NM and 0.08 NM estimated position errors respectively after a 1000 foot dive and transition into ADCP bottom lock after about two hours. Since STRONG produces a position with the aid of the IMU as a highly accurate compass, the heading errors are more illustrative. In the same dive to 1000 feet and post 90° maneuver, the T-16 and T-24 showed heading errors of 3 milrad and 0.5 milrad over the same two hour period (Alameda, 2002).

Basic application of the course error to a typical 1500 meter REMUS leg yields a basic cross track error for both heading sources. At the magnetic compass error of 0.5°, the cross track error at the end of the leg would be over 13 meters per leg. Allowing conservative Kearfott heading errors of 0.05°/hour (T-16) and 0.01°/hour (T-24), one leg at 2 m/s would yield about 0.3 meters and 0.05 meters of cross track error per leg respectively. This error would obviously be cumulative and combine with any uncorrected speed errors to be an error of uncertainty that does not grow as a circle. Although no usable long term leg to leg data was collected with an inertial compassed vehicle, the traditional magnetic directed vehicle saw higher cross track errors than this prediction. One would infer from the rough calculations that a Kearfott guided vehicle would have many more opportunities for compass correction in a mow-the-lawn scenario than needed. Additionally, long transects could require very infrequent CPA maneuvers to correct course since the heading source is very stable.

3.3.2 Doppler Velocity Log (DVL)

The DVL is an essential part to any dead reckon AUV navigation routine. Before reliable compact systems were available for vehicles, dead reckon speed was measured in various ways. Modern nuclear submarines still use electromagnetic logs that measure the movement of the water dipole transiting through an induced magnetic field. Although the system is reliable and stealthy, it only sees water movement and cannot distinguish between vehicle motion and currents or tug wash. Many AUV's use their best guess for movement with each propeller stroke and updated position based on time spent at given shaft revolutions. Again, this is an approximate speed through the water and not over ground.

The DVL echo sounds off particles to determine relative motion based on the Doppler phase shift of the returned acoustic energy. If the binned ensonification areas include the ocean floor, the motion difference is between vehicle and the earth and becomes over ground motion. The 1000 foot dive of the DVL/Kearfott combination in the previous section highlighted a gap in DVL sensor data since the instrument was obviously out of bottom lock on the decent. Although the DVL can be tuned to retain bottom lock to deeper depths, the resolution suffers; hence, military submarines often find the water depth too deep for such a system.

The RD Instruments Workhorse Navigator is the gold standard for measuring movement over the ocean bottom. It is compact and accurate with a well characterized error growth. REMUS vehicles store the altitude and three axial motion output of the instrument and generically label the device as an "ADCP" referring to its original intended use. REMUS dead reckon routines combine the best heading source and the DVL speed to update position. An offset heading is steered that compensates for the difference between "course over ground" and vehicle head in cross current situations. This arrangement works well if enough forward motion is available to balance the vehicle dynamics with vehicle reaction times. In very slow speeds or station keeping, an upward looking profiler would be useful to predict currents and react to them vice infer them

from resolved DVL motion and steered course. REMUS and STRONG operations are typically done at 2 m/s so reduced speed maneuverability is only approached in very tight turns that are quickly overcome.

STRONG geometry is weighted to favor ADCP speed measurement. As has been seen in the previous geometry sections, ADCP speed is corrected is a little more than one leg out of ten in a typical 1500 meter by 1500 meter square search area. This geometry was driven by a Monte Carlo simulation to be discussed later, but it is suffice to say that cross track correction is observable at many more vehicle positions than speed correction in a typical mow the lawn scenario. This yields an area of uncertainty that grows elongated at the head and tail of the vehicle since cross track error is robustly corrected. The limiting question becomes whether or not the vehicle can wait for a speed correction in its normal course of motion in such a survey. It is true that the vehicle can alter track and drive toward and away the ranging platform to do a speed correction any time it is deemed necessary, but an optimum situation would be one in which the corrections are obtained in the normal motions of the survey. Assuming a 100 meter lane spacing with 1500 meter legs, approximately 7500 meters of straight line travel would be covered before the next opportunity to speed correct. The correction would surely be completed by 9750 meters as the vehicle passed with minimum CPA to the transponder. Applying a reasonable 0.2% of distance traveled DVL error, along track error is expected to accrue at approximately 3 meters per leg. Hence, the theoretical along track error would be about 15 meters at the first natural opportunity for correction and at about 20 meters when a correction is certain. Radial position errors in actual experiment showed at least an order of magnitude lower along track error, and this particular example is obviously void if the search geometry is altered or the ranging platform moved. The usefulness of this exercise is to illustrate that although the compass has more drift, it also has more opportunity for natural correction; therefore, ADCP/DVL error often becomes the limiting error. This line of thinking also becomes a starting point to discuss “wise” ship maneuvers in any virtual tow scenario**.**

3.3.3 Depth Sensor

REMUS utilizes a Paroscientific quartz crystal depth sensor. The model corresponds to the depth rating of the sensor to utilize the extra sensitivity in shallower waters. The REMUS 6000 transducer is capable of 7000 meter depths and quotes a 0.01% of full scale error pressure reading or about 0.7 decibars. The quartz substructure of the sensor yields little hysteresis and shows negligible drift with nearly unlimited cycles. In the deep experiments, the depth transducer accuracy becomes an issue. In geometries where the slant range is nearly the depth of the vehicle, errors in the depth instrument are problematic. The full scale accuracy quoted by Paroscientific can be misleading since the most significant source of depth error can be in the conversion from pressure to depth in meters. The conversion can be found in the Paroscientific application notes found at their website and can be calculated with certain MATLAB tool boxes. These calculations assume a standard ocean and correct for the change in acceleration due to gravity that varies with latitude. The most exact equation can be found in the UNESCO 1983 report.

$$depth = \frac{C_1 P + C_2 P^2 + C_3 P^3 + C_4 P^4}{g(\phi) + \frac{1}{2}\gamma P} + \frac{\Delta D}{9.8}$$

Where P is the pressure in decibars, the C's and γ are determined constants, $g(\phi)$ is the standard gravitational correction for latitude (θ).

$$g(\phi) = 9.780318(1.0 + 5.2788x10^{-3}\sin^2\theta + 2.36x10^{-5}\sin^4\theta)$$

The $\frac{\Delta D}{9.8}$ term is the correction for the geopotential anomaly and the deviation from the standard ocean. Paroscientific does not allow for this ocean parameter correction, but it is not a large term with a maximum variance of 2 meters at REMUS 6000 depths. Straight

forward methods are available to account for this smaller portion of the error by combining pressure sensor measurements with a density profile estimate, atmospheric pressure, and tidal water measurements. The salinity effect on the density profile is determined using the Practical Salinity Scale (1978) and the standard ocean can be transformed into the local ocean (Jalving, 1999).

The maximum deviation in gravity from the pole to the equator equates to about 80 meters of potential error at REMUS 6000 depths and is the major depth correction considered in this research. The STRONG deep data set was taken at the very early part of the research, so the geometrical depth sensitivity was not anticipated. Additionally, the position of the ship while collecting data in over 3400 meters of water was not sufficiently deviated from the vehicle's track making most legs speed correct legs. Processing after considering the details showed that the REMUS depth calculation was incorrect. Recalculating the data at varying depths with the Paroscientific correction showed readings at 3500 meters to be about 33 meters too deep. At maximum depth the recorded value was off by as much as 100 meters. This error was uncorrected because this level accuracy was unnecessary in most applications. Using the thumbrule that 1 decibar = 1 meters is in itself good to 2/3%. At any rate, the deep data set required trial and error to fit the known trajectory. The empirically determined errors, such as this depth error, were compared to instrument accuracies in way of explanation. This depth recording anomaly did account for a large part of the error, but issues remain that will be discussed in more detail later. Likewise, the error can just as easily be in the slant range measurements. The equivalent error in range equates to about 7 miliseconds of unaccounted for delay time which is not unthinkable since manually inputted turnaround times can be as high as 50 miliseconds to allow for vehicle processing. Experiments are underway to determine the delay turnaround to an accuracy level not previously needed. As would be expected, the shallow data sets are free of such problems because of better geometry. To master deep water applications with near ship geometry, more data must be analyzed. Otherwise, an exclusion zone is present under the foot print of the surface ship

that has a radius linearly proportional to water depth. Better understanding and calibration of on board instrumentation are key to maximizing correction in deep water.

3.4 Geometric Errors

Although the geometric errors have been hinted at, they need to be briefly organized for the sake of formality. The x-y plane ambiguity associated with synthetic baselines is a consideration in any water depth. The near-ship, deep-water error is certainly of concern when in the realm of REMUS 600 and 6000 operations. Initial position errors have been discussed when applicable to baseline considerations (Figure 3.3). Initial position errors can be of consequence when considering the starting initial condition of a STRONG fix data period. Finally, although not a geometric error per se, the importance of relative motion for convergence must be explored.

3.4.1 Baseline Considerations

The discussion associated with Figure 3.3 explains the basic mechanics of a near synthetic baseline error, but does little to explore the associated ramifications. Once the vehicle is navigating, the fix to fix error should not sufficiently grow to make this near baseline effect a show stopper. Since the speed zone effectively removes the near baseline problem zone (Figures 3.4 and 3.5), the problem is attenuated. In a very deep scenario, one could envision the growth of a very large error on the initial decent. Whatever the reason, some course check must guard against an unintentional migration to the wrong side of the baseline. Inertial position or pure dead reckon should be sufficient to prevent such a gross error.

3.4.2 Initial Position

Initial position is an important parameter for STRONG since an error in the start position can often lead to an error in the ending position. The magnitude of the error is likewise important. Upon initial decent, the error can be quite large. Fix to fix errors are much smaller and easier to remove. The basic approach is to least squares fit the bottom range data. The initial position is then sequentially perturbed to find which starting point yields the best fit. Although simplistic, this numerical approach can yield quick convergence depending on the coarseness and scope of the search which drive the number of iterations.

STRONG navigation in the descent is not possible since the DVL/ADCP will not be in bottom lock. A possible solution would be to initialize with an inertial position if equipped. Previously quoted research (Alameda, 2002) shows that a dive to around 300 meters can yield position errors on the order of a few hundred meters. A streamlined vehicle with a drop weight augmented decent rate such as the REMUS 6000 (approx 47 meters/min decent rate) can reach 3000 meters in about an hour. The question becomes: will water column currents perturb vehicle position more than inertial drift? The answer has not been sufficiently researched to provide a definitive answer, but the jump from surface GPS position to bottom LBL track on four Bahamas' dives to around 3300 meters yielded an average horizontal position error of about 7% of water depth or about 230 meters. However, these numbers are obviously environment dependent. So, a simple comparison, in this case, indicates that it may be prudent to initialize the STRONG algorithm with the surface GPS position vice an inertial one. Likewise, the vehicle should navigate in a direction with observable correction, i.e. the ship not shadowing overhead, and STRONG should conduct a coarse perturbation of the initial condition to find the best fit of the data. These actions are no big stretch since the vehicle will most likely drive away from the ship for a DVL/ADCP calibration once in bottom lock. Likewise, the STRONG approach "wiggles" the initial condition from fix to fix to obtain the best data fit, as will be explained in more detail in subsequent chapters – the starting point after

decent is very similar, just larger. Potential alternatives with existing technology are to survey in the vehicle while moored on the decent weight or start operations from and LBL field, both of which are undesirable. One possible solution would be to maneuver above the vehicle as it descends using the measured ranges to correct position. As before, REMUS 100 operations are immune from such considerations since the short decent from a GPS position yields a much smaller error.

As stated, the initial position on each STRONG fix leg should be "wiggled" to remove any bias error that may grow over time. A simple geometric argument shows how an error in initial position could yield an error in final position (Figure 3.8).

Figure 3.8
Translation of Initial Position Error to Fix Error

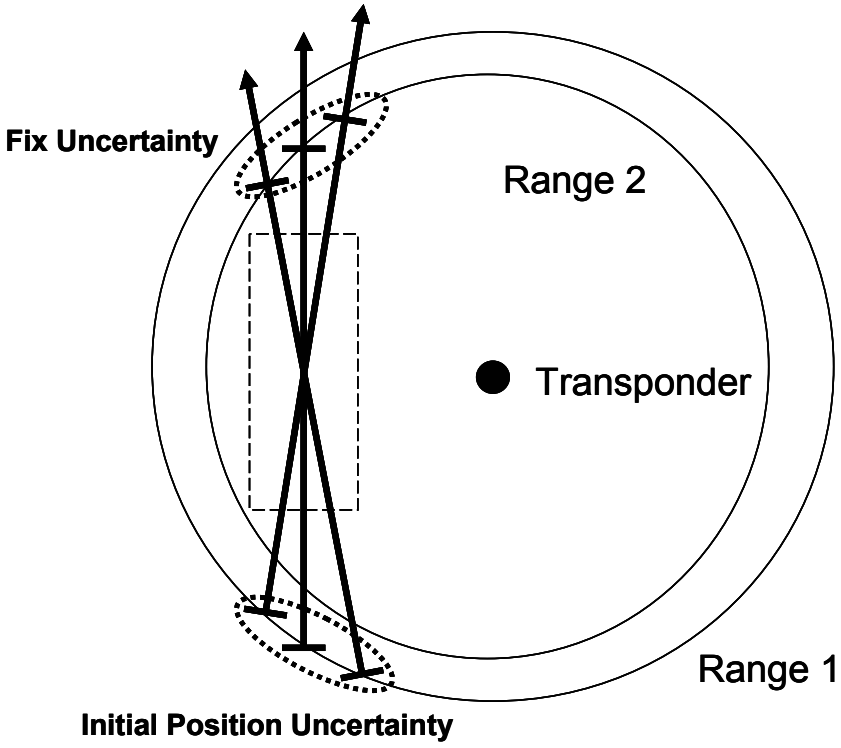

Failure to remove the initial position error will yield fix uncertainty. The dashed rectangle has limited ability to provide precise solution discrimination.

Although greatly exaggerated, the figure shows how two range measurements about a transponder can translate an initial position error into a fix uncertainty. In practice, fixes in the dashed rectangle would help discriminate between the three possible trajectories. As drawn, the solution would be impossible since the fitted trajectory could be rotated 360° around the transponder with every direction possible. Even with the added ranges in the rectangle, two identical solutions are still possible as discussed in previous sections (Figure 3.2). However, dead reckon position is sufficient to eliminate the outlying possibilities. That leaves only the small uncertainty in summing the fit errors of the two dashed ellipses and the dashed rectangle. STRONG's positional accuracy was largely dependent on finding the initial trajectory guess and perturbing the starting position to get the best fit. This approach is exactly analogous to what one would do manually to fit a constant length speed template between two or more range rings. Given data in all three areas, you would "float" the start point and adjust the trajectory to put speed ticks on subsequent circles. Your eye would integrate out any Gaussian noise in the measurements and arrive at a best fit. In the typical scale of AUV work, STRONG would arrive at a fix numerous times before the vehicle traveled through CPA to the transponder, thus eliminating some of the symmetry that exaggerates this example. However, since this geometry can be troublesome and limiting, the STRONG REMUS experimental layout was similar to this depiction. The nature of the initial condition in all experiments was explored by plotting the perturbed x – y starting position versus an average FIT VALUE to produce a "wiggle surface" that helps to illustrate the issue. The resultant plot becomes a bowl with a best fit minimum. Obviously, when this perturbing process is implemented into the final algorithm, the granularity and radial scope of the perturbation will have to balance optimum precision with run time.

3.4.3 Deep Water

REMUS 6000 operations could potentially occur at 6000 meters, but routinely happen in 3000 meters. Errors in range measurements and depth measurements have been

quantified but their affect on operations needs to be considered. Some errors scale with depth. Failure to properly model the sound speed or the vehicle advance during range measurements are pronounced at deep depths. The previously mentioned REMUS depth error was scalable deviating a negligible amount for REMUS 100 operations, but significantly in the REMUS 6000's realm. Errors in depth pressure measurement or the ranging turnaround delay are a straight bias that is the same at any depth. The cumulative experience of REMUS 100 operations allows one to deduce that no huge straight bias errors exist in range measurements. Since the vehicle is ranged frequently when on the surface with GPS, the measured ranges are certainly within a few meters (more likely less than one meter). It is safe to say that a straight bias error of 20 meters or more would be painfully obvious and long since corrected. Therefore, it is a reasonable assumption that most of the error is scalable.

An exclusion zone to prevent imaginary results in LBL navigation is nothing new and is employed in traditional REMUS operations. A 100 meter zone off baseline is geometrically off limits for three reasons in traditional REMUS LBL. First, the two nearly tangent circles cross at such a shallow angle that any range error results in a magnified position error. Second, the potential of no solution exist when the two ranges do not sum to a distance equal to the baseline. This error may be due to inaccurate ranges, or due to error in placement of the transponders. Irregardless of the reason, the undesirable effect is the same. Finally, as discussed at length, operation near the baseline puts the mirror solution close enough for positional confusion. Shifting to synthetic baselines in deep water has similar unwanted effects. The near baseline positional confusion is the same. The no solution case does not manifest in the same manner, but imaginary results are possible if the slant range hypotenuse comes up shorter than the vehicle's depth minus transducer depth. This problem can come from a slant range error, a depth error, or an unfortunate combination of both. Certainly, imaginary results can be filtered out, but a geometric derivation can put some limits on this exclusion zone so results can be ignored when underneath the ship (Figure 3.9).

Figure 3.9
Near Ship Geometry Errors

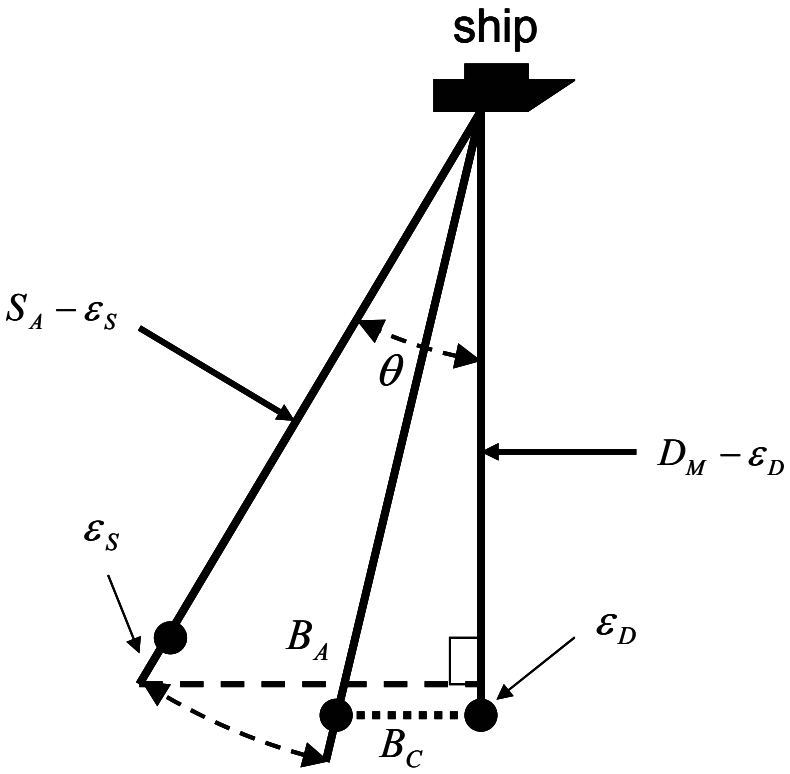

Parameters for vertical geometry are defined to explore errors in deep water beneath the ship

The measured depth is given by D_M which deviates from the actual depth D_A by a subtractive error ε_D. The actual slant range measurement is given by S_A and differs from the measured slant range S_m by a subtractive error ε_S. The errors are chosen with signs that are most restrictive. The actual bottom range and the resultant calculated bottom range are given by B_A and B_C respectively. The goal is to derive the effective bottom range and angle θ outside which a Gaussian deviation of range and depth measurements will return a minimum of imaginary results.

$$S_A = \sqrt{D_A^2 + B_A^2} = S_M + \varepsilon_S$$

$$D_A = D_M - \varepsilon_D$$

Rearranging and substituting,

$$B_A = \sqrt{(S_M + \varepsilon_S)^2 - (D_M - \varepsilon_D)^2}$$

Solving for the angle θ,

$$\theta = \sin^{-1}\left[\frac{B_A}{S_A}\right] = \sin^{-1}\left[\frac{\sqrt{(S_M + \varepsilon_S)^2 - (D_M - \varepsilon_D)^2}}{S_M + \varepsilon_S}\right]$$

Realizing that the limiting case is at zero angle with $S_M = D_M$, the equations become,

$$B_{\text{lim}iting} = \sqrt{(D_M + \varepsilon_S)^2 - (D_M - \varepsilon_D)^2}$$

$$\theta_{\text{lim}iting} = \sin^{-1}\left[\frac{\sqrt{(D_M + \varepsilon_S)^2 - (D_M - \varepsilon_D)^2}}{D_M + \varepsilon_S}\right]$$

Outside this bottom range, imaginary results are not likely if the error parameters are estimated with a good degree of reality. If you assume that the largest contributor to the slant range measurement is a linearly scalable sound speed error, and that the depth correction can also be approximated as a linear function of depth, then an illustrative assumption can be made. The REMUS depth correction mention earlier was not linear

but could be reasonably approximated as such over 6000 meters. The equation then becomes,

$$B_{\lim iting} = \sqrt{(D_M(1+R_S))^2 - (D_M(1-R_D))^2}$$

where,

$$R_S = \frac{\varepsilon_S}{D_M} \quad \text{and} \quad R_D = \frac{\varepsilon_D}{D_M}$$

If these ratios are treated as constant scale factors assumed to apply through all depths, a rudimentary plot can show how $B_{\lim iting}(D_M)$ restricts operations (Figure 3.10). Future careful calibration can determine the exact nature of the error depth, fit the curves better, and strive to limit this exclusion zone. However, this fact should be obvious, since perfectly calibrate instruments would have no exclusions. Figure 3.10 shows clearly that only a one percent scalable error in depth and range is unacceptable yielding an exclusion zone of radius 1200 meters at full vehicle depth. However, a tenth of a percent of error is much better resolving at a maximum of 75 meters exclusion. The goal zone assumes that through calibration one can eventually measure slant range to 6 meters and depth to 0.6 meters at full depth. This reasonable post calibration goal allows for significant Gaussian deviation and results in a radial exclusion zone on the order of 3 meters.

Figure 3.10
Exclusion Zone Size Comparison

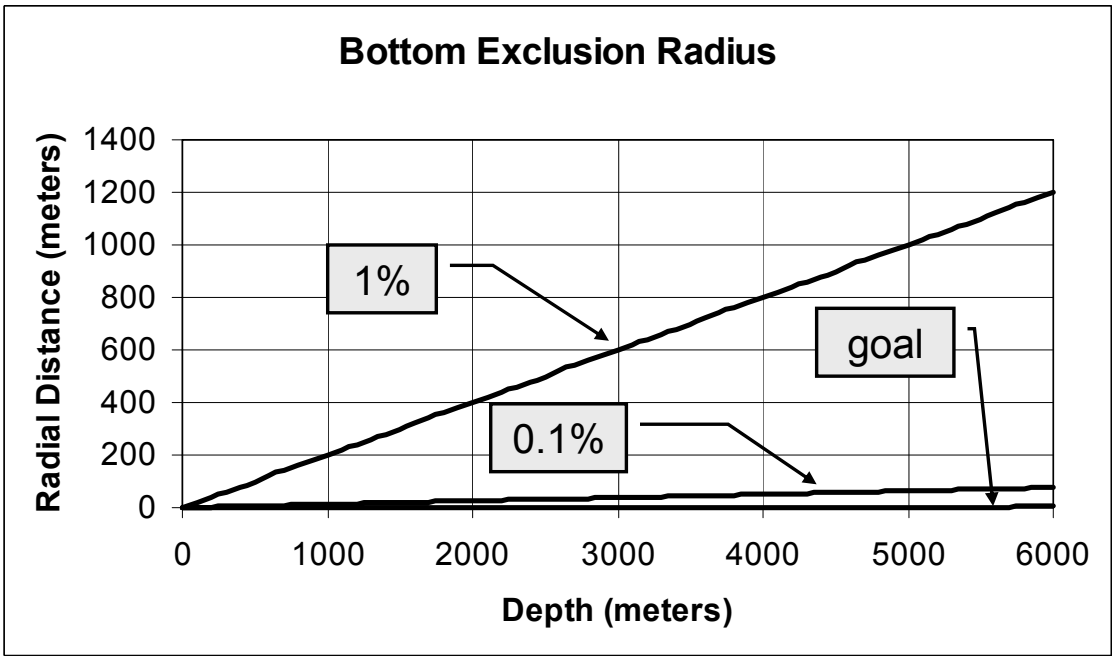

Exclusion zone radius with increasing water depth. Operations outside this zone minimize the likelihood of imaginary results with simple Gaussian errors. The 1% and 0.1% curves show the radii if the errors in depth and range scale as a percentage of depth. The "goal" curve shows the exclusion zone for slant ranges measured to 6 meters and depths measured to 0.6 meters in 6000 meters of ocean depth.

The final consideration of depth related error concerns how the depth measurement subtends the arc of the range measurement. Hence, although the vehicle might easily be outside exclusion zone to prevent imaginary results, small errors in range and depth close to the shadow of the ranging platform yield larger errors than ones farther a field. If the depth-range plane is examined and the assumption is made that the range wave fronts are nearly linear over the small depth error, an approximate geometry can be defined (Figure 3.11).

Figure 3.11
Geometric Dilution of Accuracy in Deep Geometry

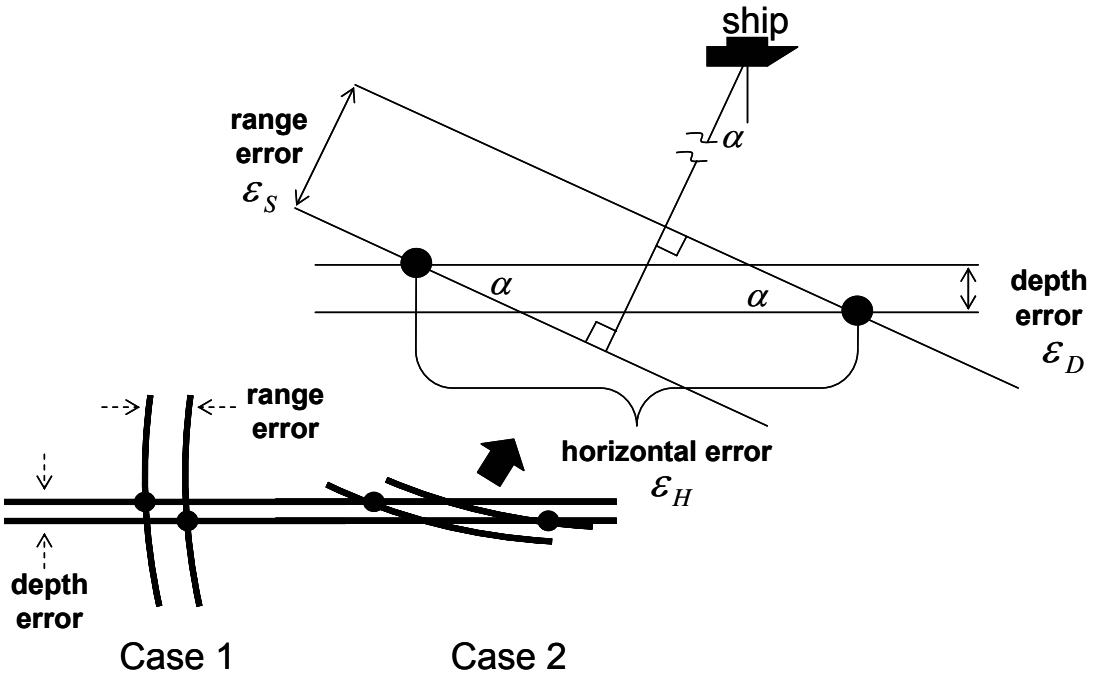

Two different cases illustrate how errors in depth and slant range measurements combine to form a variable horizontal error that exponentially increases beneath the footprint of the ship

The lower left diagram demonstrates how the horizontal range error at α 's approaching 90° is just the slant range error ε_S (Case 1). However, as the angle becomes small, the horizontal range error becomes greater than the sum of ε_S and ε_D (Case 2). The horizontal error ε_H is given by,

$$\varepsilon_H = \frac{\varepsilon_S}{\sin\alpha} + \frac{\varepsilon_D}{\tan\alpha}$$

Making the same somewhat simplified linear error assumptions concerning depth,

$$\varepsilon_H = \frac{R_S D_M}{\sin\alpha} + \frac{R_D D_M}{\tan\alpha}$$

Assuming the goal zone from Figure 3.10, the curves at two different depths are plotted (Figure 3.12). As can be seen in the equation, the solution blows up near the origin as the geometry equates to parallel lines and not triangles. The curves are truncated at the bottom range and depth at which the slant range exceeds 10,000 meters, the published range limit of REMUS 6000 operations. One can imagine that REMUS 100 shallow operations would display negligible error on such a plot at all but the origin. However, if slant range can only be calibration to 6 meters and depth to 0.6 meters, the area of uncertainty around vehicle position will be less than 20 meters if you stand off from the vehicle for at least 2000 meters of bottom range. Therefore, based on this affect, a usable radial range zone for sub 20 meter accuracy would be from 2000 meters to over 8000 meters. Conversely, restricting operations to 3000 meters yields 5 – 10 meter accuracy for a radial zone between 1000 and nearly 10,000 meters. Of course, better calibration and shallower depths equal more usable correction area. The previously mentioned exclusion zone error that occurs when the right triangle is not longer a right triangle is often eclipsed by this related affect since operations tend toward the right on the curves.

Figure 3.12
Geometric Dilution of Accuracy Plot

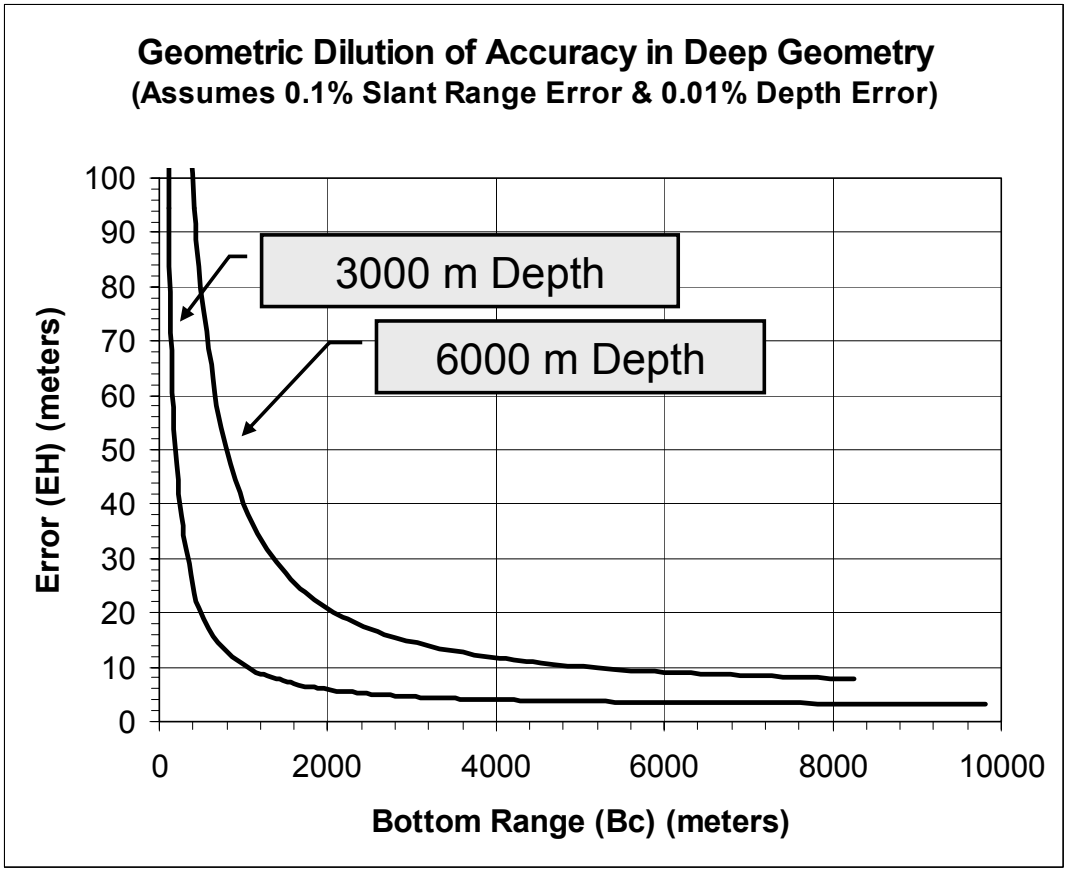

Small instrument errors in slant range and depth geometrically combine to produce an exponentially increasing area of uncertainty beneath the ship. Assuming these errors scale with depth, the curves show the best expected STRONG accuracy for an AUV position in depth and bottom range.

3.5 Sound Velocity Errors

Assuming ray theory, sound path lines from a surface transponder bend based on the sound velocity profile (SVP). The amount of bending is also dependent on how much vertical and horizontal distance sound travels in any only radial direction between source and receiver. Operations with bottom mounted transponders or shallow vehicles require no correction since the horizontal range is much greater than the depth difference

between vehicle and transponder. Mathematics for the deep case are well understood, but the calculations are numerically lengthy and cumbersome resulting in the identification of likely eigenrays. The goal in the case of STRONG is to do as before and decide if a simpler and faster approximation is warranted within the operational space of REMUS.

3.5.1 Ray Bending Model

Since STRONG will use a single ship mounted transponder, exact time measurements must be made and converted to ranges. The model assumes the maximum REMUS 6000 acoustic range of 10 kilometers, a historical Bahaman SVP, and a maximum depth of 5000 meters. With such long slant ranges, one might expect that ray bending will have some effect on the measured travel time, and hence, the measured range (Figure 3.13). The ray trace program aptly named "RAY" developed by Woods Hole Oceanographic Institution Scientist Jim Bowlin was employed to numerically explore the model space. RAY was run at iterative slant ranges and the resultant horizontal bottom ranges were compared to approximations considered for STRONG. Although the choice between the two approximation methods could have been surmised from experience alone, this exercise helped bound the expected error and determine if any approximation was warranted.

Figure 3.13
Horizontal Range Error from Sound Speed Error

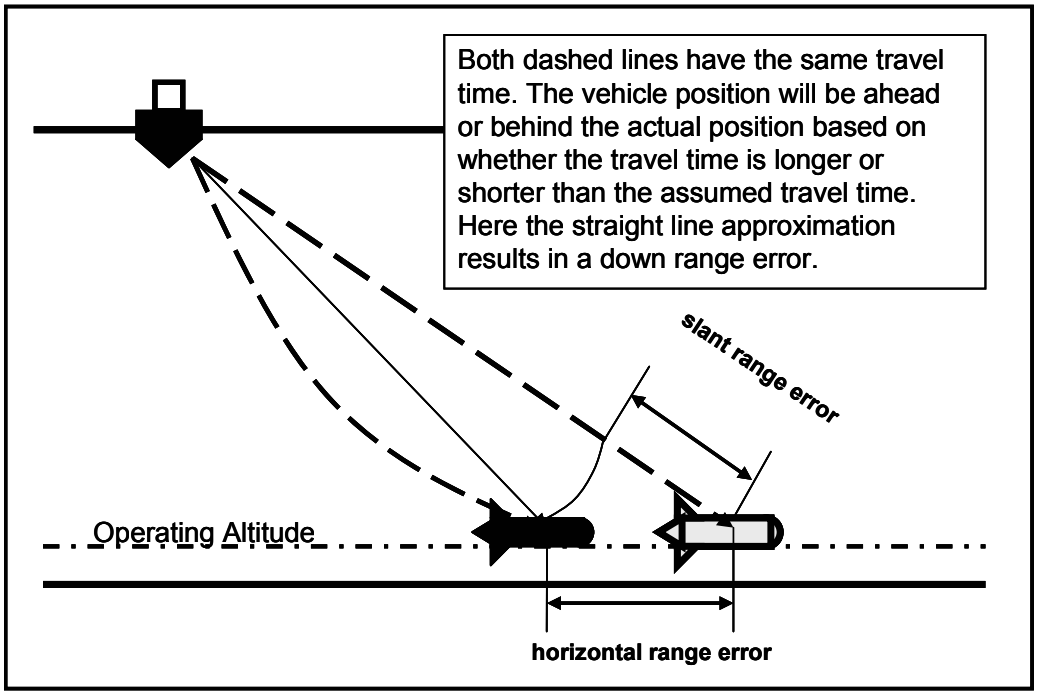

3.5.2 Bahaman Case Study

A single summer sound velocity profile was chosen as a precursor to REMUS 6000 operations in the Bahamas (Figure 3.14). The chosen water depth was 5060 meters with a 60 meter operating altitude. The ship transponder was fixed 7.5 meters below the surface to simulate a transducer pole. Range points were chosen from 0.2 km to 30 km and spaced to illuminate the most interesting parts of the error curve when plotted against increasing range. The parameters chosen were a decent approximation of actual operations although subsequent missions in the Bahamas only reached about 3500 meters.

MATLAB programs were written to execute the two different approximation methods. Each MATLAB code executed the RAY program and did different approximate calculations for comparison with the RAY output. RAY is a C++ compiled code that requires an input SVP file and an input parameter file. The historical SVP was used and

no attempt to vary sound speed radially was made since REMUS operations usually rely on one sound trace per operating area. The input file has many facets, but for this simple study, only range and the launch angle were varied. The launch angle had to be periodically adjusted as the range varied to ensure some path would go from source to receiver. The angle spread shot rays every $1/10^{th}$ of a degree for a total vertical wedge of 40°. Launch angles varied from about 80° to 20° below the horizontal as range stepped from 0.2 km to 30 km. The RAY output matrices were read in using MATLAB code and perused for travel time and distance results. The ray traces (yellow) and eigenrays (blue) for each range step were plotted (Figures 3.15 and 3.18). A sub-routine was written to exploit the eigenrays and extract the minimum ray travel time and travel distance. The two different approximation methods were compared with RAY output to determine a horizontal range error.

The first method used simple straight line geometry to find the slant range and divided by the average sound speed of 1517.45 m/s to get travel time. This time was subtracted from the RAY output to get a one way travel time error. This error was then doubled to find the two way error. The time error was then converted to a range error using the average sound speed again. This slant range error was then converted to a horizontal range error. This approach is flawed since the sound speeds do not weight with depth as the second method does. However, this simple average is included because it was the standard method for REMUS operations when surface range was not a critical parameter.

The second method used a more exact approach by piecewise calculating travel time and distance of the modeled range using the average sound speed at each sound trace depth to add up the travel time and the traveled range. Although no correction was done for the ray bending in the individual zones, this approximation was much more accurate since it coarsely took into affect the changing sound speed. The calculation for the range correction was much the same as the previous method once the differences in range and travel time were reached.

Figure 3.14

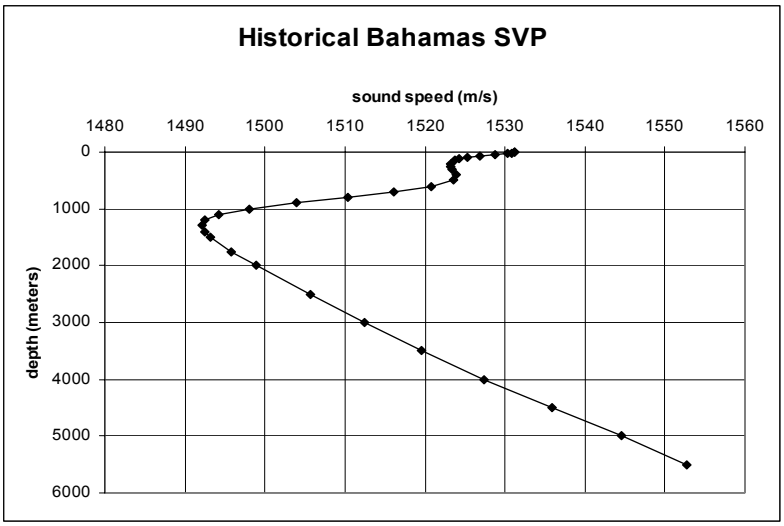

Figure 3.15
Eigenrays and Ray Traces 4 KM Range

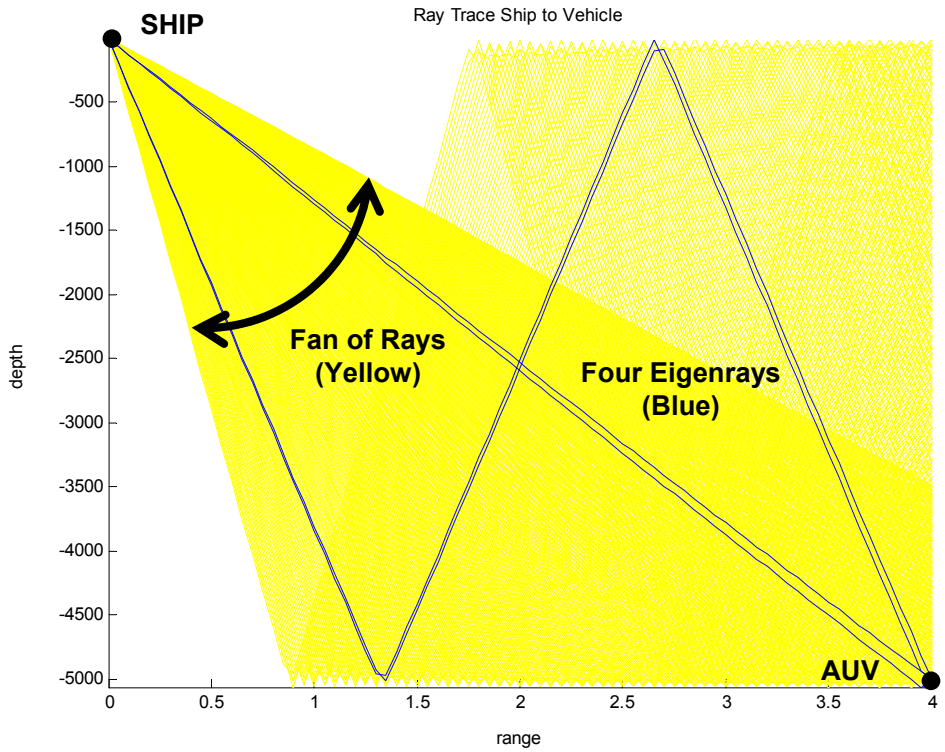

Ray acoustic trace program was used to determine the impact of ray bending on horizontal range error

3.5.3 Limitations of the Ray Model

The RAY program was originally developed for long range ray tracing. As such, the program appeared to have severe problems when bottom ranges less than about 0.2 km were used. Reasonable explanations are that the ray coverage is too sparse to pass through the receiver or that there are too many eigenrays in that region causing an overflow of a set buffer. Since a straight line approximation and a ray trace solution merge near ship, the breakdown is irrelevant even if a ray bending correction becomes necessary a distant ranges.

Also, RAY relies on the input file being changed manually for each iteration. So in implementation there is no easy method to control or modify that file when in the middle of executing MATLAB code. Hence, to use RAY as a onboard correction, large matrices would have to be set up in zones with already executed data stored for reference and correction. Storing and searching these files would eat up valuable processing time and may make the prospect daunting. Eventual use may require a custom module vice this canned application if ranges exceed the limits of this study.

Finally, RAY needs range of the receiver as an input so that it can output travel time. In practice with a navigating vehicle, travel time is measured and range is calculated as an output. This means the output and input really need to be swapped for effective use of this program, another argument for a custom application. One could cheat the system by again pre-developing large matrices so you could search the fan of rays to find which one matches the measured travel time and passes through the vehicle's known depth. This task is certainly not ideal and memory intensive.

3.5.4 Average Sound Speed

The first method used average sound speed and straight line approximation to arrive at an error estimation (Figure 3.16). Again, the plotted values show undesirable behavior underneath the ship when one would expect the error to approach zero. This can

be attributed to the break down of RAY in very short ranges as discussed earlier. Likewise, a bias can be seen as you step out in range. The error settles to an approximate average bias of 35 meters horizontal range error. Some of the bias comes from the error in assuming the sound speed numbers were taken over constant depth intervals. Although an easy correction, the end result represents less than 1% error and is acceptable for non-STRONG, "feel good" tracking.

Figure 3.16

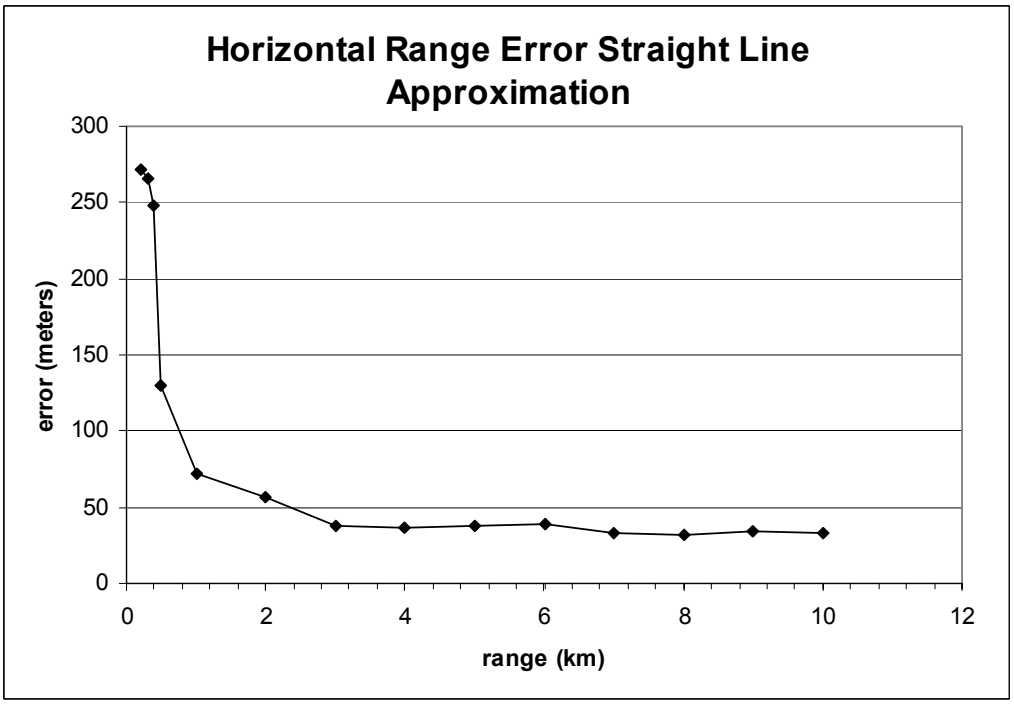

A simple average of the SVP speeds was often used for brevity for "feel good" tracking. However, failure to distribute the speeds over the varying depth intervals introduces approximately 35 meters of horizontal range bias.

3.5.5 Depth Weighted Sound Speed

Method two corrects for the sound speed change with depth by assuming a constant angle at each interface vice using Snell's Law. Although no bending is

accounted for, the travel time is a truer representation than the first method. In theory, the only source of error should now be in the distance the ray bends when the approximation does not. Certainly, a third method could be devised to include an angular deflection at each interface, but the contribution would be very slight. The near range behavior lowered in amplitude and became oscillatory but did settle out. Again this behavior is attributed to the break down of RAY. The midrange error levels to a value very near zero from approximately 3 km to 7 km (Figure 3.17). Once past 7 km the error grows as expected since the ray trace becomes more bent. Ray trace graphs of the mid range area showed very little bending while longer ranges became noticeably curved (Figure 3.15 verses Figure 3.18).

Figure 3.17

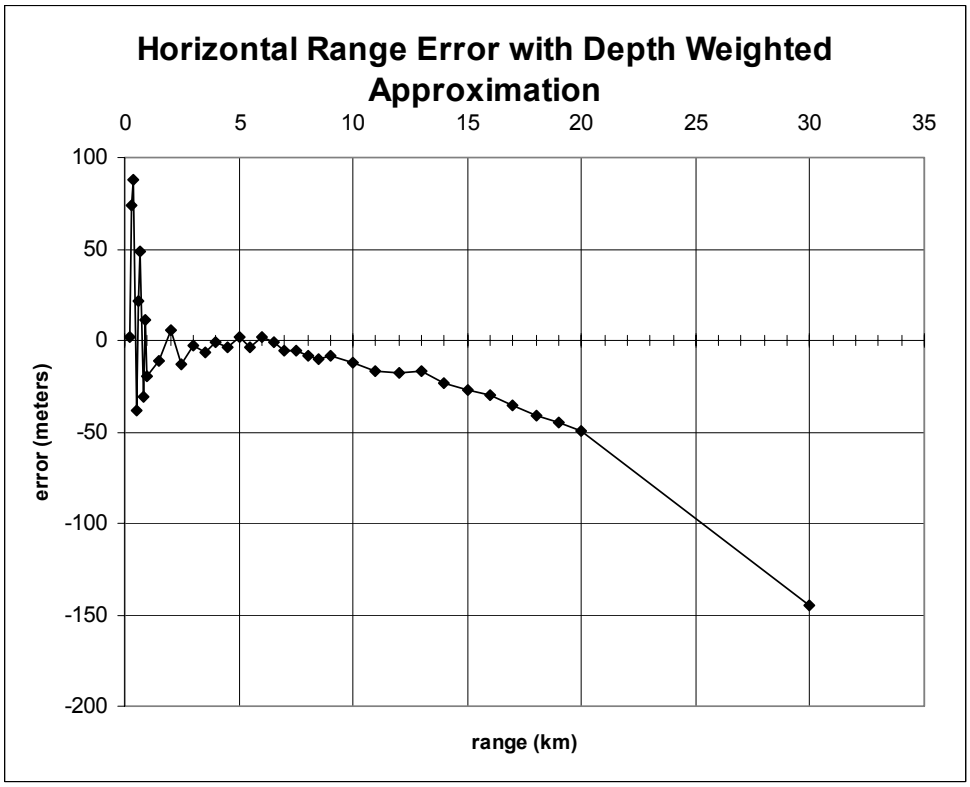

Sectioning the ocean into horizontal slabs of constant sound speed and computing travel time ignores bending but results in near zero horizontal speed error out to 7 km. Since this range is well outside the longest REMUS acoustic reception ranges, ray bending effects can be ignored.

Figure 3.18
Eigenrays and Ray Traces 30 KM Range

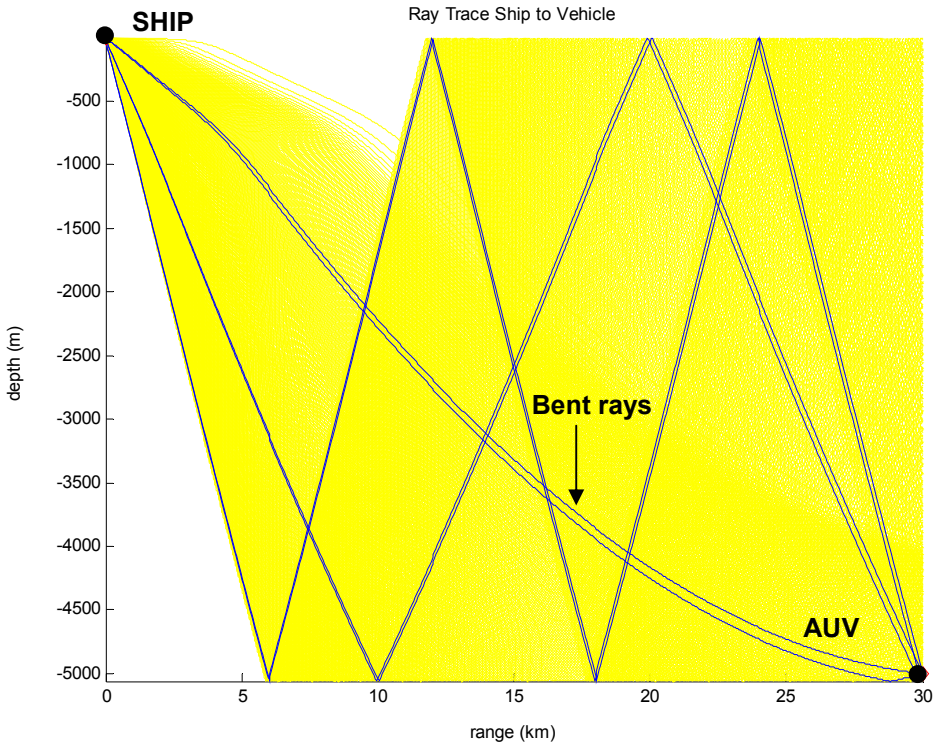

The limit range of the simulation shows visible ray bending of the eigenrays at 30 km

The depth weighted correction method appears to introduce an acceptable error into the range. The average error over the 3 km to 7 km section is -2.3 meters with a standard deviation of 3 meters (a negative error simply means the range call is short of the ray trace value). These errors are tolerable for the REMUS 6000 operation. Past 10 km, it is certain that some correction must be made for the ray bending to accurately update an AUV's navigation suite with single ship transponder information. Certainly a third compromise approach could add in Snell's law at the interfaces to recover some of the bending error. However, the point is somewhat immaterial since a 10 km bottom range in deep water surpasses the REMUS acoustic slant range limit by over 1000 meters.

3.6 Single Leg Algorithm Noise Model

In the beginning of this effort a simple geometric model was constructed to explore possibilities. The approach was as initially intended to explore possibilities for the REMUS 6000. The initial noise parameters consequently reflected a vehicle with a Kearfott inertial heading source and a RD Instruments ADCP used as a DVL. Initial experiments were done with a REMUS 6000, but operational constraints limited the data set. Additionally, initial analysis indicated that a shallower geometry with a REMUS 100 would eliminate deep water issues not completely understood in these early operations. Since the geometry was already derived from the initial noise model, it was applied to REMUS 100 operations with a magnetic compass and a comparable DVL. This application was done with some trepidation since the heading source was much noisier than the original model and there was no guarantee that this increased noise, even if Gaussian, would not manifest as an incorrect bias. In mitigation and as expected, ten times more REMUS 100 data was available to build confidence in a much noisier vehicle configuration.

The geometry model began with a stationary ranging platform and a constant course vehicle starting from a known initial position. This geometry is advantageous because the zones can be transferred from the vehicle to a geographic layout as described in Section 3.1.2 and Figure 3.5. In this manner, a vehicle could complete a straight leg in a course correct zone, a speed correct zone, or a combination of both. A vehicle course was chosen and the vehicle was advanced with a given speed. A constant course or speed error could be input with a Gaussian component. The vehicle position was then converted to a resultant range time series. This series was noisy due to the random walk of the model and no extra noise was added for the range measurement. The course or speed error was found in a least squares sense when enough range measurements were collected to overcome the Gaussian jitter overlaid on the actual error. Additionally, the original exploratory model was done in a two dimensional plane with no depth concern. Of

course, when real results were analyzed, the depth and ranging platform motion was coded.

Another assumption was made concerning the course and speed corrections of STRONG. As mentioned, the model was based on single straight line experiments correcting the parameter, course or speed error, that is observable. As discussed in Section 3.3.2, a simple box geometry allows for more course correcting opportunities than speed. Experience and the instrument parameters indicate that course correction, or cross track error, requires more frequent correction, especially in a magnetic compass vehicle. However, there is no way to resolve the range error into a percentage of course error and a percentage of speed error since their behavior in the short term looks the same and one must be known absolutely to have enough information to completely determine the system. However, the approach used is to assume that speed is known with absolute certainty during cross track corrections and vice versa when correcting along track.

3.6.1 Random Walk Noise Model

As mentioned, a simple random walk model was used to simulate vehicle motion with a noisy error bias. The parameters where chosen based on the long term quoted performance of the given instruments. Since one leg of data falls in between quoted long term and short term estimates, the parameters chosen were somewhat of a starting point guess with the realization that actual instrument behavior on the given time scale would vary. The parameters should easily be sufficient to build a working algorithm. In the case of course or along track correction, the resultant x – y walk (Figure 3.19) was converted to a range versus time plot and overlaid onto a family of range curves that represent perturbed trajectories of the intended course (0.05° resolution). On a swim by, the ranges start long, reach a minimum at the closest point of approach (CPA) and again increase as the vehicle moves away from the ranging platform. The perturbed courses make range buckets over which the noisy range deviation is plotted (Figure 3.20).

Figure 3.19
Random Walk Model for Cross Track Correction (Course)

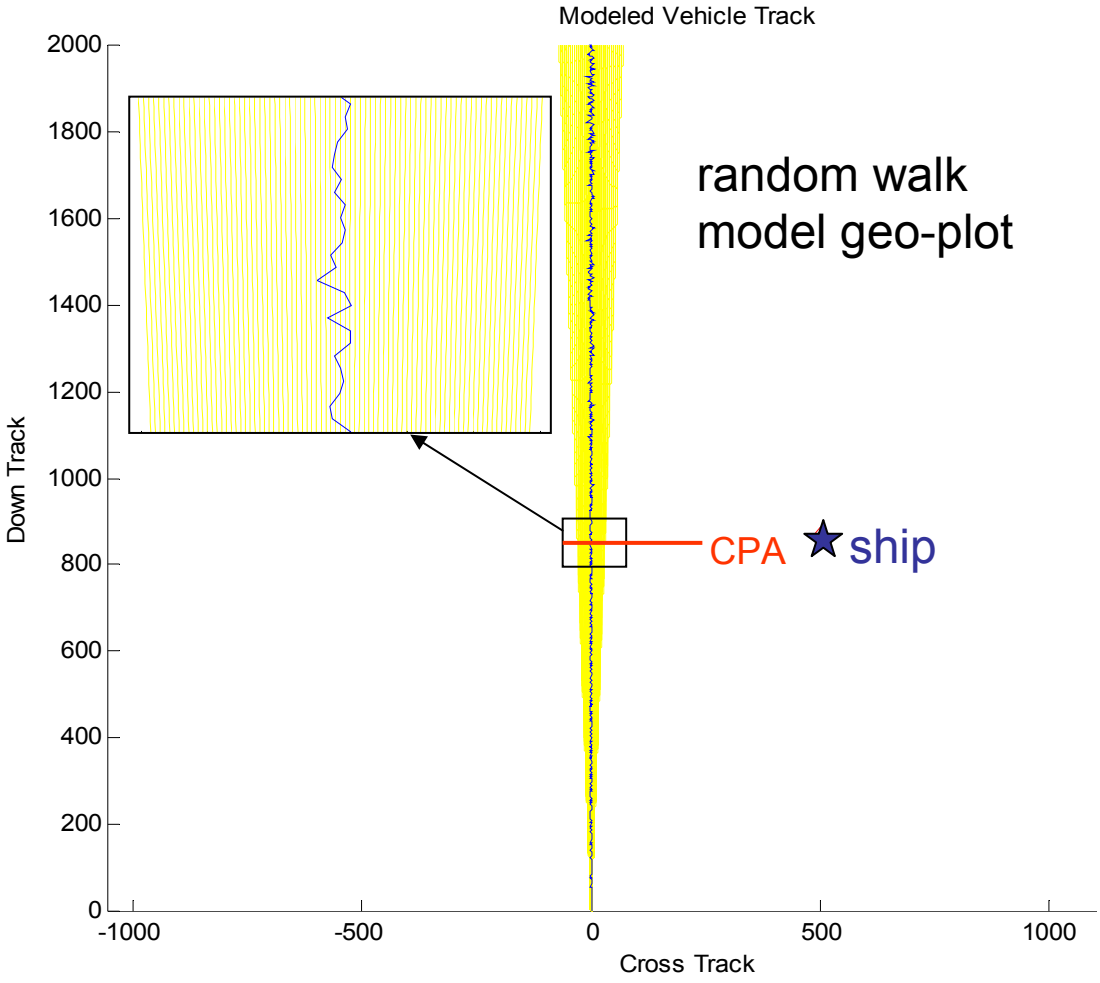

Figure 3.20
Range Bucket Perturbations with Overlaid Course Signal

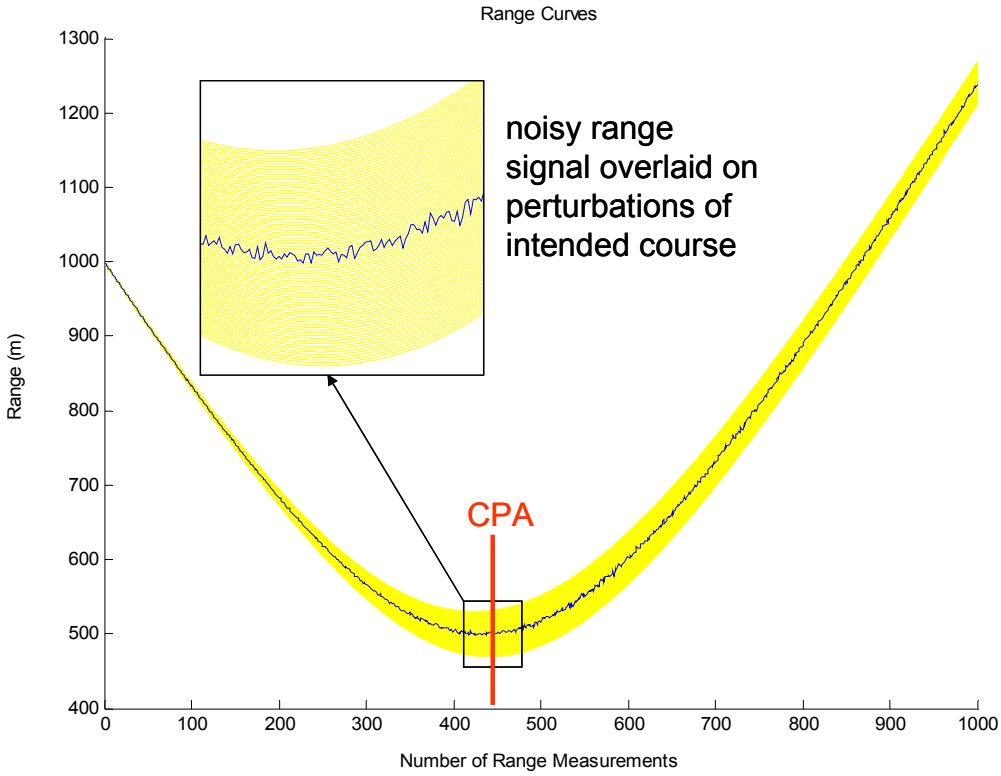

The curves spread vertically in range and see maximum deviation from one another at CPA. One can easily see that an actual course can be chosen from the perturbed values through a recursive least squares approach. The perturbed speed family results in similar curves that see spread along the time axis since a faster speed covers more range than a slow one. The details of these families and their fit method will be covered in Chapter 5; however, a small preview is required to appreciate the noise model.

One can easily observe that the model generated range data set is much more robust than actual data sets since true received ranges are delayed by travel time as much as 2 seconds for REMUS 100 and 14 seconds for REMUS 6000. For simplicity the one second interval of the model was not extended since the goal was to determine the convergence geometries, not an absolute time to converge. Convergence interval is much more germane when thought of as the number of range pings required for a solution. Since the number of ranges received in any given leg depends on travel distance, acoustic

conditions, and software settings, the algorithm had to be structured to recognize convergence when enough data was collected. As long as the range measurements are evenly distributed about a mean error, the number of measurements to converge should be relatively constant given all enjoy observable geometry. If the number is say, 30 pings, then a deep water vehicle will travel much farther before the convergence data is received than a shallow one.

3.6.2 Parameters and Assumptions

The basic parameters of the noise model assumed a Gaussian error in course of 0.1° and speed of 0.005 m/s. The course constant bias error used varied on different realizations from 0.01° to as much as a ten degrees around an arbitrary heading. The speed bias error was modeled on different realizations as high as 0.01 m/s around a reasonable REMUS speed of 2 m/s. The majority of the modeling was done concerning course since it represents the majority of the correction opportunities. Once the geometries were identified in which a course error could reliable be corrected, the remaining zones for speed were checked for validity. The MATLAB models were:

vehicle course = intended course + constant bias error + 0.1°(RANDN)
and,
vehicle speed = 2 m/s + constant bias error +0.005 m/s (RANDN)

These separately modeled random walks were translated to the range time series plots mentioned previously and used to explore the geometric space of REMUS operations. The variation in range from typical modeled cross track and along track noise (again, considered separately) is plotted in Figures 3.21 and 3.22.

Figure 3.21
Range Variation with Modeled Cross Track Error

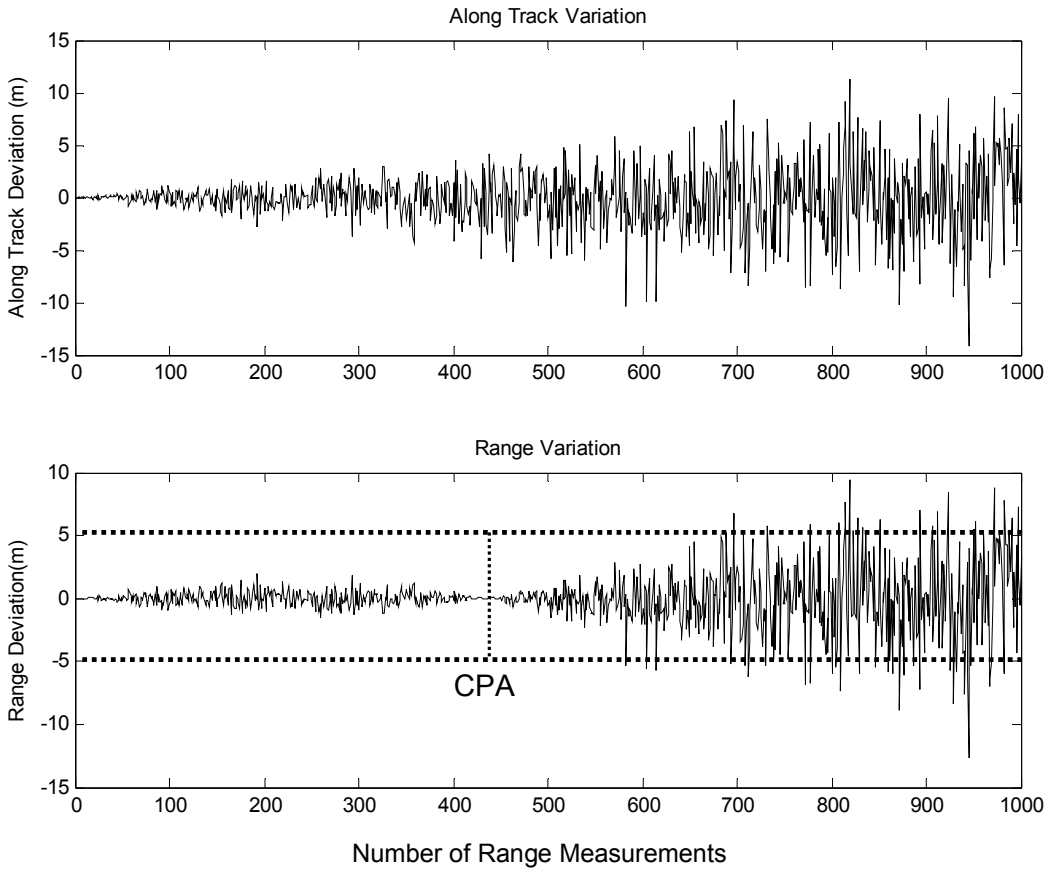

Figure 3.22
Range Variation with Modeled Along Track Error

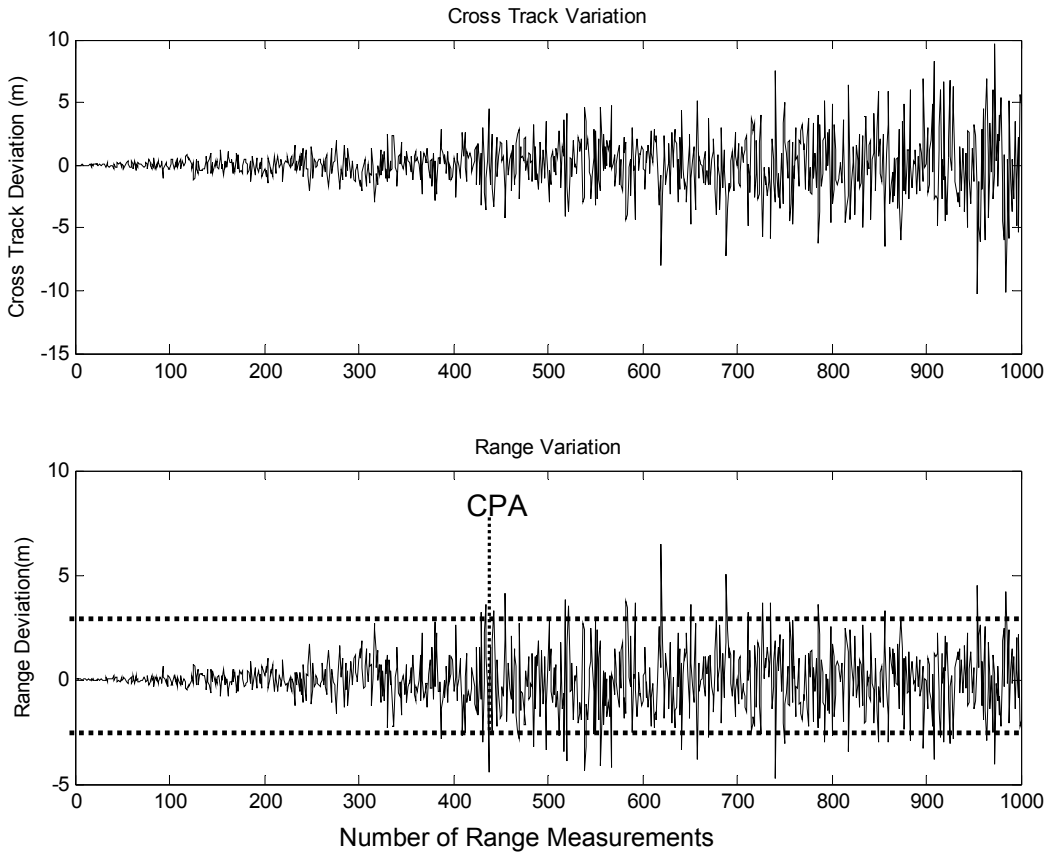

The plotted range variations exhibit the general expected behavior at the end of each leg and at CPA. In Figure 3.21, the cross track variation becomes the range variation at CPA when they are equal and dissipate as the sine of the Angle-to-CMG approaches zero. Consequently, the along track behavior behaves in a cosine nature minimizing at CPA. Additionally, the modeled along track error became about twice the cross track error at the end of the leg. This manifestation was a surprise as the experience of REMUS engineers would suggest at least the opposite. However, since each error is considered separately on a single leg, the relative magnitudes are of limited importance. The combination of the errors becomes significant when considering multiple legs and was explored through the operational experiments of subsequent chapters. Again, the simple goal of this model was to determine geometric zones for which noisy cross track and along corrections where observable.

3.6.3 Monte Carlo Simulation and Geometric Zones

A simple Monte Carlo simulation was used to find the geometric convergence zones for course (cross track) and speed (along track) correction. By keeping the ranging platform stationary and varying the starting position in bearing and range, the algorithm was repeatedly run to see if an input course bias error could be predicted at the end of a converging leg. The steps in bearing and range were sufficiently small to cover the geometry on a sub-meter level. Each starting position was run ten consecutive times averaging the number of wrong answers. The vertical axis represents the average number of wrong answers, and the flat floor is zero indicating 10 out of 10 successful predictions (within a very small tolerance). Since the ranging platform is stationary, the principle of reciprocal bearings allows a direct correlation from a view with the ranging platform in the middle to a view with the AUV in the middle (Figure 3.23).

Figure 3.23
Monte Carlo Simulation of Correction Zones

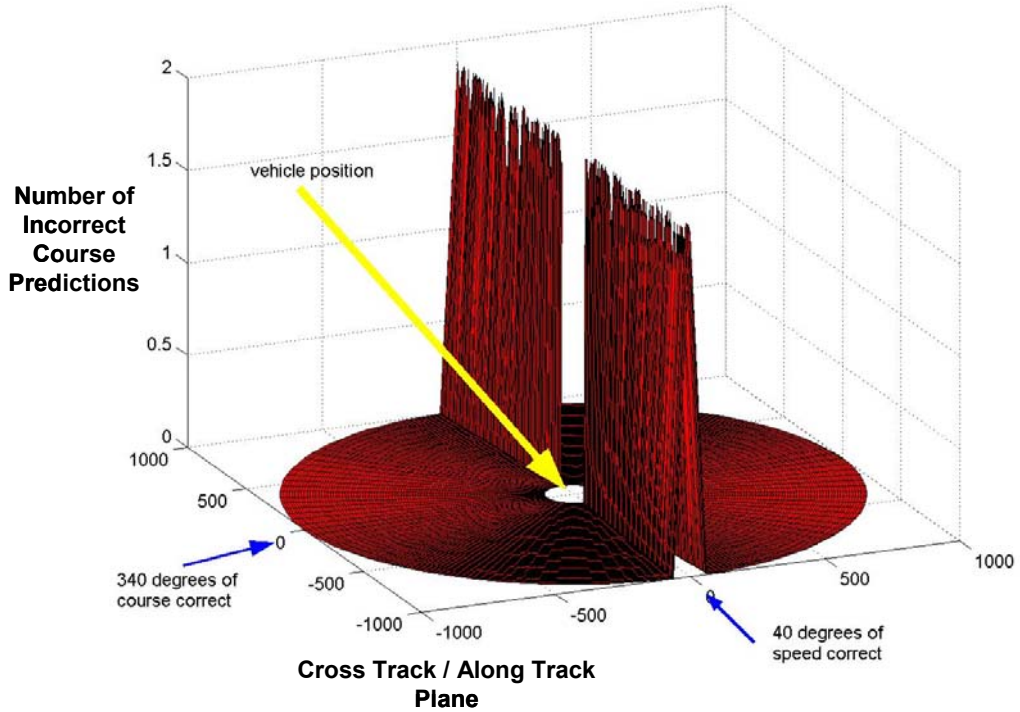

As expected, course correction was observable in all but small slices when the vehicle was heading directly toward or away from the ranging platform. These small slices yielded large numbers of errors when predicting course bias errors (resulting peaks) but are ideal for predicting speed bias errors. This analysis was the genesis of the polar plot around the AUV for Figure 3.4. Close inspection shows that the Cross Track / Along Track Plane of Figure 3.23 becomes Figure 3.4.

The resulting course correction zone was 340° leaving 20° at the bow and stern of the AUV for speed corrections. The speed correction zones are conservatively stated at 20°, the actual minimum swath is about 16° (8° on either side of centerline). One is tempted to figure speed correction quickly by straight range difference with a small angle approximation and thus ignoring the available course made good. A simple calculation shows that 8° of curvature results in about 39 meters of along track position error for a 4000 meter range. However, since determination of speed would rely on the range difference between two subsequent ranges, the real question becomes how different is range closure on track versus 8° off track? Again at 4000 meters, the difference in closure difference is off by about 10 centimeters. Irregardless, the heading is available, so the algorithm was designed to fit the speed correct just like the course correct ranges since the final speed correction will be turned into a positional fix (during which the 39 meters comes back into play and becomes important). The resulting correction plot around the vehicle is the same that was presented earlier with minimal explanation (Figure 3.4).

CHAPTER 4
Field Experiments and Data Sets

4.1 General Approach

All data was post processed in a sequential nature to simulate a single leg vehicle navigation routine. Future versions of STRONG will handle turns and maneuvers, but the simplest geometry was sought in this algorithm design stage. An appropriately designed box survey yielded numerous single leg realizations of STRONG in one long mission. A LBL field was seeded to provide a known starting and ending position. The vehicle was programmed to navigate between these positions based on DVL assisted dead reckon only, simulating the sole navigation capability of a STRONG enabled vehicle between fixes. Meanwhile, a ranging platform collected a range time series over the leg. Later, the onboard vehicle state data and the range series could be fed into STRONG code to predict a fix at the end of the leg. Then a comparison was done between two vehicle on board dead reckon positions, the STRONG position, and the LBL fix. Since a REMUS without GPS and bottom transponders relies solely on dead reckon position, the goal was to prove that a better position could be attained with the integration of a STRONG single transponder range time series.

4.2 At Sea Data Collections

Experimentation began with the deep vehicle REMUS 6000 design, hull 2. Data was essentially grabbed within the myriad of shakedown and delivery tests on board USNS Pathfinder. Since STRONG was in the early modeling stages, much of the deep data became a primer to design follow on, more flexible REMUS 100 experiments. Since STRONG operations required the vehicle to navigate without the benefit of LBL fixes, confidence had to be established in the new vehicle before it was left to solely dead reckon in a STRONG experiment in 3000 meters plus depth. Some shallow data was analyzed to learn the REMUS data architecture off Charleston S.C. Some rudimentary

observations were possible with this set since the vehicle operate between GPS fixes in about 30 meters dead reckon navigating from fix to fix (similar to the planned experimental approach).

4.2.1 Charleston S.C.

Charleston operations were the first stop on a month long shakedown of REMUS 6000, hull 2. The water depth of 20 – 30 meters and the sea conditions included a 2 knot set and drift to the north-north-east with 10 knots of wind and sea state 2 swells rolling in from the south. The goal was to bring the Kearfott Inertial Navigation Unit on line by doing the three stage alignment. Two stages are done on every launch, but the final one aligns the ADCP with the inertial unit and requires a two hour surface run with GPS. The geometry is a box run path 1.5 kilometers on each side consisting of at least three laps. GPS was required and available, but the vehicle was allowed to "swim" down to the bottom for parallel camera testing. The vehicle would come up and the end of each leg and get a fix. The geometry would have been good for STRONG since each side leg was dead reckoned between ground truth GPS fixes. However, the GPS antenna was a new design sharing air time with wi-fi communications. This combined with a water shedding issue and sea state led to a significant wait time on the surface before a GPS fix was on board. The result was an end of leg fix that could not reliably be dead reckoned back to a reasonably accurate bottom position. Some fixes required on the order of ten minutes drifting on the surface to complete. In this time, the ADCP experienced some excessive and degrading pitch and roll effects. However, a single leg was processed to become comfortable with the data streams. The fit of the data and the proximity to the last measured range was used to rudimentarily judge the accuracy with guarded optimism. Incidentally, the Kearfott alignment was unsuccessful for position and the system was degraded to a highly accurate compass, which was fortunately the only data needed by STRONG.

4.2.2 Bahamas

Once the coarse adjustments were made in shallow water, operations moved to deep water off the Bahamas. The first set was north of Great Island of the Bahamas in about 1500 meters of water. Regrettably, problems with the recovery float, depth control, and acoustic modem wiring filled all mission opportunities with troubleshooting efforts. Operations then moved to deep water about 25 NM north of Nassau. The initial runs were done to image seeded barrels leaving the last two missions as possible data runs for STRONG. The first attempt was set to run four 4000 meter legs in dead reckon, but the vehicle struck a rock outcropping at about 3400 meters and subsequently aborted. The final mission of the cruise did run STRONG legs but a failed ship gyroscope and inexperience with depth / accuracy effects explained earlier left all but one long leg unusable since the ship drifted over each of the legs failing to provide proper stand off for the water depth through the entire leg. Piecemeal corrections were abundant, but a ground truthing LBL fix was only possible at the end of the 4000 meter legs. However, environmental conditions were ideal with a long flat bottom, minimal bottom currents, and a pristine surface recovery sea state.

4.2.3 Buzzard's Bay

A REMUS 100 collection was advantageous since the vehicle was more accessible. A box survey geometry was again used to get an opportunity at course and speed corrections with each leg constituting a new single leg realization. The layout was the exact deep water geometry except that max range from the LBL truthing field was in line with a REMUS 100 vice a REMUS 6000. Additionally, the water depth in Buzzard's Bay was about 15 meters substantially easing the water depth dependent errors. A total of thirteen legs were planned, but surface conditions forced an abort when partially done with leg ten. Although bottom currents were less than 0.5 knots, the surface weather built to four foot seas dragging the zodiac on anchor over 300 meters.

The LBL transponders were placed on a north / south axis 1500 meters apart (Figure 4.1). The leg lane spacing was 100 meters with a 200 meter offset from the LBL baseline. The first and last 100 meters of each leg allowed LBL navigations to get a good starting and ending fixes. These zones allowed the vehicle to stabilize and get back on track prior to each leg. Also, the first acoustic fix at the end of the leg would show an error offset between the vehicle's magnetic compass / DVL dead reckon positions and the acoustic fix. One REMUS dead reckon position benefits from the LBL fixes at the leg ends and updates the estimate based on these positions (influenced dead reckon). Another dead reckon position assumes the vehicle launch to be truth and accepts no outside information to update its compass / DVL estimation of position (straight dead reckon). The number of legs was limited to thirteen to keep the maximum range from any transponder under the maximum recommended transponder range. The final geometry (if all legs had been completed) left twelve legs of course correction, one of speed correction (passing nearly under the zodiac), and two on each side of the zodiac that were a mixture of speed-course-speed. The zodiac was anchored in the middle of the box and the vehicle launched. Ideally, the run to the start point (directly away from the zodiac) should have been used to corrected for a DVL speed bias at the beginning, but a setup problem delayed data collection until the vehicle turned on the first leg. The speed correction in the middle of the geometry was, however, successfully applied to the initial legs. The ranges were collected through a custom deck box housing REMUS acoustic modem and digital ranging cards and saved in a special data file time stamping the vehicle range and the corresponding zodiac GPS position. The vehicle was recalled in the middle of leg ten resulting in nine plus 1300 meter dead reckoned legs for post analysis.

Figure 4.1
Buzzard's Bay REMUS 100 Operations

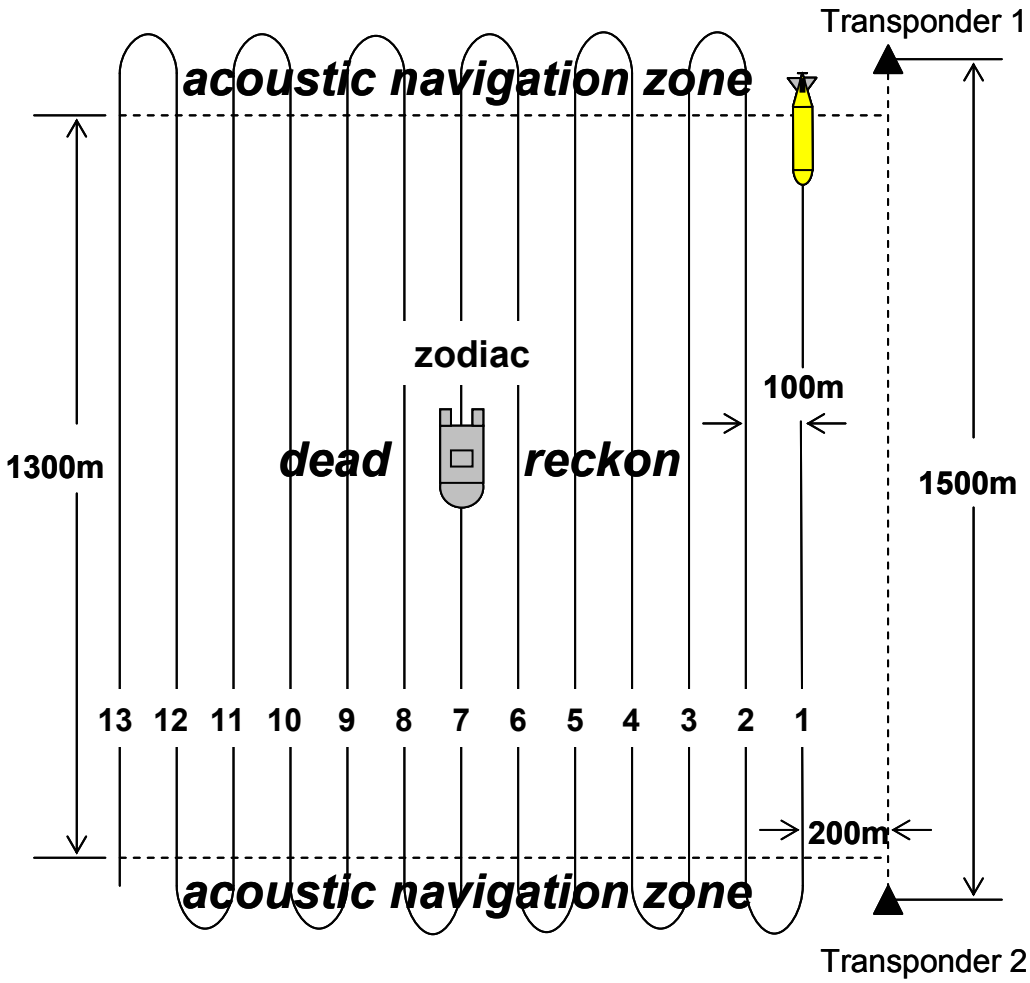

4.3 Post Processing Approach

The REMUS mission .rlf file and the range / position time series were combined with the STRONG algorithm to predict position at the end of each leg. Of course, the goal application is to run a STRONG routine on board the AUV. The algorithm would use all the vehicle's sensed state information including ranges to a single ship mounted transponder. Via acoustic modem, the vehicle would receive a GPS time series of ship's position that would allow the ranges to be corrected for relative ship motion. Given the

data, STRONG would output an “LBL-like” fix that could be used to update dead reckon or even feed into an inertial unit Kalman filter. However, in these early stages, confidence had to be demonstrated in the algorithm prior to significantly altering on board software. Therefore, post processing was used exclusively for this research.

4.3.1 General Data Preparation

Data manipulation was no easy task requiring interface with multiple programs to manage the data. The REMUS user interface was used to export all ADCP and STATE data to text files. The ranger file is directly stored as a range, transponder position, and time text file. All text files were ingested into EXCEL so the data could be easily viewed. An LBL fix was chosen at the beginning and end of each leg to position and a start and stop time. The turns outside of these start times were ignored, and the individual legs were export again from EXCEL to leg specific text files. These files were then used by over 800 lines of STRONG MATLAB code on a leg by leg basis to output a STRONG fix. Even though convergence to a solution was early in the leg, the solution was delayed until the ending fix time for easy comparison with both dead reckon positions. STRONG code attempted to simulate the leg run by executing instructions in a time sequenced loop vice taking advantage of time saving matrix manipulating steps. The goal was first to simulate and second to develop code that could easily be converted to eventually run onboard REMUS.

4.3.2 REMUS Data Streams

REMUS records much more data than needed for STRONG calculations. The essential STATE streams are both dead reckon positions, compass heading, and heading offset for current. The essential ADCP streams are vehicle depth, vehicle altitude, ADCP velocities in three dimensions, and acoustic LBL fixes. STATE and ADCP are data grouping names in the REMUS software that do not necessarily mean the information

was derived from the ADCP. For example, the heading offset is calculated with ADCP velocities, but is exported as STATE. Likewise, the depth comes from the CTD, but is listed in the ADCP export. As discussed, the transponder (ship) position and the ranges constituted the RANGER stream. One issue involved the logging cycle of the data. STATE, ADCP, and RANGER data are logged on different and fluctuating intervals, so the data sets had to be average or interpolated to common times. The intervals vary with mission length to optimize data storage. The chosen data set to time synchronize with was the RANGER set since it was obviously the most sparse. One leg may have only 60 ranges on the order of 5 to 10 seconds apart, but the ADCP and STATE data sets are recorded to tenths of seconds. When appropriate, data with cumulative affect, such as ADCP velocities, were average over the interval to give a truer indication of vehicle motion. Some data, like depth, was chosen as the simple interpolation between recorded values. This time leveling of the data was one of the most significant deviations of the STRONG simulation from a real time navigator because it assumes the entire data set apriori. This obstacle is easily overcome in application with simple time synchronization modifications in the data recording software. In many cases, the closest available value is good enough since the system is not incredibly dynamic and has favorable noise characteristics.

4.3.3 LBL Fixes as Ground Truth

The LBL transponder net was in place but only used in the turns and the ends of each leg. The starting position was chosen as the last reasonable LBL fix prior to shifting to dead reckon only navigation. Since REMUS navigates on the average of LBL fixes vice knee jerk correcting from fix to fix, the dead reckon position often did not match the chosen LBL position. The vehicle's dead reckon tracks were simply offset by the difference between the time zero fix and the like influenced dead reckon position (the straight dead reckon was left uncorrected since it accepts not fix information from launch). This action essentially reset vehicle position to a known LBL start point. This

correction was only on the order of a meter or two, but was necessary to start each leg as a separate realization.

The ending fix position did not always exactly correspond in time to the STRONG predicted fix which was tied to RANGER time. A small snippet of vehicle influenced dead reckon was used to advance the STRONG position to match time with the LBL ending fix position. Again, advancement is no more than 10 seconds, so the error in dead reckon position over that interval was considered negligible. However, this advance was necessary to produce comparable results.

The final factor to be considered with this LBL truthing method is the most obvious one – error in the placement of the beacons. Although discussed at length for deep seeding in section 1.2.1, the error in shallow transponder seeding must be considered. Although the weights for these transponders were placed within two meters of their intended positions, a three meter error in GPS and a meter of buoy current tend can yield a varying error value throughout the transponder field. Experience indicates that even these shallow moorings yield a LBL fix accuracy of no better than 5 meters.

CHAPTER 5

SINGLE TRANSPONDER RANGE ONLY NAVIGATION GEOMETRY (S.T.R.O.N.G.) ALGORITHM

5.1 Flow Chart of Approach

The conceptual ideal of STRONG is flow charted in Figure 5.1. In a single leg, steady course or speed sense, the center down flowing leg has been implemented post process. The peripherals and upward flows will come after the center leg is forged to be a generic navigation tool able to handle maneuvers. Chapter 6 will devote effort to outline a notional approach for the more generic form. Chapter 5 explores the specific case algorithm to describe the two part method at the heart of the center down flowing leg. This two part method has dual legs for course or speed correction. Part one is the convergence upon a fitted solution from perturbed trajectories with the best available initial condition. Part two involves repeating part one with a sequentially varying initial condition in aim to find a better fit and subsequent correction. Simple plots will be used to illustrate the method followed by the same plots featuring actual data.

Figure 5.1 *Start* **STRONG Flow Chart**

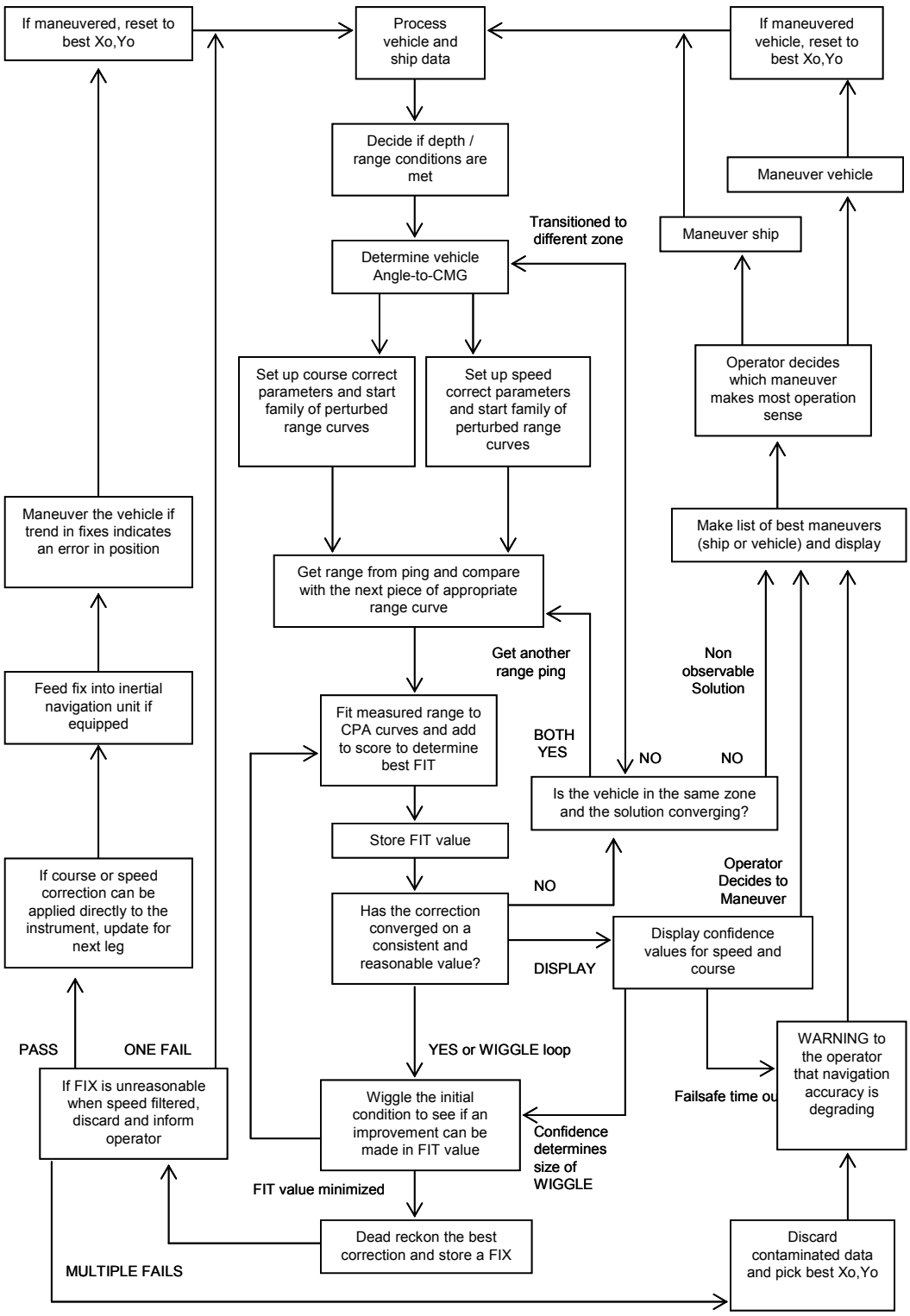

5.2 Integration of Ranges (Part One)

The STRONG approach utilizes a simple non-linear least squares approach to fit the range data time series $R_N(t)$. Variance is allowed in the parameters of course, speed, Xo, and Yo. Initial position and either course or speed are inputs to generate the iterative comparison range $\widetilde{R}_N$.

$$\min\left(\sum_{1}^{N}\left|\widetilde{R}_N(course, speed, Xo, Yo) - R_N(t)\right|^2\right)$$

The minimization is done with the simple MATLAB function at each iteration to form a prediction. The variance of these predictions is used to decide when the chosen course or speed error is a suitable to produce a reliable output positional fix. A similar method used in simulation is the least square root method (Scherbatyuk, 1995). A least squares approach is sound given the following criteria are met (Brook and Arnold, 1985):

1. Time values are not random variables
2. Deviations are independent
3. Deviations have a mean about the desired correction
4. Variance of the deviation is constant and does not depend on time
5. Deviations are normally distributed

Assuming all significant instrument biases that degenerate proportional to time can be removed as discussed, the noise level is within reasonably assumed values, and the resultant range measurements have a Gaussian distribution about the mean correction, all five criteria should be valid.

5.2.1 Course Correction

Course correction produces a fix when the vehicle has navigated enough time in the proper geometry to support convergence. To produce the most accurate cross track

correction, you must have an accurate speed (i.e. recently corrected) and a good initial position (wiggled out in Part Two). Each experimental realization was monitored with a series of plots so the process could be monitored for any ill effects. Before presenting some of these intermediate plots of real data, simple illustrations are used to easily explain the process and the graphics. Understanding of the inter workings will be essential in future implementations of the approach.

5.2.1.1 Least Squares Fitting

Course or cross track error is eliminated by minimizing the square of the range error residual. Although relative motion is subtracted out, the easiest geometry to visualize is a stationary ship (transponder) that gets passed by the vehicle on course 180° (Figure 5.2).

Figure 5.2
Course Correction Illustrative Example

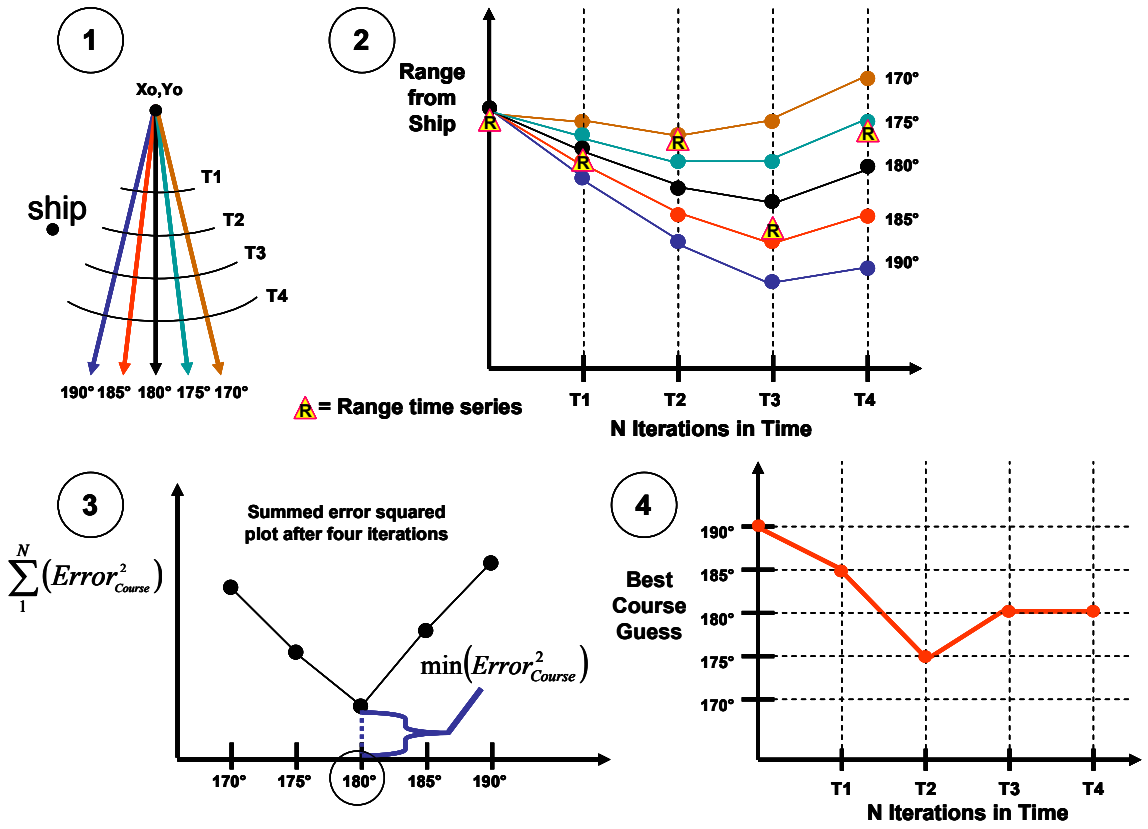

Step 1 shows the actual heading of the vehicle in black as it approached, past, and opened the ranging ship stationed to the west. A family of course curves is developed with a five degree granularity. The idea of perturbing potential trajectories has been done since the 1950's in the "method of variant orbits" to determine space object paths with radar range measurements (Liebelt, 1967). Blue, red, green and brown perturbed trajectories are developed creating a $\widetilde{R}_N$ series on peripheral of the intended course. The speed is assumed correct and is marked by T1 – T4 hashes. In this example, the speed is constant, but it need not be. The resulting graphic is a map-like geographic representation of the potential trajectories. The width of the course spread should be set to encompass the biggest feasible course error drift between fixes. The granularity of the spread will directly translate to the coarseness of the prediction. In this case, the chosen trajectories will be binned by five degree separations. The initial reaction is to push the granularity down to a hundredth of a degree and spread the fan over 90° to cover all possibilities and get a highly accurate result; however, the perturbations must be balanced with memory and processing time constraints. Since Part Two involves iteratively moving or wiggling the initial condition and rerunning the data, it is critical to only cultivate the minimum family size.

Step 2 plots the range perturbations versus time. The structure, if allowed to generate into the future would take on the appearance of a "CPA smile" that is typical of a passing maneuver between two objects. The actual measured range time series $R_N(t)$ is plotted on the family. Time synchronization has be done to make all data comparable on the T1 – T4 times. At each time, the error between $R_N(t)$ and each trajectory point is squared and saved in a running sum for each course. The $\widetilde{R}_N$ trajectories widen as CPA is approached overcoming the noise spread of the $R_N(t)$ series as long as it is evenly distributed and summed for a sufficient amount of time. The actual run geometry (box, long transect, etc.) is somewhat immaterial as long as the CPA smiles are forced with the necessary frequency to correct the error drift. In this case, the data is a simple second order polynomial, but generic motion could make this shape require a much higher order

fit. One of the biggest pitfalls of the least squares form is that the order of the fitting polynomial is usually not known apriori yielding bad approximations if the wrong order is chosen (Liebelt, 1967). However, that worry is no issue in STRONG since the problem will always reduce to a simple first order fit of the curved range perturbations.

Step 3 shows the sum of the squared errors plotted versus course family choice. As expected, a minimum points out the trajectory the vehicle most closely followed assuming all straight bias errors are removed. If the solution was a perfect fit and the initial position was exact, the curve would touch the time axis. Since the ending result is not known, the squared error residual beneath the curve is the only clue to how good the least squares fit is to the perfect solution. This error residual is a function of the noise in the range measurements and the initial position error. A FIT VALUE is defined as the square root of this residual divided by the number of iterations and is used as a quality factor. This quality factor is essentially an average of the term:

$$\left| \widetilde{R}_N\,(course, speed, Xo, Yo) - R_N\,(t) \right|$$

In Part Two of the STRONG approach, the vehicle starting point is perturbed in x and y to minimize the FIT VALUE and best approximate the vehicle trajectory.

Step 4 charts the best fits or "guesses" at a proper trajectory. The time zero range actually falls outside the family causing the guess to be "clipped" to the maximum possible guess of 190°. At time T1 the best guess becomes 185°. As the family widens, the spread overcomes the noise and answer settles in to 180°. This progression leads to discussion of the internal course trigger that determines when to act upon the error and produce a fix. The program actually operates on course difference from the intended course. This produces a comparable curve that oscillates about zero with convergence as the curve flattens. The real data plotted later for Step 4 is normalized to speed or course difference for additional clarity.

5.2.1.2 Course Trigger

The method of course triggering involves tracking a five iteration window of course guess differences. The current course prediction is subtracted from the previous one to develop an error plot. The perfect five iteration window would contain all zeros; however, this criterion is relaxed to allow jumps between adjacent family members. Essentially, if the guesses bounce between neighbors, then the output is at the limit of predictability for the chosen parameters and should be stopped. Since the family granularity is known, the trigger level is set for five toggling guesses. When below this value, the iterative loop is exited and a course is decided upon. This entire process can be repeated if necessary with a perturbed initial condition. In Step 4, three out of the five necessary adjacent member guesses are present to support convergence. This smart trigger approach is necessary since the goal is to get in as many fixes as the data will support without prematurely converging.

5.2.1.3 Fix Generation

Once the trigger is tripped, a course is generated. The algorithm actually does a subtraction and works with course error from the intended course. The choice is largely irrelative, but an error is necessary if there is any hope to correct the instrument directly. For instance, a magnetic compass has a predictable bias on certain courses. Since box surveys repeat reciprocal courses, knowing this error and applying it directly can keep the vehicle on a truer course without the need to find the same correction repeatedly. Conversely, inertial heading sources lack these errors, but also accept few direct corrections and prefer fix input as the only influential external source. Since STRONG is intended to work with inertial units, the corrections often have to become fixes.

Part Two wiggling of the initial condition is temporarily skipped so the development of the fix can be discussed. Once an acceptable course is decided upon, the vehicle starts with best initial condition and dead reckons from this point with the

assumed correct speed. This end point is converted from grid position to latitude and longitude and would readily be available to influence REMUS positioning or feed into the inertial unit for a better estimated position.

5.2.2 Speed Correction

Speed correction produces a fix on the occasion that the vehicle points toward or away from the ranging platform. Assuming an adequately corrected heading and initial position, along track can be removed with the STRONG algorithm. As in the previous fashion some simple graphics will be reviewed to illustrate basic concepts.

In parallel fashion, speed or along track error can be found by minimizing the square of the residual range error. Again, a stationary ranging platform was chosen for simplicity (Figure 5.3).

Figure 5.3
Speed Correction Illustrative Example

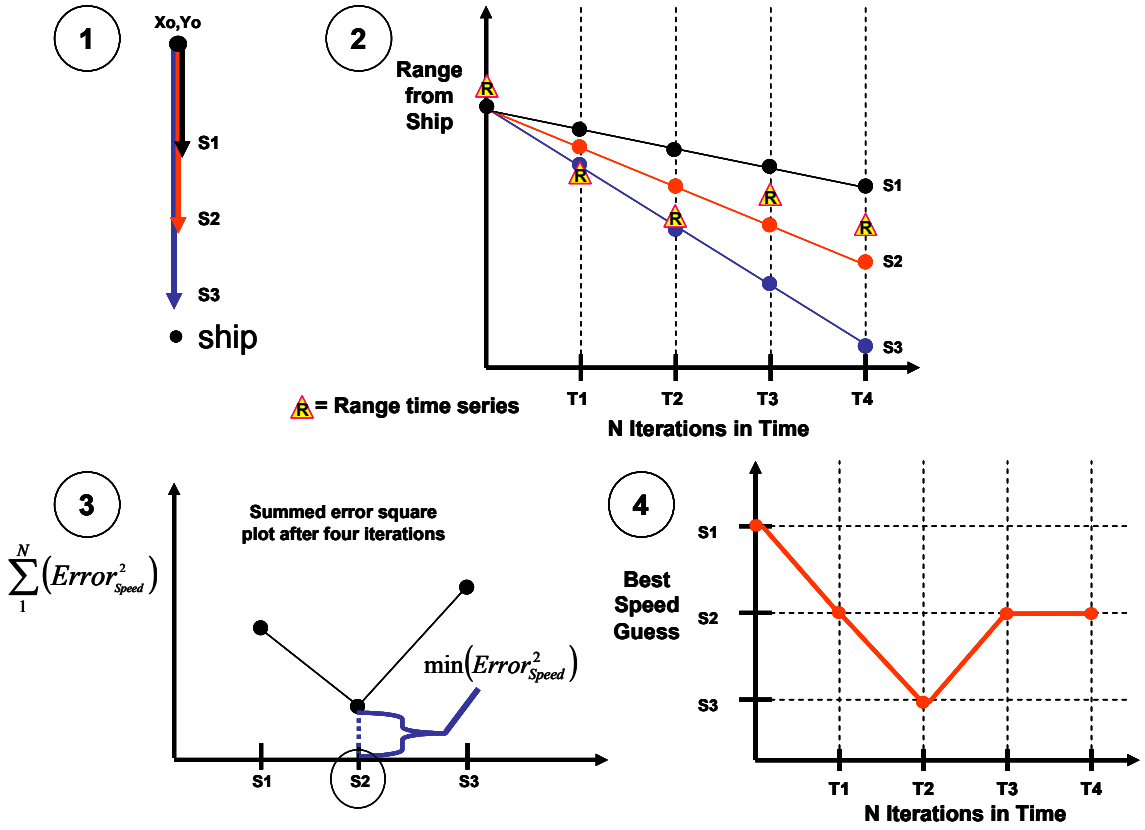

Step 1 builds the family of speeds on a known course. The course can vary, but here is shown constant bearing down on the ship. The lengths of the errors correspond to increasing speeds. In this example, the red speed is closest to the actual vehicle speed. Again, proper initial condition is an essential component to success. It must be close enough to be wiggled out in Part 2.

Step 2 shows the range family of curves. If the trajectory is poised to pass directly beneath the ship, the curves become straight lines with a slope equal to the range rate. In this case, both the zero and first components of $R_N(t)$ are clipped on opposite sides of the $\widetilde{R}_N$ curves. A guess cannot be made outside the family. If the measured ranges remained on one exterior side an improperly widened family, the limit speed (or course would be chosen). Eventually, the vehicle would be nudged back toward the intended course, but

the process would take too long. Again, the family must be wisely chosen. If left to generate through CPA, the curves would sequentially bottom out and then ramp up at a mirror range rate downstream.

Step 3 again results in a minimum at the proper trajectory speed. As with course, the ends of the curve grow with an increasing number of iterations to make the minimum more defined and poignant.

Step 4 shows guesses at each edge of the family. Although the granularity of the speed spread is greatly exaggerated, convergence is progressing nicely as four out of five guesses bounce between adjacent family members. The trigger operates identically to the course section so needs no additional explanation. Fix generation is likewise comparable.

5.2.3 Duality of Course and Speed

The interdependence of course and speed has been alluded to since the correction of one requires an assumption of correctness on the part of the other. Unless this simplification is made, a solution is not possible since the system is under determined and cannot be separated into course and speed error portions. The worst part of the coupled nature is that if there is an error in both, the singularly sought correction will be contaminated. To keep this under control, corrections must be done frequently with regard to instrument drift rates.

5.2.4 Speed – Course Transition

Each individual correction having been explained, some thought must be given to the transitions between course and speed zones. For the test algorithm used in these experiments, transitions were more dependent on geographic location vice vehicle orientation (reciprocal bearings). Irregardless, a steady course may drive the vehicle from course correction to speed correction or vice versa. The problem arises because the noisy data makes the transition vague and can cause rough starts and ill seeded memory

positions. One approach is to ignore data when on the cusp of a transition. Whatever approach, care must be taken to keep memory positions clean.

5.3 Wiggling the Initial Condition (Part Two)

Once a course or speed correction is arrived at, the initial condition is perturbed and the ranges re-run. This process was done manually at detailed resolution to sufficiently explore the concept. A simple loop was used to step the initial condition in polar fashion out from the best fix position. Over 1600 starting points were run on each leg to see how much the FIT VALUE could be improved with a perturbed initial condition.

5.3.1 Simulated Annealing of the Initial Condition

As discussed in Section 3.4.3 and illustrated in Figure 3.9, any initial condition will result in a data fit. As explained, the geometry can result in directional bias that shows very little change in FIT VALUE in certain directions. A wiggle surface was plotted on each leg in order to get some intuition with these biases and hopefully provide input to the design of a "smart wiggle" that could find a better starting position without 1600 starting points. The wiggle surface plots Xo, Yo for each iteration against the FIT VALUE for that run in the vertical direction. The surface has a pancake like appearance because the starting points were spiraled out from the initial fix position. The minimum of the pancake would theoretically represent the best fit and be the choice since no other internal quality factor is available. For comparison, a second surface plotted the same Xo, Yo positions against radial distance from the ending acoustic fix. Although flawed by up to ten meters, the ending acoustic fix shows some relative accuracy of this approach (Figure 5.4).

Figure 5.4
Wiggle Surface for Leg 3 REMUS 100

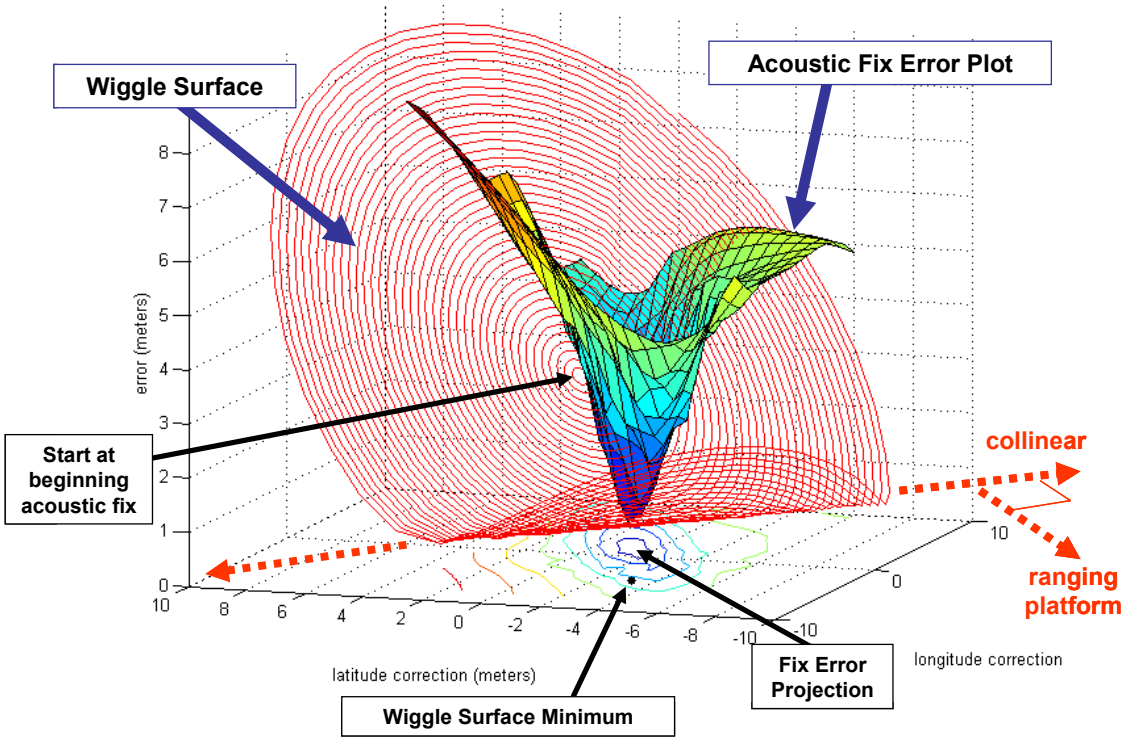

A wiggle surface uses the hind sight of a controlled experiment to explore how well the apriori FIT VALUE can improve accuracy. Closeness of the Wiggle Surface Minimum and the Fix Error Projection implies the method is successful. The distance from the center of the "pancake" to the fold shows how much initial position error was removed with the wiggle.

A black dot is provided below the minimum of the wiggle surface and contours below the ending error surface to show the distance between the two in the x – y plane. Ideally, the two would fall on top of one another solidifying the approach; however, the best to hope for, is that the two agree on the scale of the controllable error and are much less in magnitude than the error being removed. In this case, the two are on the order of six meters apart. All ending results of STRONG were tallied from the strict minimum of the wiggle surface. In every case, the ending accuracy was improved, often times, significantly when compared to Straight Dead Reckon. This improvement should be expected if all error biases are removed and the remaining range time series only has evenly distributed noise about a mean correct answer.

5.3.2 Smart Wiggle

Since some version of the wiggle will be necessary at each STRONG fix, minimizing the computational impact can be significant for a real time navigator. Re-intializing the process every time will prevent any position error from migrating and summing from fix to fix. The robustness of the wiggle will depend on the following factors:

1. Quality of last fix
2. Time since last fix
3. Resolution desired from STRONG fix
4. Geometry

The wiggle must cover the maximum expected error from the last fix. As discussed in Section 3.4.2, the initial condition after vehicle decent in depth will likely require the largest wiggle. However, subsequent wiggles may be relaxed in scope if the STRONG fixes are frequent with good geometry. The coarseness of the initial position step should be on the order of the accuracy wanted at the fix prediction end. There is no need to wiggle in millimeters when meter fix accuracy is expected. The wiggle grid used here was a wasteful spiral. There are several routines like a concentric box approach that can find the minimum of a surface in a miserly number of steps. This approach is often used in USBL systems to find the center of the main lobe for bearing calculation.

A final consideration in the wiggle surface correction is to correct the error to first order. The surface takes on a "folded pancake" appearance with a steep parabola on one axis and a very shallow one in the orthogonal direction. This shape is no accident and was seen with every run leg. The reason can be explained with Figure 3.8. The total error can be thought of as a sum of three parts:

$$Error_{Total}^2 = Error_{oval-start}^2 + Error_{rectangle}^2 + Error_{oval-end}^2$$

The wiggle surface shape is determined by how the FIT VALUE changes as the

trajectory slides upon the range circles. As explained in section 3.4.2, without the rectangle section, two ranges on symmetric side of CPA could be slid 360° around the ranging platform with no observable variance in the data. The rectangle term becomes the saving grace, but is very sluggish to respond since the trajectory becomes more and more tangential to the circles (and orthogonal to range) as CPA is approached. Conversely, the solution is very sensitive to advances toward or away from the ranging platform as the oval terms sum in opposite direction on either side of CPA strengthening their position. The end result is a folded pancake that has its long axis collinear with the long range circles (in the limit that small concentric circle arcs approach parallel lines) and orthogonal to the ranging platform bearing (Figure 5.4). Therefore, a smart first order wiggle would be to march the initial condition toward or away from the ranging platform approximated bearing until the well defined minimum is reached. Does it take out all the error? No, but a significant chunk can be removed by moving a short distance in a known direction. For further accuracy, you can search for a minimum along the collinear shallow axis, but using the initial fix guess of position in this direction may be a more fruitful approach since a few incorrect ranges in the rectangle term can adversely influence the final solution. In fact several of the legs arrived upon a minimum skewed all the way to the edge of the wiggle surface. These initial positions were left in for conformity, but this deviation was certainly at the limit of any reasonable beginning fix error and would have been more accurate if left with a first order smart wiggle.

5.4 Charleston, S.C. Data

The Charleston and Bahamas data were starter sets with few concrete results; however, some loose conclusions can be drawn from each. With the details of the Charleston collection already discussed, a simple geographic view shows the ship and vehicle tracks (Figure 5.5). There is no reliable ending fix, just a final range. The vehicle fix influenced dead reckon position and the STRONG fix are plotted. The STRONG fix is much closer to the ending range and there is an overall better fit to the ranges (all but

first and last ranges were omitted for clarity). This depiction appears to be hopeful, but a final ending range is not as exact as a fix and relying on one range for truthing is flawed since it is not independent of the data set and the single final range may have an inherently large error. With that said, the data did lay out to fit a course with an error not unreasonable for an uncalibrated inertial compass.

Figure 5.5
Charleston REMUS 6000

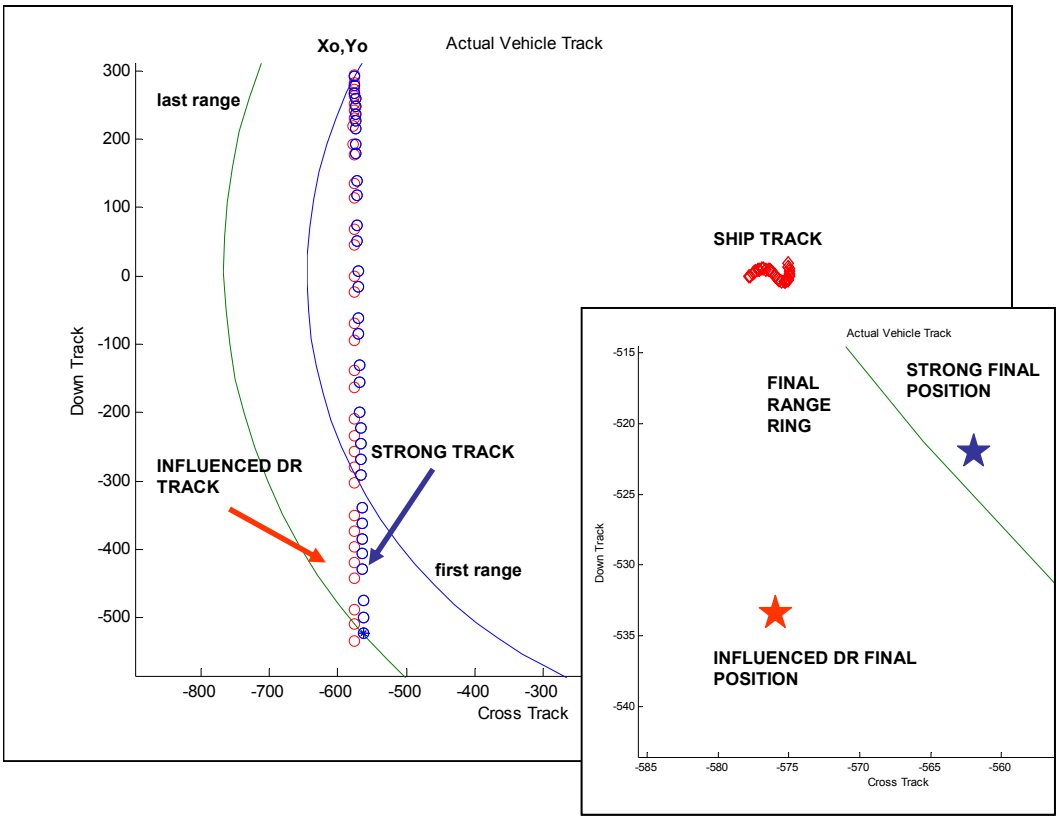

Figure 5.5 is similar to Step 1 of the Figure 5.2 explanative illustration. Steps 2 through 4 are also provided to characterize the Charleston fit (Figure 5.6). Note that the red range dots fit around the chosen range trajectory with an evenly distributed nature. This observation is not meant to prove that some unidirectional range bias is not present, but in a case of a gross bias, the fit would distort at the ends. The family spread in Step 3 does not touch the vertical range axis indicating that a small wiggle was necessary. The

FIT VALUE is good nearly touching the vertical axis. Notice that the Step 4 inset shows the answer was arrived at in about 22 iterations (course difference curve flattens) but was delayed to use the remaining data.

Figure 5.6
Charleston REMUS 6000

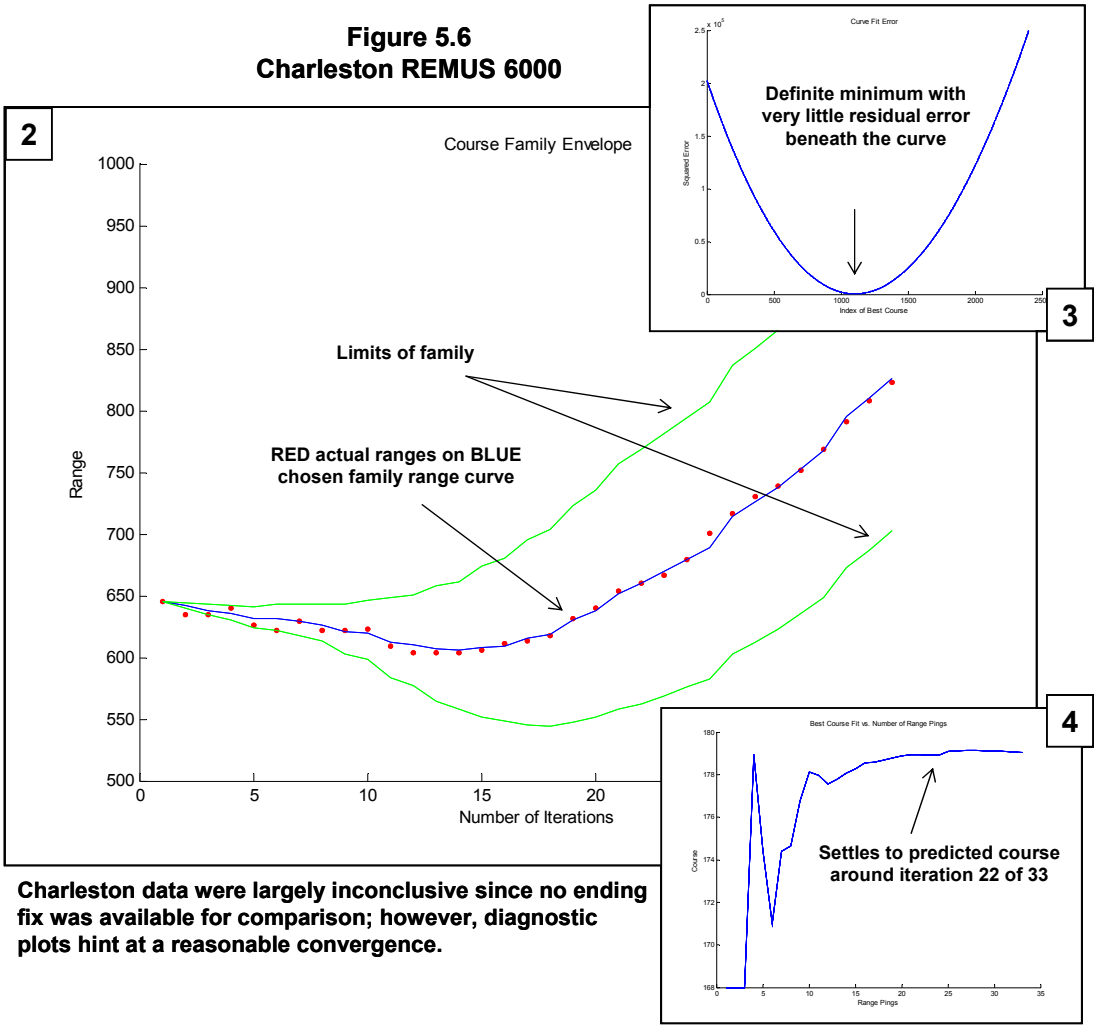

Charleston data were largely inconclusive since no ending fix was available for comparison; however, diagnostic plots hint at a reasonable convergence.

5.5 Bahamas Data

The Bahamas data set was a challenge particularly since it was deep (3400 meters) and one of the first full legs carried through the algorithm. There were several errors that made fitting the data difficult until the project gained more maturity. A time

synchronization error, the near geometry breakdowns, and a slant range discrepancy slowed down the analysis until each issue could be logically addressed. Since each bias could only be found by manually wiggling each major player in the data set (and all were inter dependent), smoothing the data set and making sense of the errors literally took weeks. The range data for each CPA leg has a necklace appearance with the vertical length proportional to the length of the leg (Figure 5.7). The raw ranger data is a dense mess spanning eight different channels, two vehicles, and multiple bounce returns (Figure 5.7 inset). The proper channel was chosen and a simple speed filter was used to reject ranges that were impossible. As feared, the data density is no where near the random walk model of Figure 3.19. However, there are sufficient pings to allow convergence prior to end of each leg. The leg processed was leg one. An equipment problem blanked out part of legs five and six. The data density was halved because REMUS 6000 Hull 1 was also in the water navigating. This fact meant Hull 2 received, at best, half as many ranges as possible.

Figure 5.7
Bahamas REMUS 6000 Range Variation

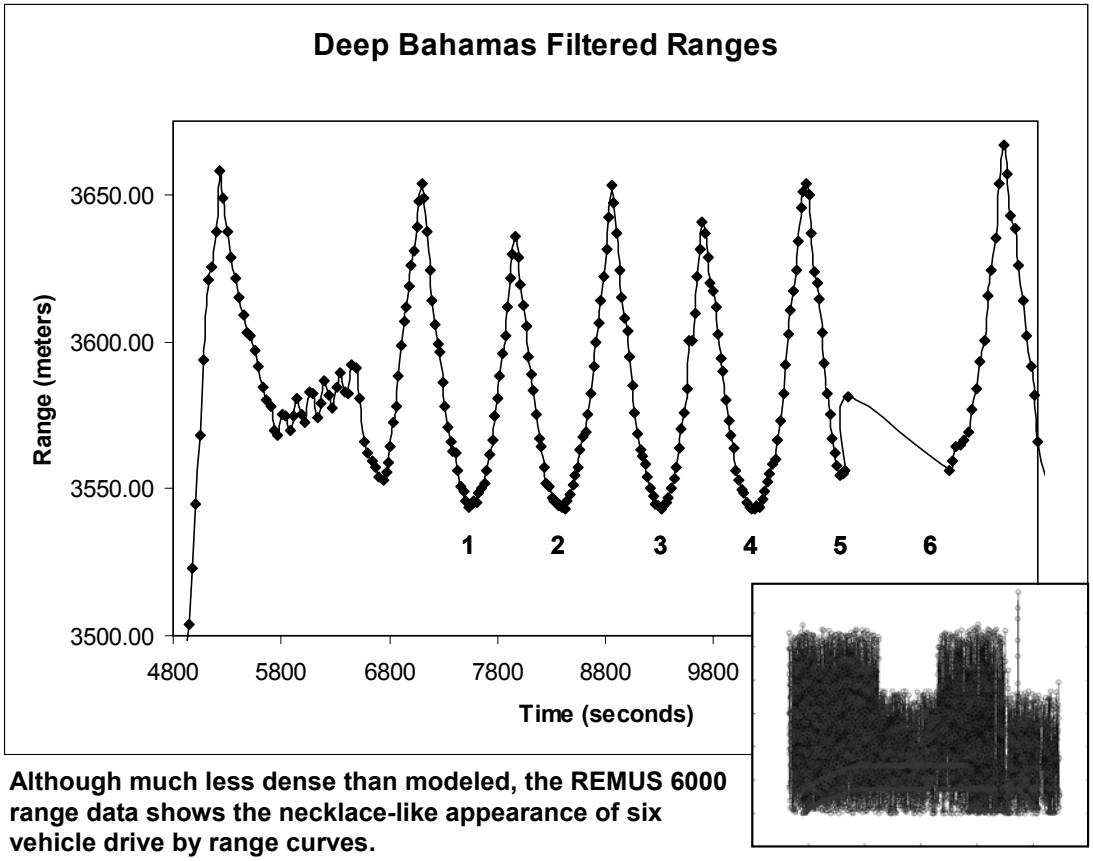

Although much less dense than modeled, the REMUS 6000 range data shows the necklace-like appearance of six vehicle drive by range curves.

The near geometry effects for deep water discussed at length in Section 3.4.3 explored expected limits for STRONG navigation deep areas given certain instrument accuracies. Figure 3.10 shows that a 1% depth error potentially yields imaginary results when within 700 meters of bottom range. Since the ranges varied from 800 meters to a CPA of about 100 meters, the data definitely fell into the questionable region. In fact, there was a significant (to STRONG) depth error in the REMUS software that had to be corrected before the depth error percentage was low enough to process the leg. Similarly, Figure 3.12 shows that even with excellent depth accuracy, a mission in 3000 meters of water can be troublesome at near ranges. The processed deep leg spans the curve where it begins to exponentially increase. The error from Figure 3.12 was averaged over the deep

range time series to find the best expected resolution of a fix with this geometry. This rough value of 30 meters became the measure of success for the leg. In other words, if the data could be adjusted to within reasonable limits of instrument accuracies, the process could be expected to eventually work. The following adjustments were made to pull the fit and ending fix errors in line:

1. 30 second time error
2. 0.01 m/sec ADCP speed error
3. 50 meter Xo error
4. 35 meter Yo error
5. 14 meter slant range error

The time error was a simple discrepancy. Incorrectly, an assumption was made that the vehicle time is exactly synchronized with GPS time by procedure. The launch procedure only requires the two to be within one minute since no other process requires such precise time comparison. The error was found by trial and error and is reasonable.

The ADCP speed error was within the accuracy expected. Similar errors were found in REMUS 100 operations. The drift rate is low, so when the speed error is found, it is relatively constant over the entire mission.

The Xo and Yo errors seem large, but are well within the accuracy of the transponder field. A correction was attempted as described in Section 1.2.1. However the correction was manually done with a drafting compass. The width of the pencil mark was on the order of 20 meters, so renavigation error plus inherent GPS / seeding errors can explain this offset. These errors were found by wiggling the initial condition.

The 14 meter slant range error is the most troublesome. In 3400 meters of water, it is certainly a small deviation from the whole. However, the sensitivity of the solution beneath the ship requires that the error be known at least to a few meters. A slight error in sound speed could explain a small portion of the error, but the Section 3.5.2 ray trace study puts that error no more than a couple meters. If converted to travel time, the discrepancy in on the order of 9 milliseconds. The transponder turn around times can vary on the order of tens of milliseconds based on the installed electronics. For instance,

this run had the turn around time adjusted from 9 milliseconds up to 50 milliseconds. Since sub meter accuracy beyond a return relative sense is not needed in REMUS 6000, no exact test has been done to determine the exact delay time. Further testing with the equipment is necessary to determine how much, if any, of this error can be explained away. However the potential correction is on the order of the error. This error was found by trial and error.

Although not perfectly explained, the deep REMUS leg does fit within the prescribed limits with reasonable and, hopefully, correctable error. The radial fix errors and FIT VALUE can be seen in Figure 5.8. Step 1 only plots every fifth range for clarity. To show the fit, the dead reckon position that goes with an adjacent range ring has a dot in the center color matched to the ring. Step 2 shows that the final fit has evenly distributed range dots. A time synchronization error simply shifts the dot set left or right. A range dependent error narrows or widens the v-shape. Step 3 shows an interesting behavior in that the curve has a double hump with two minimums. The second hump is the ghost solution of Figure 3.3. The vehicle is so close to the base line that the algorithm sees the good fit on the other side of the baseline. Again, a good initial position makes that hump only a local minimum. Step 4 shows through a course difference plot that the algorithm would have again converged early on ping 20 of 33 if not delayed for fix comparison.

As expected, the shallow REMUS 100 legs were much easier to process without the deep depth affects. There is usable data in the remaining deep legs, but the trial and error shifting required to process the first leg led to a refocusing on shallow water data first. Future data collection with some simple calibrations would make a much more approachable data set. However, the deep lessons learned are very important.

Figure 5.8
Bahamas REMUS 6000

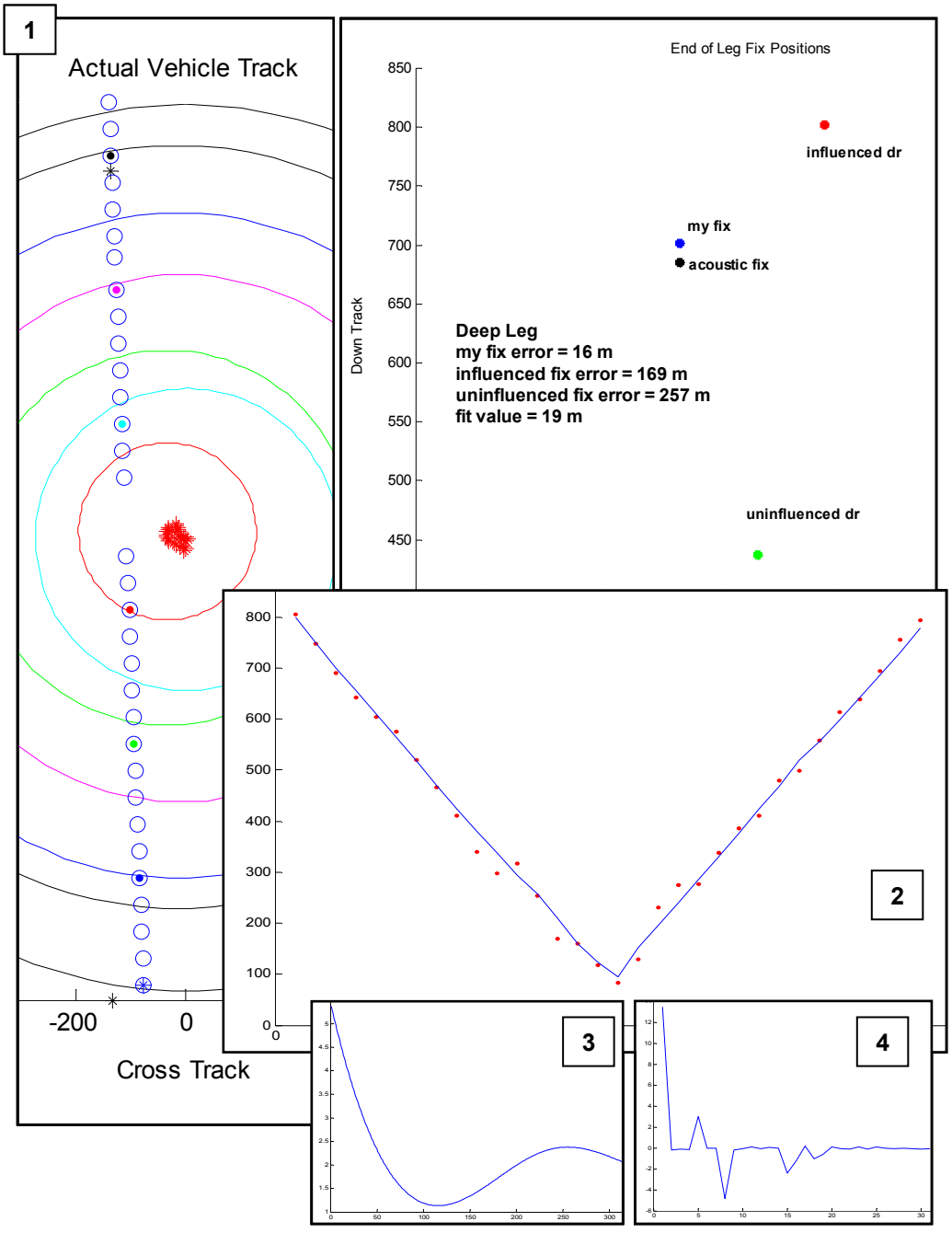

A REMUS 6000 survey leg in over 3400 meters of water gave credence to deep STRONG operations but challenge current methods of instrument calibration.

5.6 Buzzard's Bay Data

The box geometry of Figure 4.1 was attempted in Buzzard's Bay with a REMUS 100. Only nine legs were fully completed, but the partial leg ten did have an ending fix when the vehicle was aborted early due to rough surface conditions that were threatening safe passage home to Woods Hole in the zodiac. Heavy seas dragged the zodiac even at the maximum anchor scope. Again the data was downloaded, dissected in EXCEL, and ingested into the STRONG algorithm. The result was ten course correct legs, two speed-course-speed correct legs, and one speed correct leg.

It is no secret that the noise model designed for an inertial compass REMUS 6000 does not sufficiently characterize a REMUS 100 magnetic compass guided vehicle. The DVL capabilities are similar with the smaller 100 having the more capable ADCP model. However, the threat becomes a heading so noisy that false trajectories could come from short term error bias. Since each leg is reinitialized, the individual legs can be thought of as individual experiments building some rudimentary statistical base to prove that STRONG can prevail outside the limits of the simple model.

A Step 1 – 4 Figure could be produced for every leg; however, the results become more pertinent when end of leg data is compared. Three legs were chosen to profile: a course leg, the speed leg, and aborted leg 10. Leg 10 is particularly interesting because it involves large scale relative motion as the zodiac hauls anchor and motors to the intercept point while ranger data is recorded. The filtered range data set is dense and generally consistent (Figure 5.9). The edges of the necklace structures are asymmetric because the zodiac drifted from the center of the survey box. The symmetry on either side of leg 7 can also be seen re-enforcing the fact that legs on each side of the center baseline are mirror images and indiscernible without a reasonable starting position. This speed leg is sparse, but returns a correction that was applied to all legs. Likewise, leg 10 is sparse, but converges quickly assisted with relative motion.

Figure 5.9
Buzzard's Bay REMUS 100 Range Variation

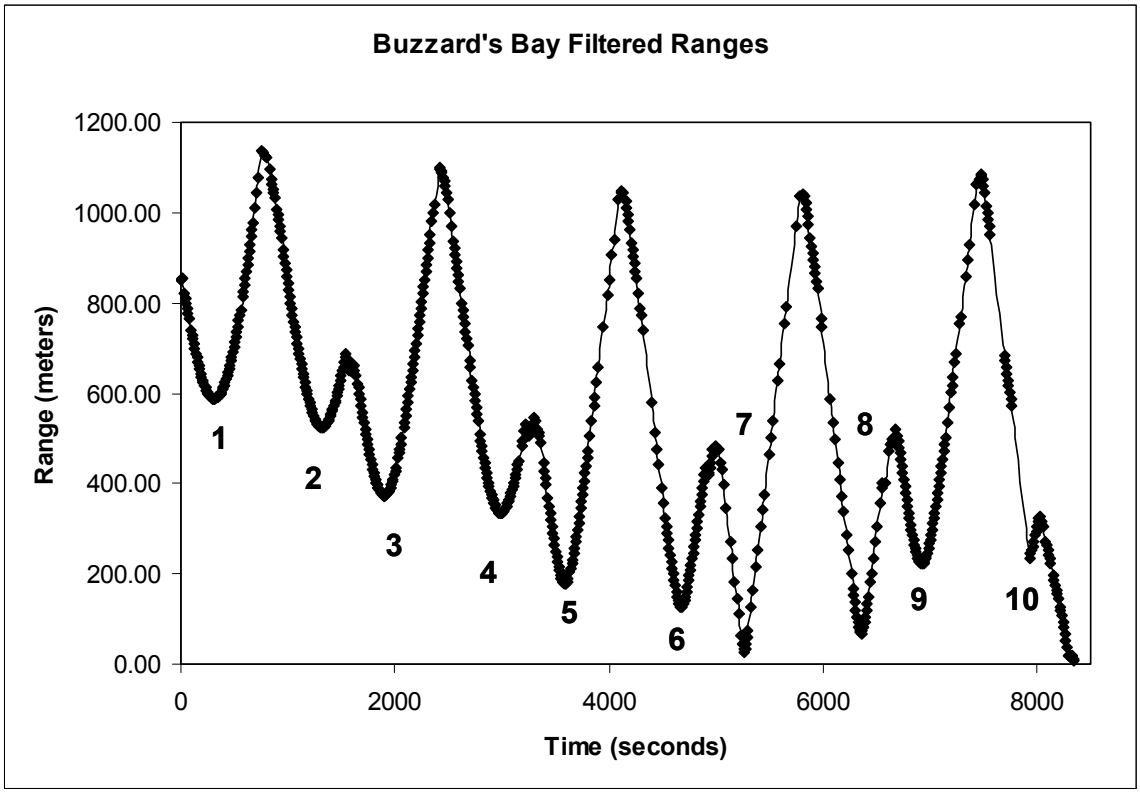

Ten legs of shallow water data were collected and analyzed to valid the STRONG algorithm.

Leg 3 is a standard south bound course correct leg (Figure 5.10). The FIT VALUE of 1 meter and the fix error of 3.4 meters are excellent. Step 1 shows the fit of every fifth range and ending fix layout. Step 2 shows a good range fit of red ranges on the blue family. Some small deviations on the opening side of the parabola correspond to data time gaps and small zodiac drift when the anchor was reset. Step 3 shows an excellent fit. The Step 4 course difference plot shows that the course error could have been predicted as early as iteration 15 out of 70. Potentially, three to four fixes could have been produced on this leg if the convergence had not been delayed for comparison.

Figure 5.10
Buzzard's Bay Leg 3

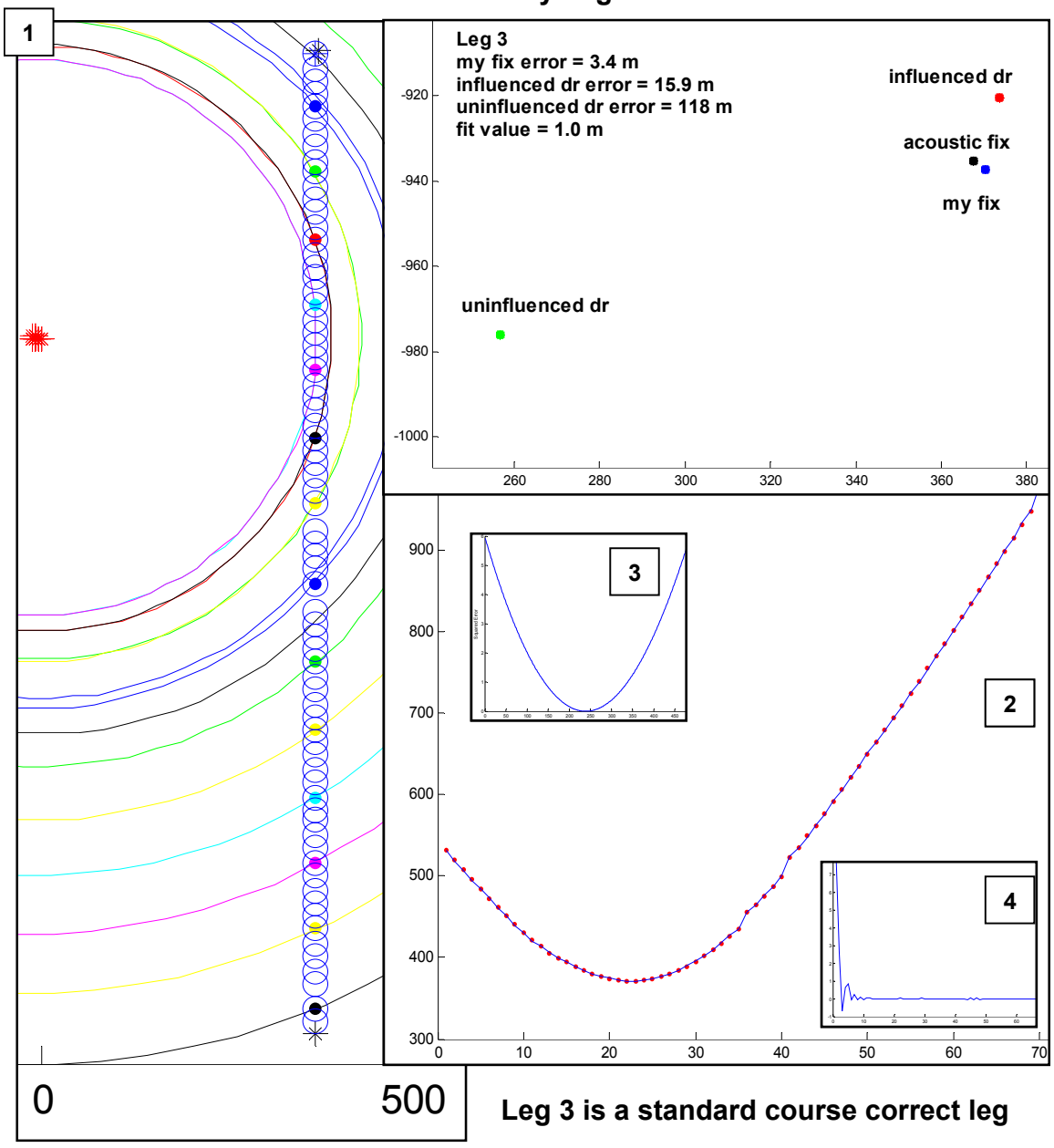

Speed correct leg 7 was sparse but produced acceptable results (Figure 5.11). The FIT VALUE is just over half a meter but the ending fix error is moderate at 8.9 meters. Step 2 shows the family limits and the chosen trajectory sequentially bottom out with

increasing speed. Step 3 confirms the minimal fit value, and Step 4 shows convergence on a speed error of 0.02 m/sec in less than 10 iterations.

Figure 5.11
Buzzard's Bay Leg 7

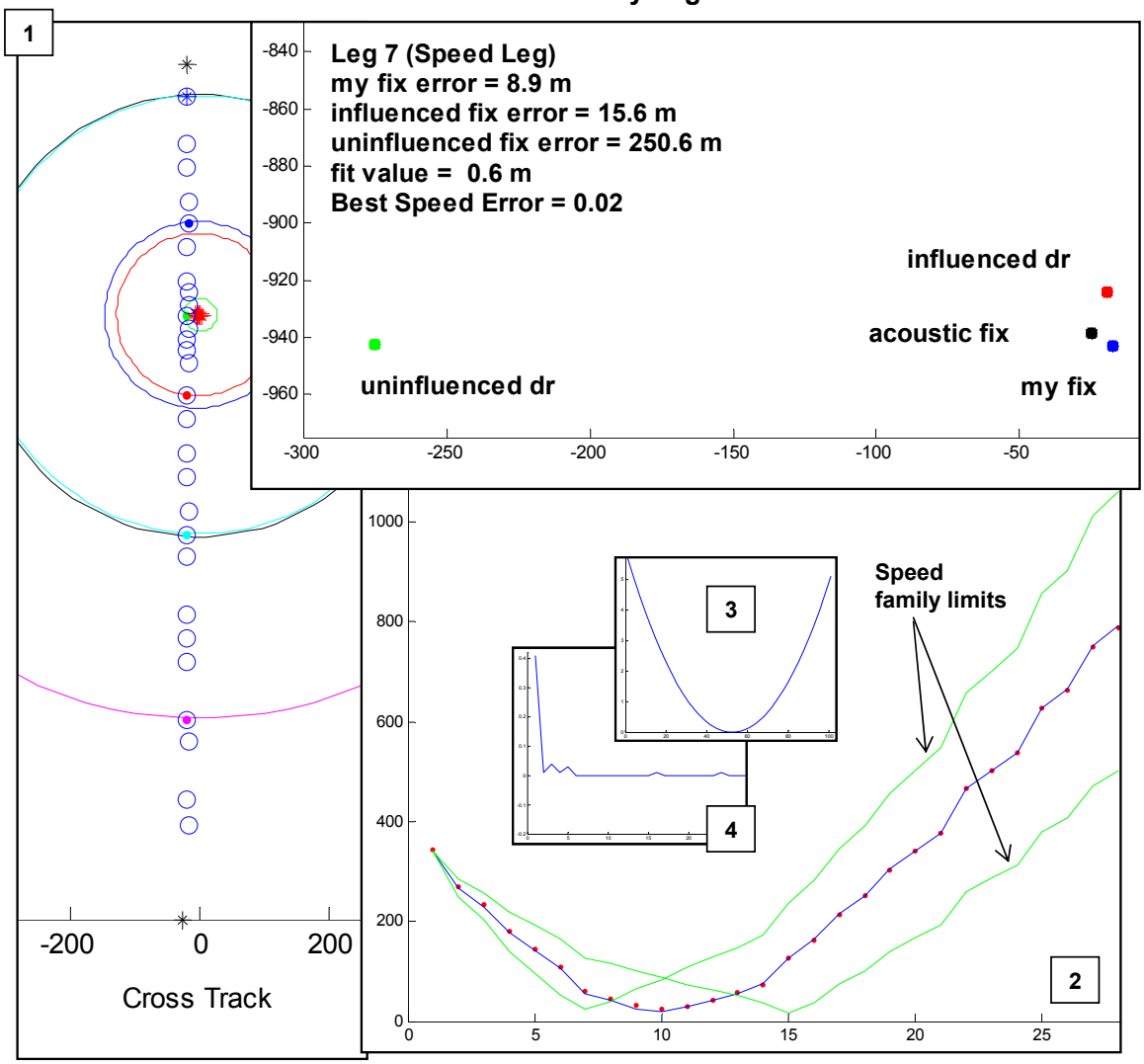

Leg 7 was a speed only leg driving beneath the zodiac

Leg 10 was terminated early, but exhibited good convergence enhanced by significant relative motion between the vehicle and zodiac (Figure 5.12). Step 1 is shown with the STRONG renavigation and the influenced dead reckon track. This dead reckon

track is much closer than the uninfluenced track. The FIT VALUE is good at 2.9 meters. The STRONG fix error has increased to 16.4 meters, but is much preferable to the dead reckon error of 55.7 and 384.2 meters respectively. Step 2 shows an unusual range fit pattern. The curve is not smooth since the horizontal axis is iterative number vice time. Hence large range time gaps with relative motion produces a jagged curve. This jagged signature becomes like a key into a lock and makes the solution hard fast and insensitive. Relative motion is good for converge. Step 3 shows a well defined minimum, and Step 4 shows early convergence once again. The Step 4 curve is flat early because the first few iterations are back in the speed zone and are ignored. The algorithm would have returned a speed correction if enough ranges were available. STRONG transitioned to course correct, reset memory positions, and produced a fix.

Figure 5.12
Buzzard's Bay Leg 10

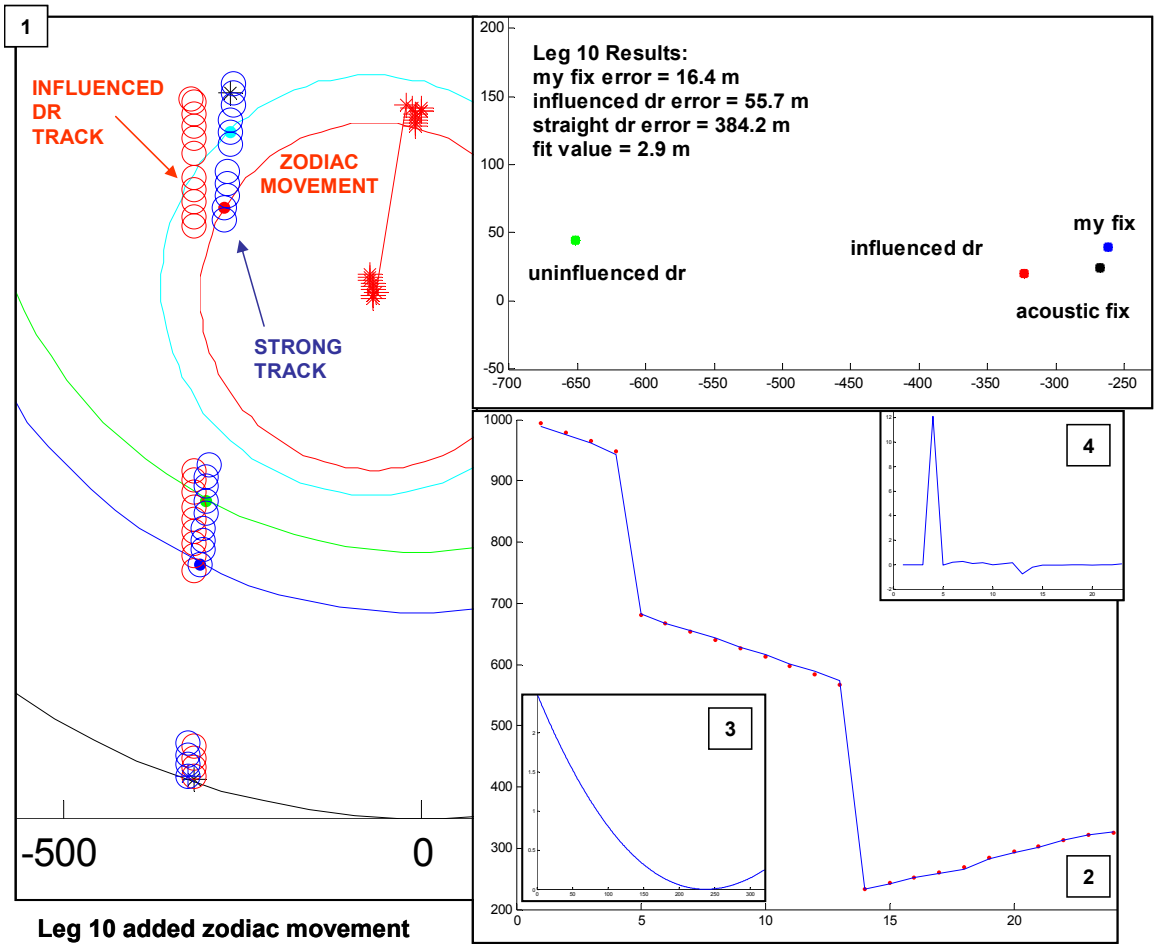

5.7 Combined Results

The data legs from Buzzard's Bay and one from the Bahamas have acoustic fix information for comparison at the end of each leg. Every time, the convergence was delayed, sometimes three fold, past the guessed trajectory. Although potentially having 10 meters or so of transponder error, this acoustic fix comparison is the most consistent ground truthing method. The ending STRONG fix was chosen simply based on a wiggle of the initial condition out to a radius of 10 meters with no regard to the ending fix comparison. A smart wiggle toward or away from the ranging platform would have been quicker resulting in nearly as good a fit (in some cases better). In 9 out of 11 legs (deep

and shallow), the wiggle produced an improvement in FIT VALUE vice using the raw acoustic starting fix (Figure 5.13). In fact, Leg 3 of the Buzzard's Bay set, the solution would not converge without the wiggled starting point. However, Legs 5 and 9 wiggled to excellent FIT VALUES of approximately 1 meter to have their STRONG fix positions deviate the most from the ending acoustic fix. Fix errors and wiggle movements were separated into North / South legs and x – y components to determine if the bias was due to an acoustic fix error or a bias in the data. Although acoustic fix error probably separated the plots on the remaining legs, 5 and 9 were biased due to an asymmetric data density. Careful study of Figure 5.9 shows that Legs 5 and 9 are mirror images about center Leg 7. Before CPA (minimum of the necklace), each leg had a wealth of data and post CPA became very sparse. This effect was probably due to the environment, but it did skew the results slightly since the small bias errors in range approaching were not balanced with opening ranges. A filter could be applied to adjust the wiggle results. However, the resultant error is small compared to the uninfluenced dead reckon positions and would not be carried through the next wiggle. Leg 10 also saw a significant increase in error. Part of this divergence is attributed to the significant change in water depth that the ranger transducer experienced when the zodiac was underway. Excluding these data points, the x – y wiggled differences show weak agreement indicating the southern transponder may have been a couple more meters to the southeast than charted. However, there is not enough data to make anything more than a judgment call. In these legs, wiggled and non-wiggled positional errors differ by less than the professed accuracy of the LBL field.

The second half of Figure 5.13 shows that the wiggled initial condition paces the acoustic "known" starting point. Comparison of the two beyond the order of acoustic fix error (10 meters) is tenuous, but the curves are very similar discarding Legs 5 and 9. The important point is that the wiggled condition tracked the acoustic starting point when vehicle uninfluenced dead reckon position grows to 384 meters in just 10 legs. Wiggling not only prevented the migration of this dead reckon error as a tainted starting point, but

also improved, in some cases, on the acoustic starting position. Therefore, wiggling is a reasonable and simple method to prevent error migration and realize the best data fit.

Figure 5.13
FIT - Error Comparison

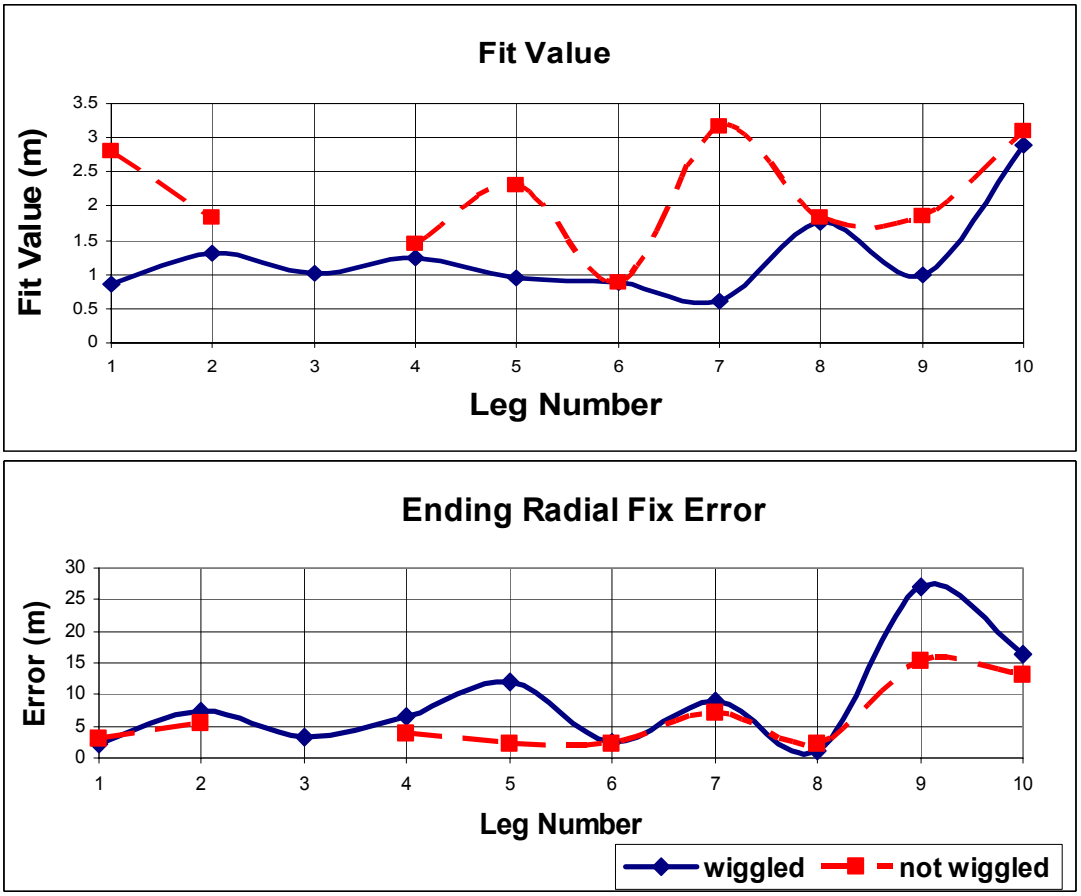

Wiggling improved the FIT VALUE in 9 out of 11 legs. The second graph illustrates how closely the wiggled initial position tracks the ground truth LBL acoustic starting point. Therefore, wiggling should prevent the large scale deviation of initial position seen in vehicle uninfluenced dead reckon (up to 384 meters in leg 10).

Figures 5.14 and 5.15 show the combined results of the mentioned 11 legs. The quoted values are radial errors in range from the ending acoustic fix. Recall that the influenced dead reckon integrates the dense acoustic fix information at the ends of each leg to re-initialize position. The uninfluenced dead reckon runs from time of launch and

does its best to update position with the heading source and the DVL. Uninfluenced dead reckon can be thought of as the best position a vehicle would have if bottom transponder navigation was not feasible and no depth transient was desirable or feasible for GPS position updates. Therefore, the most meaningful comparison is between STRONG position and the uninfluenced dead reckon position because eliminating bottom transponders and GPS leaves only these two navigators. Figure 5.14 easily illustrates why depending on uninfluenced dead reckon is problematic. There is a clear and significant divergence in the uninfluenced position as errors migrate and compound. The uninfluenced dead reckon error of 384 meters is certainly unacceptable after only 10 legs. The growth rate is over 30 meters per leg. The oscillatory nature of the increasing error is due to the bias in the magnetic compass between a north and south course. REMUS does eliminate this 10 – 15 meter error with software after a given number of legs, but this feature was defuncted to keep the different realizations as comparable as possible. STRONG even beats the influenced dead reckon error on all but one leg proving that, in the majority of cases, a single leg of 1300 meters accumulates enough dead reckon error to require STRONG correction. The deep leg manifests even more error (Figure 5.15). In a single leg, the uninfluenced dead reckon has degraded to 257 meters. Albeit there is a larger potential error in the acoustic fixes, but the STRONG results agree well with the fix information.

Figure 5.14

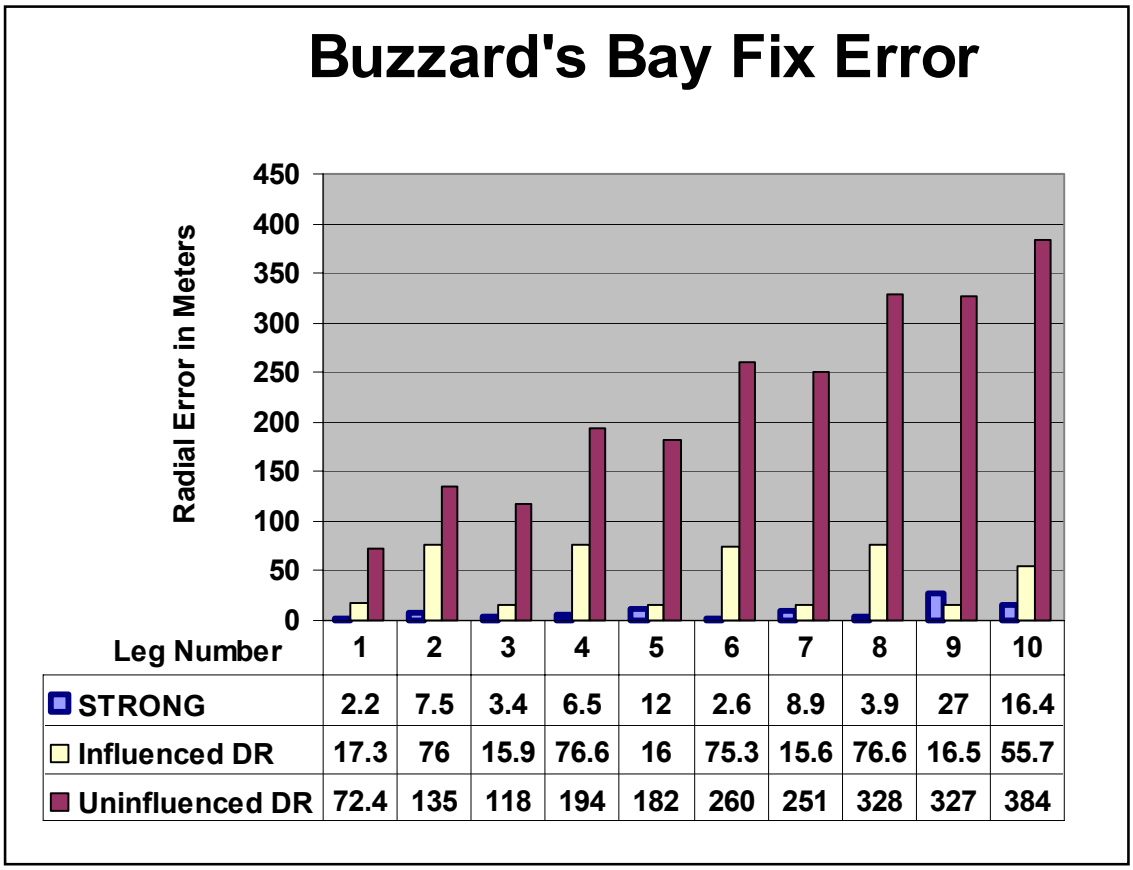

Leg Number	1	2	3	4	5	6	7	8	9	10
STRONG	2.2	7.5	3.4	6.5	12	2.6	8.9	3.9	27	16.4
Influenced DR	17.3	76	15.9	76.6	16	75.3	15.6	76.6	16.5	55.7
Uninfluenced DR	72.4	135	118	194	182	260	251	328	327	384

Over the entire mission, the REMUS position without external correction grows steadily over 10 legs to almost 400 meters. On each individual leg, the reset dead reckon position is often over 50 meters by the end of the leg. STRONG is more accurate than both dead reckon positions in all but one case.

Figure 5.15

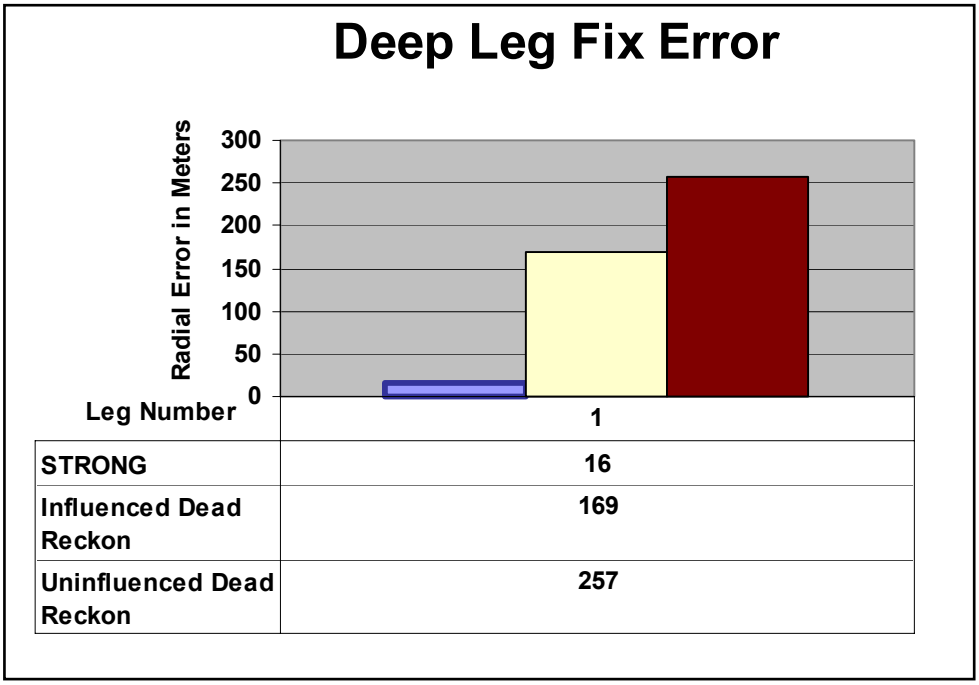

Leg Number	1
STRONG	16
Influenced Dead Reckon	169
Uninfluenced Dead Reckon	257

After adjustments, the STRONG ending position was significantly better than both dead reckon positions

CHAPTER 6
FUTURE WORK

6.1 Transition to Generic Problem

To make STRONG a viable navigation tool, the algorithm must become a generic navigator that can withstand arbitrary vehicle movement and catch corrections as they become observable. As with navigation routines on large manned submarines, divergence from reality can lead to catastrophic results. Experience and testing with a working, in vehicle routine will provide future data for the confidence building necessary to turn an AUV loose with single transponder navigation. Chapter 6 is not meant to circumvent any of this necessary testing, but to thumbnail an approach to building a generic routine able to deal with maneuvers.

As described at length, the single leg version built a family of perturbed possibilities around the mission preplanned course and speed boot strapping between along track and cross track corrections in hopes of containing positional inaccuracies. The geometric inter-relation of the vehicle and the ship in the x-y plane is utilized to determine when certain corrections are fruitful. The z dimension comes into play when instrument errors and / or appreciable depth combine to exacerbate vehicle plane errors in position. In the generic form, the vehicle's actual motion becomes more telling than the planned trajectory. For instance, the turns onto course in a box survey can significantly vary from the planned trajectory as vehicle and environmental dynamics cause deviations. Therefore, the more logical baseline to perturb is not the intended track but the dead reckon position. This approach seems strange given that previous chapters sought to prove that this navigator is largely flawed and degenerates with time. However, a dead reckon trajectory is accurate on a relatively short time scale between fixes and is the best indication of vehicle motion for perturbation. If the vehicle is equipped with an inertial navigator, another option would be to perturb the filtered inertial position. However, many vehicles will not have this system, and inertial navigators are prone to unwanted oscillations with periods small compared to a typical mission. Likewise, one of

the goals of STRONG was to produce an independent position that could potentially be used for fix input to a Kalman filtered inertial navigator. Figure 6.1 illustrates how a non constant course and speed dead reckon position could be perturbed to provide "fitable" trajectories. The zones around the vehicle are still sensitive to vehicle Angle-to-CMG and fall into speed and course correct zones.

Figure 6.1
Generic STRONG

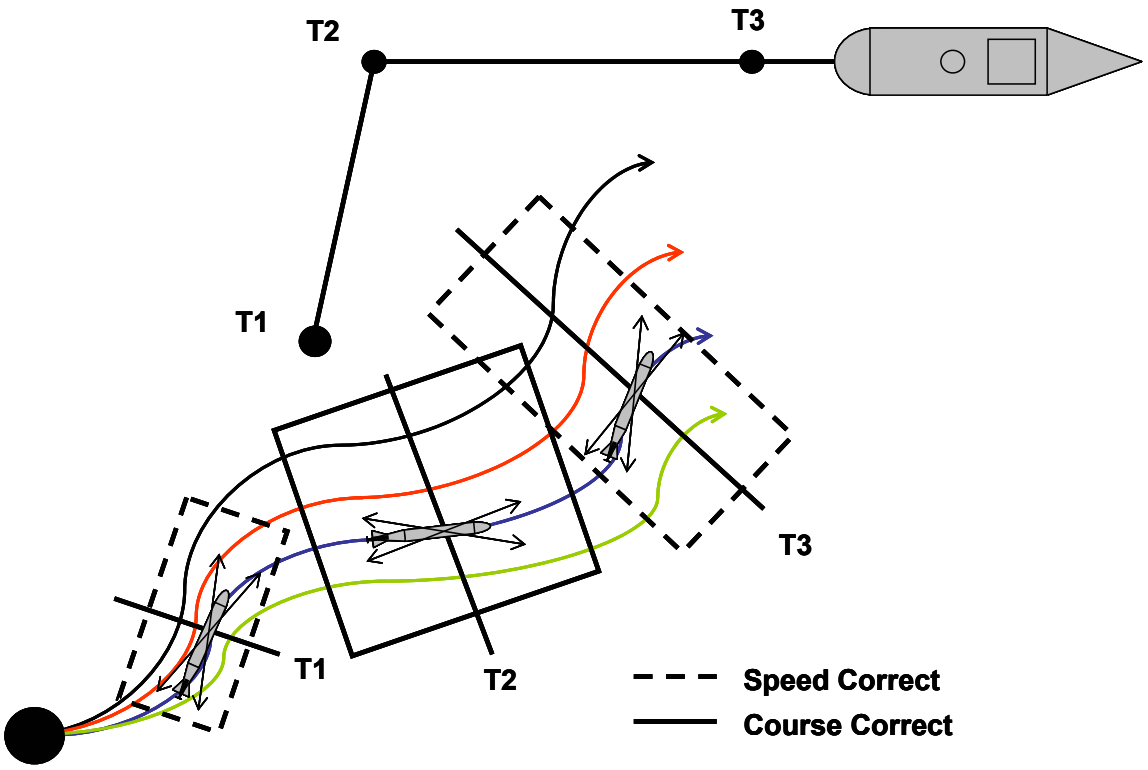

STRONG can be applied in a more general sense to glean corrections when possible and prompt operators to action when a directed maneuver is needed

The interdependence of course and speed and the existence of multiple local minimum with initial condition remain unchanged. The key again is to correct course and speed at every opportunity and build safeguards and operator aids to make the correction frequency high enough to prevent aliasing of speed error to course correction and vice versa. Additionally, resetting the initial condition with a wiggle radius proportional to

maximum expected error and of x-y resolution comparable to the needed STRONG fix accuracy is essential to prevent convergence on multiple false minima and migration of positional error to subsequent fixes. Finally, the importance of attaining and preserving maximum instrument accuracy cannot be understated. Especially in deep depths, errors in sound speed, depth measurement, and range can overwhelm all hopes of reasonable accuracy when the single transponder is surface ship mounted.

6.2 Processing Locations

The smartest location to process data requires some consideration. Assuming the most advantageous application of a maneuvering ship as the ranging platform, it may be tempting to process some data topside unloading the burden on the vehicle brain. However, since all data through put must reach the vehicle via acoustic modem in an environment that is plagued with unwanted noise, the wisest decision is often to process as much information as possible onboard the vehicle. No doubt, acoustic modems are on the cusp of significant improvement, but vehicle processors and memory storage are growing more quickly. The only information required from the ship would be the GPS track. The ship to vehicle ranges could be processed on board the vehicle as with traditional LBL vice the topside method employed with this research. This shift leaves the problem of time synchronizing ship position with the measured range. Therefore, ship position must be sent more frequently than vehicle ranging to allow interpolation and on a time scale to capture the granularity of ship movements. Since only the digits expected to change must be sent, the packets of information can be small in size. They must, however, be frequent since the information is essential to calculations and real time STRONG fix production cannot be more frequent than data packet reception. Since ranges are produced on the order of 5 – 10 seconds, small bursts of ship position could be inserted between ranges and interpolated to range time. If need be, larger, less frequent, transmissions are possible if time late fixes are accepted and dead reckoned to present vehicle time with small snippets of dead reckon track. Some time lateness is inevitable

since fix processing with a significant wiggle can take a couple range cycles to complete. Irregardless, a data transmission protocol must be developed to minimize transmission without delaying STRONG fix generation.

6.3 Flow Chart

A simple flow chart is necessary as a starting point for the generic algorithm (Figure 6.2). Combined with the operator feedback flavor of Figure 5.1, a process can be cultivated. The most significant deviation of Figure 6.2 is the dual processing of course and speed information. Previous versions of STRONG retained no memory of past correction that failed to mature producing no fix. When the geometry transitioned from speed to course correct, the speed information was dumped. The idea behind the generic approach is to build broken data sets of each type of correction over time and carry them along for range to range convergence. These "course and speed tails" will be populated based on how much observable correction was available for each type of correction. For instance, a vehicle that has operated frequently in the course zone will have a robust course tail with very young data points. The parallel speed tail would have an identical number of points but span a much longer time period. Each addition of a new range would push in a new point in either tail and sum the data points to see if convergence criteria are still met. If so, a new fix will be produced from the best history of course and speed. If the new ranges show a consistent deviation from the dead reckon position, and not just Gaussian noise, a different perturbation will be picked and the best course or speed will be updated.

Tail length is a debatable issue that is dependent on the noise level and the error drift rate. STRONG work in both deep and shallow water showed convergence in 10 – 30 ranges. A conservative length of 50 points should be sufficient to overcome the noise but be less than the instrument drift error. In practice, ADCP error has much less drift than course error and requires less frequent correction. However, typical box geometry has fewer opportunities for speed correction. This fact combined with similar Gaussian

behavior means the tail lengths should be roughly equal in length. In fact, the tail length can be variable growing with the smart convergence criteria of the STRONG work already done. This approach makes the tail sufficient to promote convergence, but short enough to reduce computational load.

Figure 6.2 Generic STRONG Flow Chart

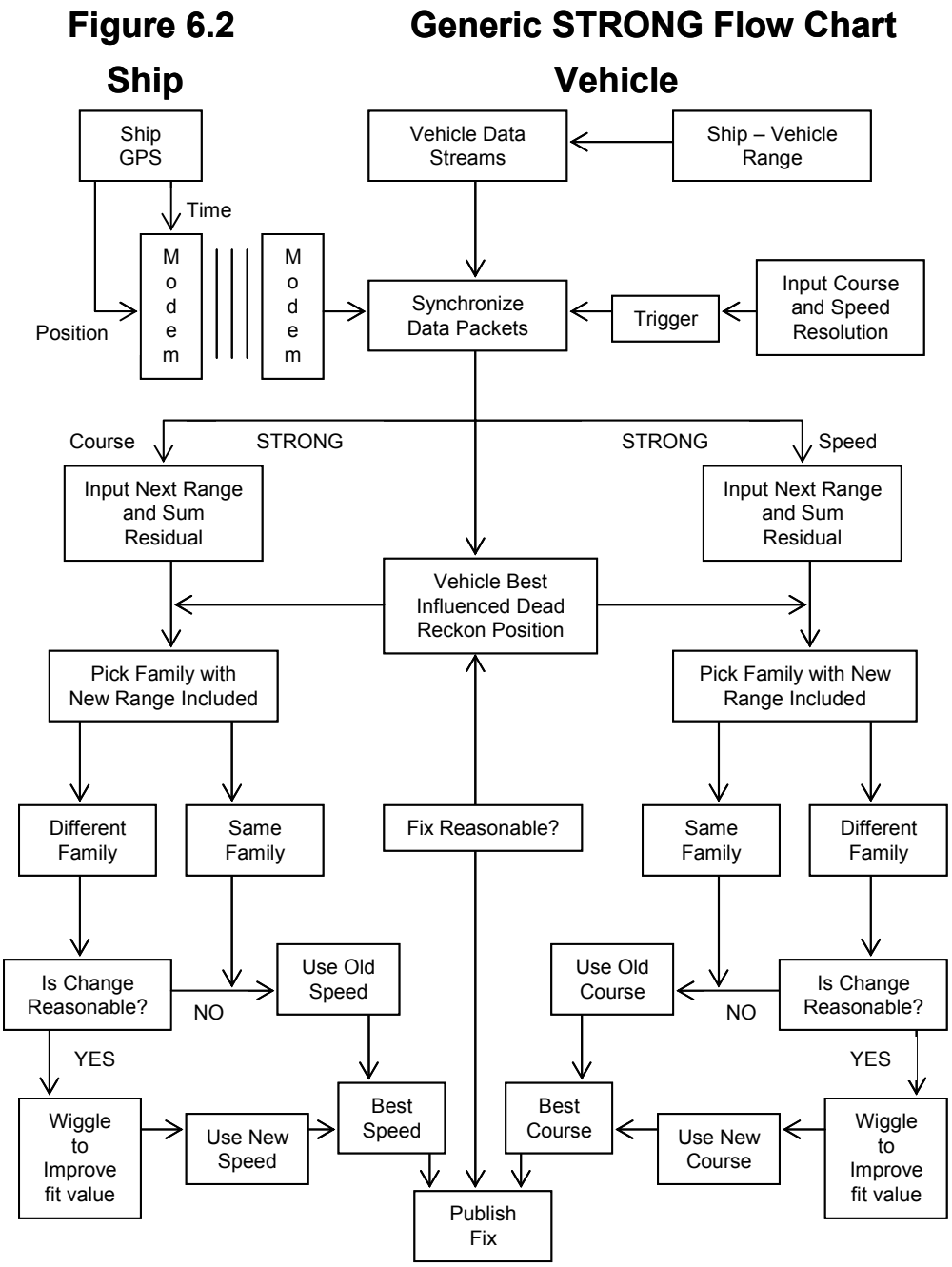

6.4 Operator Feedback

STRONG indicators must be used to alert the operator when a correction is suspect. Data density and fix age are good generic indicators that some changes must be made. The FIT VALUE was discussed at length as good health indicator of the correction. Although FIT VALUE is dependent on the environmental conditions, the value should be consistent within comparable operational conditions. For instance, REMUS 100 operations off Nantucket will yield a much better fit than REMUS 6000 operations in the Sea of Japan. However, there should be little difference between mission legs of each. REMUS dead reckoning uses a wide array of similar smart filtering to through out absurd data. No matter the method, feedback should get back to the operator to indicate that convergence is considered poor.

As discussed, a huge factor in the failure to converge is the lack of relative transponder to vehicle motion. Given feedback that convergence is suffering, a good course of action is to maneuver the ship or the vehicle to provide more observable data. Actually, a little education can prepare a smart ship driver to proved good target motion without prompting. It is fairly obvious that the long "virtual tow" missions of Section 1.2.2 benefit from frequent CPA's (Figure 6.3).

Figure 6.3
Zoned Corrections Transformed to a "Mowing the Lawn" Pattern

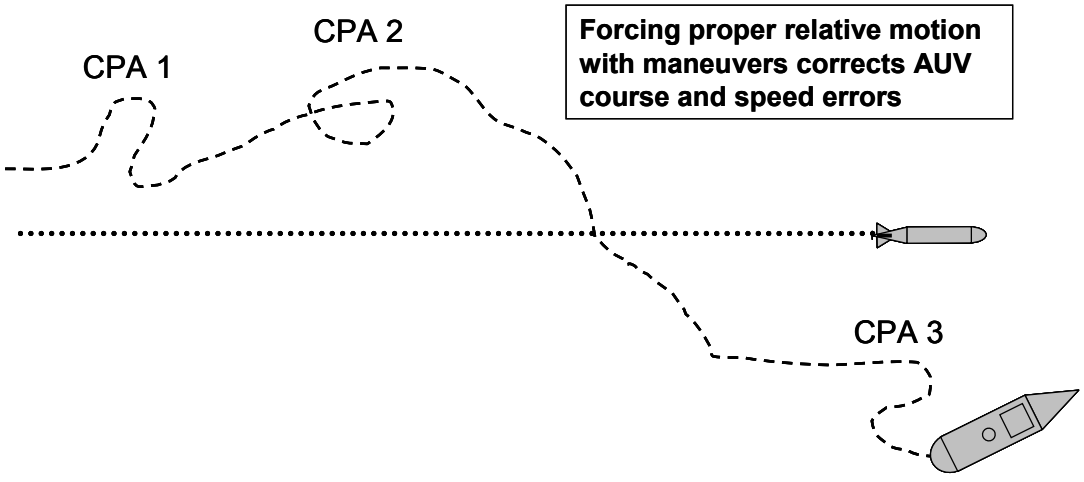

6.5 Final Notes

Early versions of STRONG were conceived much in a vacuum combining a planned development for the REMUS 6000 system and submarine tracking principles permanently burned into my brain by a little repetitive training and a wealth of undersea experience. Research into the field of AUV navigation reveals different approaches to very similar problems. STRONG remains a direct, very mechanical method to solve a complex problem. Although the problem was simplified and constrained to fit into a masters level curriculum, this body of work indicates the method holds promise and some of the theoretical calculations and curves can be applied directly to future operations.

BIBLIOGRAPHY

Stokey, R. and T. Austin. 2002. SAMS: Transponder Deployment and Calibration Procedure Rev. A 3/1/02. Woods Hole, Ocean Sciences Lab.

Marquet, W., D. Webb, and K. Fairhurst. 1969. "A Recoverable Deep Ocean Navigational Beacon." Marine Sciences Instrumentation, 325 – 346.

Spindel, R., R. Porter, W. Marquet, and J. Durham. 1976. "A High-Resolution Pulse-Doppler Underwater Acoustic Navigation System." IEEE Journal of Oceanic Engineering, Vol. OE-1, No. 1, 6 – 13.

Cestone, J., R. Cyr, G. Roesler and E. St. George Jr. 1976. "Latest Highlights in Acoustic Underwater Navigation." International Navigation Congress 1997 Boston, MA, 2 – 15.

Austin, T. C. 1994. "The Application of Spread Spectrum Signaling Techniques to Underwater Acoustic Navigation" Proceedings 1994 Symposium on Autonomous Underwater Vehicle Technology, 443 – 449.

Larsen, M. B. 2000. "Synthetic Long Baseline Navigation of Underwater Vehicles." Proceedings of OCEANS 2000 MTS/IEEE, 2043 – 2050.

Baccou, P. and B. Jouvencel. 2002. "Homing and Navigation Using One Transponder for AUV, Post-processing Comparisions Results with Long Base-Line Navigation." Proceedings of the 2002 IEEE International Conference on Robotics & Automation Washington, DC, 4004 – 4008.

Newman, P. and J. Leonard. 2003. "Pure Range-Only Sub-Sea SLAM." Proceedings of the 2003 IEEE International Conference on Robotics & Automation Taipei, Taiwan, 1921 – 1926.

Song, T. 1999. "Observability of Target Tracking with Range-Only Measurements." IEEE Journal of Oceanic Engineering, Vol. 24, No. 3, 383 – 387.

Jalving, 1999. "Depth Accuracy in Seabed Mapping with Underwater Vehicles." Proceedings of Oceans '99. Vol. 2, 973-978.

Alameda Jr., W. 2002. "SEADeViL A Totally Integrated Inertial Navigation System (INS) Solution." Underwater Intervention Symposium New Orleans, LA, 1 – 6.

Scherbatyuk, A. 1995. "The AUV Positioning Using Ranges from One Transponder LBL." MTS/IEEE, NEW YORK, NY (USA). Vol. 3, 1620 – 1623.

Brook, R. and G. Arnold.1985. Applied Regression Analysis and Experimental Design. New York: Marcel Dekker, INC.

Liebelt, P. 1967. An Introduction to Optimal Estimation. Reading: Addison-Wesley Publishing Company.